DIFFRACTION AND SCATTERING OF ELECTROMAGNETIC WAVES IN ANISOTROPIC MEDIA

Benjamin Ruf

Research Report No. PIBMRI-1262-65
Contract No. AF 19(628)-2357

Project No. 563501
Task No. 5635

for
Air Force Cambridge Research Laboratories
Office of Aerospace Research
United States Air Force
Bedford, Massachusetts
26 April 1965

MRI

POLYTECHNIC INSTITUTE OF BROOKLYN
MICROWAVE RESEARCH INSTITUTE

ELECTROPHYSICS DEPARTMENT

NOTICES

Requests for additional copies by agencies of the Department of Defense, their contractors, or other government agencies should be directed to:

Defense Documentation Center (DDC)
Cameron Station
Alexandria, Virginia 22314

Department of Defense contractors must be established for DDC services or have their "need-to-know" certified by the cognizant military agency of their project or contract.

All other persons and organizations should apply to the:

Clearinghouse for Federal Scientific
and Technical Information (CFSTI)
Sills Building
5285 Port Royal Road
Springfield, Virginia 22151

AFCRL-65-429

DIFFRACTION AND SCATTERING OF ELECTROMAGNETIC WAVES IN ANISOTROPIC MEDIA

Benjamin Rulf

Polytechnic Institute of Brooklyn
Electrophysics Department
Graduate Center
Route 110
Farmingdale, New York 11735

Contract No. AF 19(628)-2357

Project No. 563501

Task No. 5635

PIBMRI-1262-65

26 April 1965

Prepared for

AIR FORCE CAMBRIDGE RESEARCH LABORATORIES
OFFICE OF AEROSPACE RESEARCH
UNITED STATES AIR FORCE
BEDFORD, MASSACHUSETTS

ACKNOWLEDGEMENT

The work presented here is to be submitted as a dissertation to the faculty of the Polytechnic Institute of Brooklyn, in partial fulfillment of the requirements for the degree of Doctor of Philosophy in Electrophysics.

The author wishes to express his gratitude to Professor L. B. Felsen who was the thesis adviser, and to Professors Shmoys, Hessel and Tamir for their interest and useful comments.

This research has been sponsored by the Air Force Cambridge Research Laboratories, Office of Aerospace Research (USAF), Bedford, Massachusetts, under Contract No. AF-19 (628)-2357.

ABSTRACT

This study deals with several two-dimensional scattering and diffraction problems in anisotropic media. The intent is twofold: First, to generalize mathematical methods applicable in isotropic regions to a certain class of anisotropic problems; and Second, to study the solutions of the anisotropic problems in such a manner as to highlight certain common properties which point the way toward the construction of approximate solutions for configurations with more general structural shape or anisotropy. In the low-frequency range, the method of multipole expansion is used. It is demonstrated that the rigorous solution for the problem of scattering of a plane or cylindrical wave by an obstacle which is small compared to the wavelength may be expanded in a series whose terms correspond to multipole radiation in the anisotropic medium. As an illustration, the excitation coefficients of the first few terms arising from scattering by a narrow conducting ribbon are calculated. In the high frequency range, geometrical optics, the first-order asymptotic solution of Maxwell's equations is considered first. The ray refractive index is calculated, and the laws of propagation and reflection of rays, which define the trajectories of energy transport, are derived from Fermat's principle. To obtain an insight into diffraction phenomena, two types of representative problems -- -- diffraction by a straight edge, and diffraction by a smoothly curved object -- are discussed. Rigorous solutions are found which are then expanded asymptotically for high frequencies. The diffracted field contributions are phrased in a manner which emphasizes the local character of the diffraction process by exhibiting an explicit dependence on the local properties of the scattering object and on the adjacent medium. The asymptotic expressions may be put in a form which constitutes a generalization of Keller's geometrical theory of diffraction, thereby providing a method for constructing high frequency solutions for a rather general class of diffraction problems in anisotropic regions.

Special attention is paid to the case for which the medium parameters are complex or negative real, so that the results apply to a certain class of plasmas with losses or with "hyperbolic" refractive index characteristics.

TABLE OF CONTENTS

TABLE OF FIGURES

TABLE OF FIGURES (continued)

CHAPTER I

INTRODUCTION AND SUMMARY

To gain an understanding of the phenomena of scattering and diffraction of electromagnetic waves by objects embedded in anisotropic dielectric media has been the goal of many investigators in recent years. The general problem is rather complex, but various special problems have been solved, both for their own sake and for the sake of extrapolating the obtained results to other, more difficult configurations. In the following investigation, the same course has been chosen. Several special problems have been treated, and an attempt has been made to find the limits of validity of the methods used.

Throughout this work we assume that the surrounding medium is anisotropic and can be characterized by a dielectric tensor $\underset{\sim}{\hat{\epsilon}}$ the elements of which are known functions of frequency and other parameters[1]. Thus, at a fixed frequency (steady state). the tensor elements are regarded as constant, independent of the fields under investigation. The limitations of this approach have to be kept in mind. However, results obtained from such an idealized model for the medium are known to furnish workable approximations in such studies as communication through the ionosphere, radio wave propagation around the earth etc.. where the propagating fields are not very intense. Of the mathematical methods used in this work, two should be specifically mentioned: L. B. Felsen[2] devised a method of reducing boundary value problems which arise from a certain class of electromagnetic wave problems in uniaxially anisotropic media to other boundary value problems, corresponding to wave propagation in isotropic media. This is accomplished by means of a simple transformation of variables. The transformed problems may then be treated by known methods, and the solutions transformed back to the original variables. Although this method is applicable only for a rather restricted class of problems, its value lies in enabling one to find rigorous solutions. These solutions may then be evaluated approximately by asymptotic methods in the various wave-

length ranges. The asymptotic results may be interpreted in physical terms, and their forms indicate how solutions of more complicated problems (to which it might be impossible to find rigorous solutions) should appear. This, in effect, is the main goal of this investigation.

In finding asymptotic solutions in the short wavelength ("quasi optic") range, use has been made of the method formulated by J. B. Keller[3] for isotropic electromagnetic problems. With the help of his technique, one may construct asymptotic solutions to a rather broad class of wave problems. It is important to note that this theory has not yet been shown to hold generally. Instead, many specific problems which can be solved rigorously have been shown to agree with this theory. In order to extend the applicability of Keller's theory to anisotropic media, it is therefore necessary to find rigorous solutions of various prototype problems, (with the help of Felsen's method, or otherwise), and to deduce from their asymptotic behavior the extension of Keller's method to a class of electromagnetic wave problems in anisotropic media. It has been mentioned that the elements of the dielectric tensor $\hat{\underset{\sim}{\epsilon}}$ are regarded as constants at any given frequency. These constants may be complex numbers and, for example, in a magnetoplasma, may lie on the negative real axis of the complex plane. Under these conditions, the wave equation for some of the field components becomes a hyperbolic rather than an elliptic equation. Although Felsen's method may be applied formally even if the elements of $\hat{\underset{\sim}{\epsilon}}$ are not real and positive, the solutions have to be carefully examined to find whether they are still physically meaningful. The solutions of several problems have been investigated as functions of the complex elements of $\hat{\underset{\sim}{\epsilon}}$ and the regions of their validity has been determined.

In Chapter II the class of physical problems which is considered in this work is described, the corresponding boundary value problem formulated, and Felsen's method of solution is outlined. In Chapter III, this method is used for finding an exact solution to the problem of diffraction by an elliptic cylinder. This solution is then expanded asymptotically in the long wave range ("multipole expansion"), and the special case of a narrow conducting ribbon is worked out in some detail. Chapter IV covers several aspects of the short wave diffraction problem. First, in order to utilize ray concepts, geometrical optics is dis-

cussed and some general properties of the geometric optical field are derived for our class of problems. Next, diffraction effects are investigated, from the point of view of Keller's geometrical theory of diffraction. A representative problem for the treatment of edge diffracted rays is the diffraction by a conducting half-plane, which is solved rigorously by means of the Wiener-Hopf technique[4]. The asymptotic expansion of the rigorous solution is interpreted in terms of geometric optical and diffracted rays. For the treatment of surface diffracted rays, two problems are solved: diffraction by a parabolic and by an elliptic cylinder. Rigorous solutions are found by Felsen's method, and again the asymptotic expansions interpreted in ray-optical terms. The diffraction coefficients and decay exponents found in that way may be used to construct solutions to more general diffraction problems of the same class, exact solutions of which are unavailable. It is demonstrated that these diffraction coefficients and decay exponents are functions of the ray refractive index in the medium. A ray refractive index may be found for more general anisotropic media than those considered in this investigation. Thus, the formulation used in this study indicates the possibility of applying Keller's theory to more general problems, of which those considered here are special examples.

CHAPTER II

FORMULATION OF THE PROBLEM

We consider two-dimensional electromagnetic problems, in which the fields are generated by z-directed line currents of constant strength and the scattering obstacles are perfectly conducting cylindrical objects whose axis is parallel to z (Fig. 1)

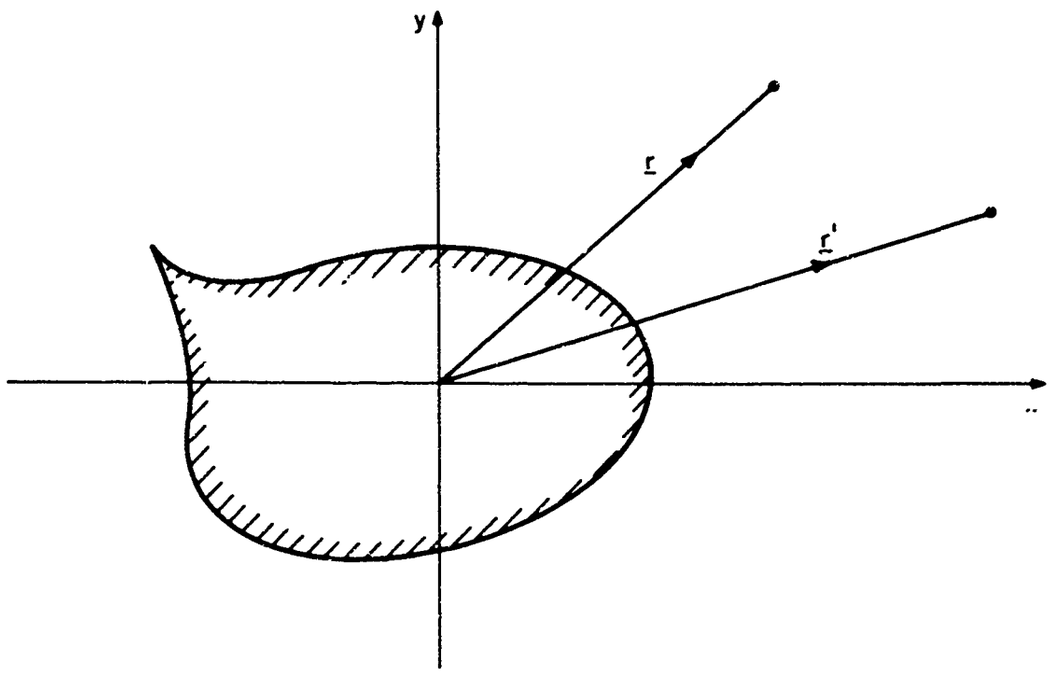

Fig. 1 The geometry of the two-dimensional diffraction problem.

The surrounding anisotropic medium is assumed to be described by a dielectric tensor having the form

$$\hat{\underset{\sim}{\epsilon}} = \underset{\sim}{\epsilon} + \underline{z}_o \underline{z}_o \epsilon_z \tag{2-1a}$$

$$\underset{\sim}{\epsilon} \rightarrow \epsilon_o \begin{pmatrix} \alpha & i\beta \\ -i\beta & \epsilon \end{pmatrix} \tag{2-1b}$$

Initially α, β and ϵ are assumed to be real and positive constants. Later on, analytic continuation into the complex plane will be investigated for some of these elements. In this class of problems, Maxwell's equations have E-mode solutions ($H_x = H_y = 0$) which are excited by magnetic line currents, and H-mode solutions ($E_x = E_y = 0$) which are excited by electric line currents. The fields in the latter category behave essentially as in an isotropic medium[14] and will not be considered further.

For an implied $e^{-i\omega t}$ time dependence, the pertinent field equations are

$$\nabla \times \underline{H} = -i\omega \underset{\sim}{\epsilon} \cdot \underline{E} \tag{2-2a}$$

$$\nabla \times \underline{E} = i\omega\mu_o \underline{H} - \underline{M} \tag{2-2b}$$

With the excitation in the form of a magnetic line current of unit strength

$$\underline{M} = \underline{z}_o \, \delta(x - x') \, \delta(y - y') \tag{2-3a}$$

the magnetic field has the simple form

$$\underline{H} = \underline{z}_o \, H(x, y) \tag{2-3b}$$

where $H(x, y)$ satisfies the wave equation

$$\left(\alpha \frac{\partial^2}{\partial x^2} + \epsilon \frac{\partial^2}{\partial y^2} + k_o^2 \Delta \right) H(x, y) = -i\omega\epsilon_o \Delta \, \delta(x - x') \, \delta(y - y') \tag{2-4}$$

with

$$k_o = \frac{2\pi}{\lambda_o} = \omega\sqrt{\epsilon_o \mu_o} \tag{2-4a}$$

$$\Delta = \alpha\epsilon - \beta^2 = \begin{vmatrix} \alpha & i\beta \\ -i\beta & \epsilon \end{vmatrix} \tag{2-4b}$$

The field components E_x and E_y can be derived from $H(x, y)$ through Eq. (2-2a):

$$E_x = \left(-\epsilon \frac{\partial H}{\partial y} + i\beta \frac{\partial H}{\partial x}\right) \Big/ i\omega\epsilon_o \Delta \tag{2-5a}$$

$$E_y = \left(-i\beta \frac{\partial H}{\partial y} + \alpha \frac{\partial H}{\partial x}\right) \Big/ i\omega\epsilon_o \Delta \tag{2-5b}$$

The boundary conditions to be satisfied by $H(x, y)$ are a radiation condition* at $r \to \infty$ and the vanishing of the tangential component of the electric field on the surface of the perfectly conducting scatterer. If the object has sharp edges as in Fig. 1 the field must also satisfy an edge condition.

The dielectric tensor defined by Eqs. (2-1a, b) represents two cases of particular interest: when $\alpha = \epsilon$ in Eq. (2-1b), the tensor represents a gyrotropic medium. It will be shown in Chapter IV that the ray refractive index for such a medium does not depend on direction (for the two-dimensional class of problems considered here). The only difference between this case and the isotropic case is in the boundary conditions at an interface, as can be seen from Eqs. (2-5a, b).

* Since the medium is anisotropic, the radiation condition requiring the outward flow of energy cannot be phrased simply as the "outgoing wave" condition familiar from isotropic problems. This aspect has received detailed attention elsewhere[5].

When $\beta = 0$ in Eq. (2-1b), the tensor represents a uniaxial medium. Ionized gases subject to a very strong constant magnetic field in the y-direction may be represented (approximately) by such a tensor. The frequency dependence of ϵ in Eq. (2-1b) for such media indicates the possibility that ϵ becomes negative in a certain range of frequencies. If losses due to collisions and other effects are considered, ϵ will be a complex number with $Im\,\epsilon \geq 0$ for the implied time dependence.* Further discussion will be limited mostly to this latter case ($\beta = 0$) as it is the simplest case which displays the anisotropy both in the ray refractive index and the boundary conditions.

It is the object of this study to find solutions of Eq. (2-4) subject to the said boundary conditions for a variety of configurations, to evaluate asymptotic expansions of the solutions at low and high frequencies, and to interpret these in physical terms. Further, the dependence of the solutions on the parameter ϵ (as it is allowed to take on complex values) will be investigated to assure that they remain valid throughout the region of interest, namely $Im\,\epsilon \geq 0$.

Felsen's method of solving Eq. (2-4) in the case $\beta = 0$ is as follows. Define a change of variables

$$\begin{pmatrix} x \\ y \end{pmatrix} = \begin{pmatrix} \sqrt{\alpha} & 0 \\ 0 & \sqrt{\epsilon} \end{pmatrix} \begin{pmatrix} u \\ v \end{pmatrix} , \tag{2-6}$$

which transforms Eq. (2-4) into

$$\left(\frac{\partial^2}{\partial u^2} + \frac{\partial^2}{\partial v^2} + k^2 \right) \hat{H}(u,v) = -i\omega\epsilon_o \sqrt{\alpha\epsilon}\ \delta(u-u')\,\delta(v-v') \tag{2-7}$$

where

$$k = k_o \sqrt{\alpha\epsilon} \tag{2-7a}$$

* In reference (1) the reader may find a detailed discussion of the properties of the dielectric tensor of ionized gases under various conditions.

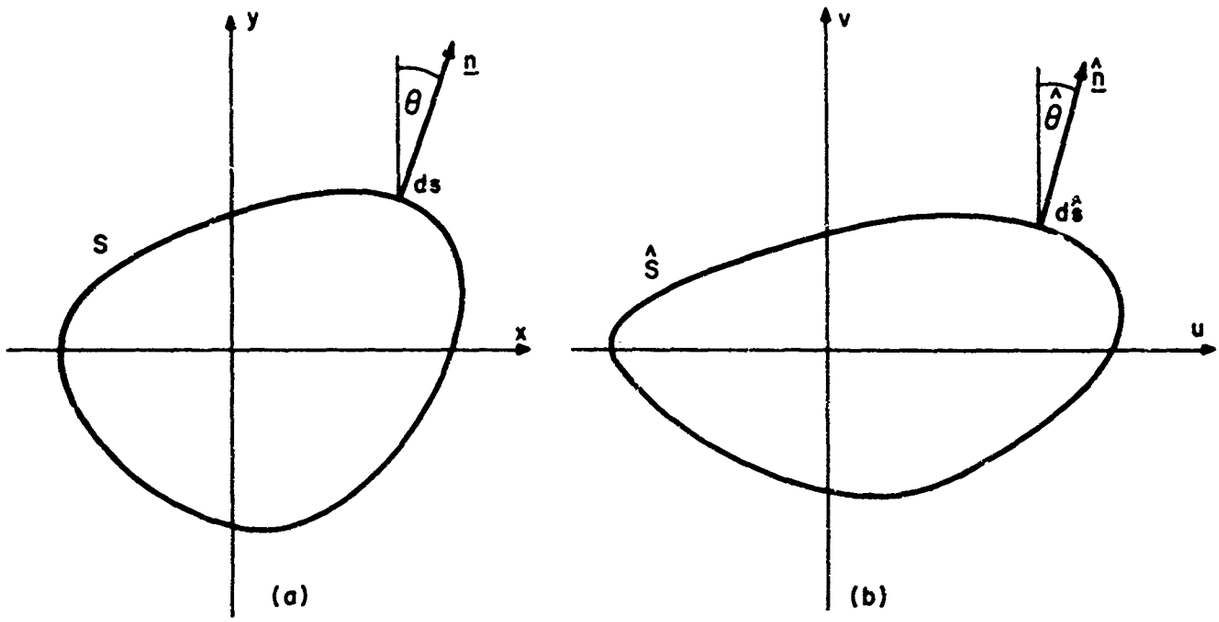

Fig. 2 (a) The real space (x, y).
(b) The transformed space (u, v).

On the surface of a perfect conductor, $\underline{E}_t = 0$, which can be expressed in terms of $\underline{H}$ via Eqs. (2-5)

$$|\underline{n} \times \underline{E}| = E_y \sin\vartheta - E_x \cos\theta = \frac{1}{i\omega\epsilon_o}\left[\frac{\partial H}{\partial x}\,\frac{\sin\theta}{\epsilon} + \frac{\partial H}{\partial y}\,\frac{\cos\vartheta}{\alpha}\right] = 0 \quad \text{on } S \tag{2-8}$$

where $\underline{n}$ is a unit vector normal to S. One notes the relations

$$\frac{\partial H}{\partial x} = \frac{1}{\sqrt{\alpha}} \frac{\partial H}{\partial u} \tag{2-9a}$$

$$\frac{\partial H}{\partial y} = \frac{1}{\sqrt{\epsilon}} \frac{\partial H}{\partial v} \tag{2-9b}$$

$$\sin\theta = \frac{dy}{ds} = \frac{\sqrt{\epsilon}\, dv}{\sqrt{\alpha\, du^2 + \epsilon\, dv^2}} = \frac{\sqrt{\epsilon}\sin\hat{\theta}}{\sqrt{\alpha\cos^2\hat{\theta} + \epsilon\sin^2\hat{\theta}}} \tag{2-9c}$$

$$\cos\theta = \frac{dx}{ds} = \frac{\sqrt{\alpha}\, du}{\sqrt{\alpha\, du^2 + \epsilon\, dv^2}} = \frac{\sqrt{\alpha}\cos\hat{\theta}}{\sqrt{\alpha\cos^2\hat{\theta} + \epsilon\sin^2\hat{\theta}}} \tag{2-9d}$$

with the quantities $\sin\hat{\theta}$ and $\cos\hat{\theta}$ defined as

$$\sin\hat{\theta} = \frac{dv}{\sqrt{du^2 + dv^2}} \tag{2-9e}$$

$$\cos\hat{\theta} = \frac{du}{\sqrt{du^2 + dv^2}} \tag{2-9f}$$

Substitution of Eqs. (2-9 a-d) into Eq. (2-8) yields the condition,

$$\frac{\partial H}{\partial u}\sin\hat{\theta} + \frac{\partial H}{\partial v}\cos\hat{\theta} = \frac{\partial H}{\partial \hat{n}} = 0 \quad \text{on } \hat{S} \quad . \tag{2-10}$$

$\hat{S}$ is given by a function $f(u, v, \epsilon, \alpha) = 0$. It is obtained from the expression of S by means of Eq. (2-6). If α, ϵ are not real and positive $\hat{S}$ does not have the geometrical meaning of a surface in the u-v space. It is seen that the oblique derivative boundary condition in Eq. (2-8) becomes a conventional Neumann type condition in the u-v space (Eq. (2-10)). If arbitrary complex values of α and ϵ are allowed, the derivation of Eqs. (2-7) from (2-4) and Eq. (2-10) from (2-8) does not change. In this case, $\hat{S}$ cannot be drawn as in Fig. 2 (b) because u and v are complex. Also $\hat{\theta}$ as defined by Eqs. (2-9 e, f) becomes

complex. Nevertheless, if a solution is found which satisfies Eq. (2-7) and the boundary condition (2-10) on $\hat{S}$ (which is given now by a function of the complex variables u, v), it will be a solution of Eq. (2-4) with the boundary condition (2-8) on S (which is a real surface) in the x, y space. If such a solution is in the form of an integral or an infinite series, with α, ε appearing as parameters, it will be meaningful only in those regions of α and ε where it is convergent and satisfies the radiation condition. The radiation condition requires radial outflow of energy from the source at distances very large compared to the wavelength. In an anisotropic medium, the wavelength is a function of direction, and the expression $kr = 2\pi \frac{r}{\lambda} >> 1$ should be replaced by $k_o N(\theta) r \gg 1$, where

$$N(\theta) = \frac{\lambda_o}{\lambda(\theta)} = \sqrt{\alpha \cos^2 \theta + \varepsilon \sin^2 \theta} \qquad (2\text{-}11)$$

is defined as the ray refractive index[6][13], and $\lambda(\theta)$ is the wavelength along a radial line from the source, which makes an angle θ with the y axis. Proof of the right hand part of eq. (2-11) will be given in Chapter IV, section B.

Using Eq. (2-11) it is easy to show that $k_o N(\theta) r >> 1$ expressed in the u-v coordinates becomes $k\sqrt{u^2+v^2} >> 1$, which is just the usual requirement in an isotropic medium. Thus the transformed problem comprises Eq. (2-7), subject to a Neumann type boundary condition on $\hat{S}$ and a radiation condition of the usual type. This is a conventional diffraction problem in an isotropic medium characterized by a wavenumber k. If its solution can be found, one may use the inverse transformation of Eq. (2-6) and thus obtain a solution for the original problem in the x-y space. As long as α and ε are real and positive, the physical nature of the origin and transformed configurations is retained, and a solution which is physical in the u-v space will be physical in the x-y space as well, because Eq. (2-6) introduces a change of scale only. If however these parameters are complex or if one is negative real, it has to be shown that solutions obtained in a formal manner via Eq. (2-6) still solve the original physical problem, by checking their convergence and the satisfying of the radiation condition. In the absence of physical boundaries (radiation in infinite space) or in the presence of a perfectly conducting plane boundary, it

has been shown that Felsen's method yields physically meaningful solutions if α, ϵ are restricted to certain regions in the complex plane[2].

CHAPTER III

SCATTERING IN THE LONG WAVE RANGE

A. FORMULATION OF THE PROBLEM OF SCATTERING BY AN ELLIPTIC CYLINDER

In this chapter we solve the problem of scattering by a perfectly conducting elliptic cylinder embedded in a uniaxial medium. The rigorous expression for the Green's function is found by utilizing Felsen's method. An asymptotic expansion is obtained which is useful when the dimensions of the cylinder are small compared to λ_o. For the special case of a narrow ribbon, the terms in the asymptotic solution are identified as multipole radiations in the uniaxial medium.

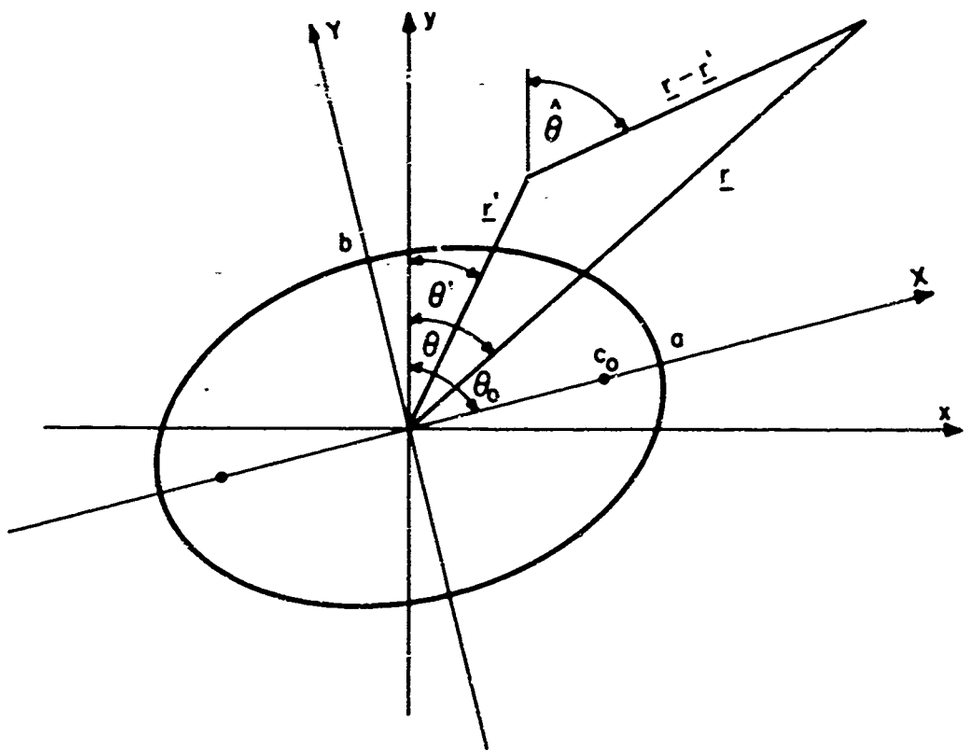

Fig. 3 The geometry of the elliptic cylinder.

It has been shown in Chapter II that all the field components are derivable from a Green's function G which satisfies the equation

$$\left(\frac{\partial^2}{\partial u^2} + \frac{\partial^2}{\partial v^2} + k^2\right) G = -\delta(u-u')\,\delta(v-v') \tag{3-1}$$

subject to the conditions

$$\frac{\partial G}{\partial \hat{r}_n} = 0 \quad \text{on } \hat{S}, \tag{3-1a}$$

Radiation condition at $\sqrt{u^2+v^2} \to \infty$ (3-1b)

The equation for the given surface S in the anisotropic x-y space is

$$\frac{X^2}{a^2} + \frac{Y^2}{b^2} = 1 \tag{3-2a}$$

which may be expressed in terms of u, v by transforming first to the x, y coordinates, and then using Eq. (2-6). The resulting equation for $\hat{S}$ in the u-v space is:

$$A(\theta_o)\,u^2 + B(\theta_o)\,v^2 + 2\,C(\theta_o)\,uv = 1 \tag{3-2b}$$

where

$$A(\theta_o) = \alpha\left(\frac{\sin^2\theta_o}{a^2} + \frac{\cos^2\theta_o}{b^2}\right) \tag{3-2c}$$

$$B(\theta_o) = \varepsilon\left(\frac{\cos^2\theta_o}{a^2} + \frac{\sin^2\theta_o}{b^2}\right) \tag{3-2d}$$

$$C(\theta_o) = \sqrt{\alpha\varepsilon}\,\sin\theta_o\,\cos\theta_o\left(\frac{1}{a^2} - \frac{1}{b^2}\right) \tag{3-2e}$$

In order to have the equation for $\hat{S}$ in a convenient form, one may perform a rotation through an angle δ in the u-v space

$$\begin{pmatrix} u \\ v \end{pmatrix} = \begin{pmatrix} \cos\delta & -\sin\delta \\ \sin\delta & \cos\delta \end{pmatrix} \begin{pmatrix} U \\ V \end{pmatrix} , \tag{3-3}$$

so that the equation for $\hat{S}$ in the U-V space may be written as

$$\begin{aligned} &\left[A(\theta_o)\cos^2\delta + B(\theta_o)\sin^2\delta + 2C(\theta_o)\sin\delta\cos\delta\right] U^2 + \\ + &\left[A(\theta_o)\sin^2\delta + B(\theta_o)\cos^2\delta - 2C(\theta_o)\sin\delta\cos\delta\right] V^2 + \\ +2&\left\{\left[B(\theta_o) - A(\theta_o)\right]\sin\delta\cos\delta + C(\theta_o)(\cos^2\delta - \sin^2\delta)\right\} UV = 1 \end{aligned} \tag{3-4}$$

If one sets the coefficient of UV equal to zero, the angle δ is determined in terms of quantities $a, b, \theta_o, \alpha, \varepsilon$,

$$\tan 2\delta = \frac{2\sqrt{\alpha\varepsilon}\,\sin\theta_o\,\cos\theta_o\left(\frac{1}{a^2} - \frac{1}{b^2}\right)}{\sin^2\theta_o\left(\frac{\alpha}{a^2} - \frac{\varepsilon}{b^2}\right) + \cos^2\theta_o\left(\frac{\alpha}{b^2} - \frac{\varepsilon}{a^2}\right)} \tag{3-5}$$

and the equation for $\hat{S}$ now has the canonical form of an ellipse in the U-V frame;

$$\frac{U^2}{m^2} + \frac{V^2}{n^2} = 1 \tag{3-6}$$

With the help of Eq. (3-5), m and n may be expressed in terms of A, B and C which are defined by Eq. (3-2c, d, e). The results are

$$m = \left\{\frac{1}{2}\left[(A + B) + \sqrt{(A - B)^2 + 4C^2}\right]\right\}^{-1/2} \tag{3-7a}$$

$$n = \left\{\frac{1}{2}\left[(A + B) - \sqrt{(A - B)^2 + 4C^2}\right]\right\}^{-1/2} \tag{3-7b}$$

Some algebraic manipulation shows that for real and positive α and ϵ, m and n (the semi-axes of the ellipse in the U - V space) are real and positive quantities. For complex or negative real values of α and(or) ϵ, U, V become complex variables, and Eq. (3-6) is no longer the equation of a real ellipse. The boundary value problem is now

$$\left(\frac{\partial^2}{\partial U^2} + \frac{\partial^2}{\partial V^2} + k^2\right) G = -\delta(U - U')\,\delta(V - V') \tag{3-8a}$$

$$\frac{\partial G}{\partial \hat{n}} = 0 \quad \text{on} \quad \frac{U^2}{m^2} + \frac{V^2}{n^2} = 1 \tag{3-8b}$$

$$\text{Radiation condition at } k\sqrt{U^2 + V^2} \to \infty \tag{3-8c}$$

B. SOLUTION IN ELLIPTIC CYLINDER COORDINATES

The boundary condition (3-8b) suggests solution of the problem in elliptical cylinder coordinates.

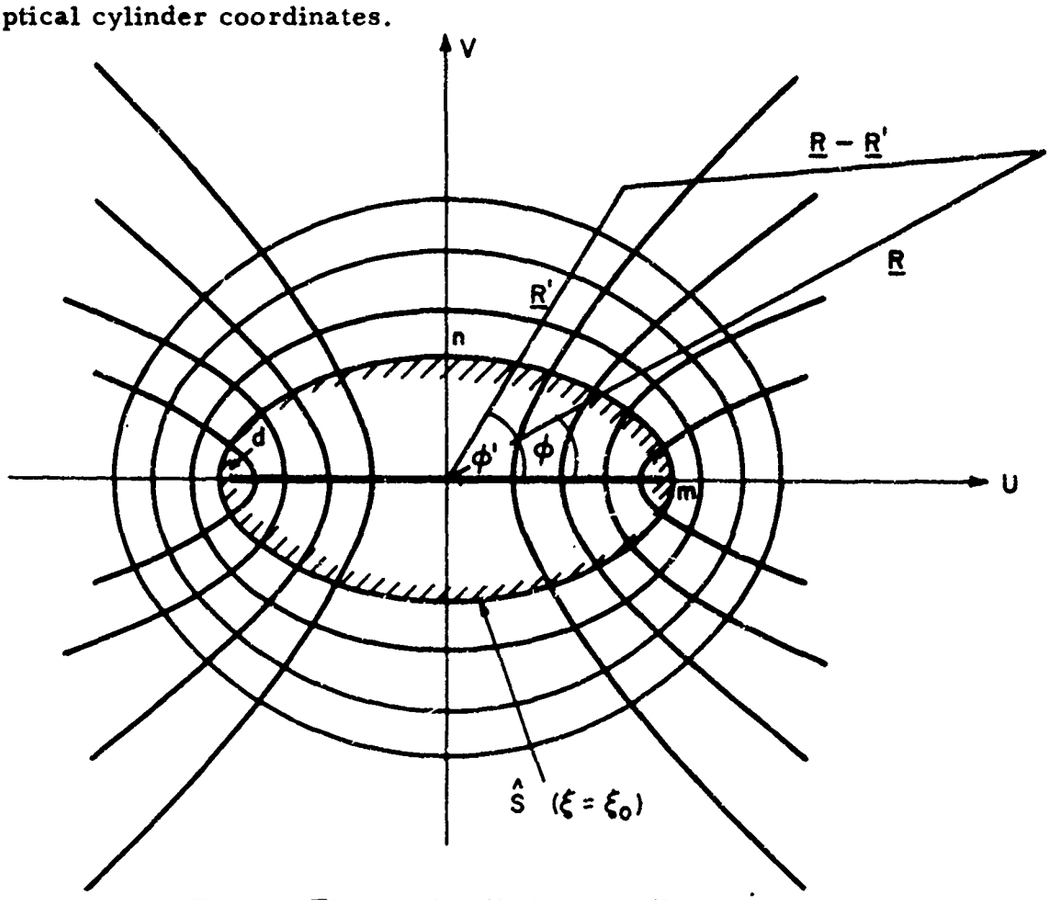

Fig. 4 Elliptical cylinder coordinates.

We introduce the usual coordinates

$$U = d \cosh \xi \cos \eta \tag{3-9a}$$

$$V = d \sinh \xi \sin \eta \tag{3-9b}$$

$$d = \sqrt{m^2 - n^2} \tag{3-9c}$$

whence

$$0 \leq \xi \leq \infty \tag{3-9d}$$

$$0 \leq \eta \leq 2\pi \tag{3-9e}$$

It follows that for $\xi \gg 1$,

$$R = \sqrt{U^2 + V^2} \sim d \cosh \xi \tag{3-9f}$$

$$\varphi = \tan^{-1} \frac{V}{U} \sim \eta \ ; \tag{3-9g}$$

the differential operator in Eq. (3-8a) then becomes:

$$\frac{\partial^2}{\partial U^2} + \frac{\partial^2}{\partial V^2} + k^2 = \frac{\partial^2}{\partial \xi^2} + \frac{\partial^2}{\partial \eta^2} + 2h^2 (\cosh 2\xi - \cos 2\eta) \tag{3-10}$$

where

$$h^2 = \frac{1}{4} k^2 d^2 = \frac{1}{4} k^2 (m^2 - n^2) \tag{3-10a}$$

and the boundary condition (Eq. (3-8b))is

$$\frac{\partial G}{\partial \xi} = 0 \quad \text{on} \quad \xi = \xi_o \quad (*) \ . \tag{3-10b}$$

The solution to Eq. (3-8a) is well known and found in terms of Mathieu functions [8][11]. It has to be periodic in the η variable, which calls for Mathieu functions of the first kind and integral order [9] $ce_m(\eta ; h^2)$,

*) From Eq. (2-9e, f) and (3-9a, b) it is easy to show that the condition given by Eq. (3-10b) is identical with condition (2-10) even for complex α, ε.

$se_m(\eta;h^2)$, or their linear combination $me_m(\eta;h^2)$. The "radial" Mathieu functions[10] $M_m^{(i)}(\xi;h)$ are so defined as to behave like outgoing or incoming waves (or their linear combinations) as $\xi \to \infty$. In terms of these functions the solution to Eqs. (3-8) is

$$G(\xi,\eta;\xi'\eta') = \frac{i}{4}\sum_{m=-\infty}^{\infty} me_m(\eta')\, me_m(-\eta)\, M_m^{(3)}(\xi_>)\cdot$$

$$\cdot\left[M_m^{(1)}(\xi_<) - \frac{M_m'^{(1)}(\xi_o)}{M_m'^{(3)}(\xi_o)}\, M_m^{(3)}(\xi_<)\right] = G_d + G_s \qquad (3\text{-}11)$$

where

$$\xi_> = \begin{cases} \xi \text{ when } \xi > \xi' \\ \xi' \text{ when } \xi' > \xi \end{cases} \qquad (3\text{-}11a)$$

$$\xi_< = \begin{cases} \xi \text{ when } \xi < \xi' \\ \xi' \text{when } \xi' < \xi \end{cases} \qquad (3\text{-}11b)$$

and

$$M_m^{(1)}{}'^{(3)}(\xi_o) = \left.\frac{\partial M_m^{(3)}(\xi;h)}{\partial \xi}\right|_{\xi=\xi_o}; \qquad (3\text{-}11c)$$

the derivation of Eq. (3-11) is given in appendix A.

The first part of Eq. (3-11)

$$G_d = \frac{i}{4}\sum_{m=-\infty}^{\infty} me_m(\eta')\, me_m(-\eta)\, M_m^{(3)}(\xi_>)\, M_m^{(1)}(\xi_<) \qquad (3\text{-}12)$$

is a representation of the primary field, for which a closed form expression

is known[11]*:

$$G_d = \frac{i}{4} H_o^{(1)}(k|\underline{R} - \underline{R}'|) = \frac{i}{4} H_o^{(1)}\left[k\sqrt{(U-U')^2 + (V-V')^2}\right] =$$

$$= \frac{i}{4} H_o^{(1)}\left[k\sqrt{\frac{(x-x')^2}{\alpha} + \frac{(y-y')^2}{\epsilon}}\right] = \frac{i}{4} H_o^{(1)}\left[k_o N(\hat{\theta})\,|\underline{r} - \underline{r}'|\right] \qquad (3\text{-}13)$$

with $\underline{R}, \underline{R}', \varphi$ and φ' defined in Figure 4, $\underline{r}, \underline{r}'$ and $\hat{\theta}$ defined in Figure 3 and $N(\hat{\theta})$ defined by Eq. (2-11). Eq. (3-13) may of course be derived directly by applying Felsen's method to Eq. (2-4) in an unbounded space. This will be done in Chapter IV, section B. The second part G_s of Eq. (3-11) is a representation of the scattered field. It is known[9-12] that this representation may be expanded as a power series in h^2. If $h<<1$ and $\xi_o<<1$, i.e. when the dimensions of the scattering obstacle are small compared to wavelength, this series is rapidly convergent[11-12]. The form of the scattered field G_s becomes quite simple in the "far field" region, i.e. when both source and observation points are located at large distances (compared to wavelength) from the obstacle. Then $h<<1$ and $\cosh\xi>>1$, in which case[10]

$$M_m^{(1)}(\xi) \sim J_m(kR) \qquad (3\text{-}14a)$$

$$M_m^{(3)}(\xi) \sim H_m^{(1)}(kR) \qquad (3\text{-}14b)$$

Because of the rapid convergence of the series expansion of G_s, only a finite number of terms contribute effectively, and it is permissible to replace $H_m^{(1)}(kR)$ by its large argument asymptotic approximation $H_o^{(1)}(kR)\,e^{-im\pi/2}$. Thus G_s is written as

$$G_s \sim \left[\frac{i}{4} H_o^{(1)}(kR)\right]\left[\frac{i}{4} H_o^{(1)}(kR')\right] g(\varphi, \varphi') =$$

$$= \left\{\frac{i}{4} H_o^{(1)}\left[k_o N(\theta) r\right]\right\}\left\{\frac{i}{4} H_o^{(1)}\left[k_o N(\theta') r'\right]\right\}\hat{g}(\theta, \theta') \qquad (3\text{-}15)$$

* There are differences between the definition and notation of Mathieu functions in references (8) and (11). In this study, the notation of reference (8) is used.

where it is understood that the large argument approximations of the Hankel functions are implied (i.e., the result is good to $0(1/\sqrt{kR})$ and $0(1/\sqrt{kR'})$), and where

$$g(\varphi,\varphi') = -4i \sum_{m=-\infty}^{\infty} (-1)^m \, me_m(\eta') \, me_m(-\eta) \, \frac{M_m^{(1)}(\xi_o)}{M_m^{(3)}(\xi_o)} \quad . \tag{3-15a}$$

g may be expanded as a power series in h^2 which, due to the condition $h<<1$, will be rapidly convergent. According to Eq. (3-9g), η and η' in this expansion may be replaced by φ and φ'. All pertinent formulas for this expansion are given in references (9) and (10), and the calculation has been carried out in detail in reference (12). The scattered field, given by Eq. (3-15), has the form of a cylindrical wave radiated from the obstacle, with an amplitude proportional to the incident field at the location of the obstacle and to a "scattering coefficient" $g(\varphi,\varphi')$, which is a function of the geometry of the scatterer and the properties of the medium. The identification of $g(\varphi,\varphi')$ as a superposition of multipole radiations in the given medium will be carried out in the next section for the special case of $\xi_o = 0$, i.e. where the elliptic cylinder reduces to a strip.

C. SCATTERING BY A NARROW STRIP

If the ellipse in Fig. 3 reduces to a strip, then b=0, and $a=c_o$ is its half-width. To find the half-width m of the transformed strip (n=0 in this case), one may use Eqs. (3-2) and (3-7). The calculation is rather involved since one has to determine $\lim_{b\to 0} m(a,b)$ in Eq. (3-7a) in order to obtain the desired result. A more straight-forward approach may be used in this special case. It consists of transforming the end points of the strip, which are $P_1 \equiv (c_o \sin\theta_o, \; c_o \cos\theta_o)$ and $P_2 \equiv (-c_o \sin\theta_o, \; -c_o \cos\theta_o)$ in the xy space, into the uv space via Eq. (2-6). The result will be

$$m = \frac{a\,N(\theta_o)}{\sqrt{\varepsilon\,\alpha}} \tag{3-16}$$

where $N(\theta_o)$ is defined by Eq. (2-11). Eqs. (3-10a) and (3-9a, b) then yield

$$h = \frac{k_o a}{2} N(\theta_o), \tag{3-17a}$$

$$\xi_o = 0 , \tag{3-17b}$$

and the expansion of $g(\varphi,\varphi')$ is performed as follows. Using the relations[9-10]

$$me_m(z;h^2) = \sqrt{2}\ ce_m(z;h^2) \qquad m = 0, 1, 2 \ \ldots \tag{3-18a}$$

$$me_{-m}(z;h^2) = i\sqrt{2}\ se_m(z;h^2) \qquad m = 1, 2, 3 \ \ldots \tag{3-18b}$$

$$M_m^{(i)}(z;h) = Mc_m^{(i)}(z;h) \qquad m = 0, 1, 2 \ \ldots \tag{3-18c}$$

$$M_{-m}^{(i)}(z;h) = (-1)^m Ms_m^{(i)}(z;h) \qquad m = 1, 2, 3 \ \ldots \tag{3-18d}$$

one may write

$$g(\varphi,\varphi') = \sum_{m=1}^{\infty} g_m(\varphi,\varphi') = -4i \sum_{m=1}^{\infty} (-1)^m\ se_m(\eta')\, se_m(-\eta)\ \frac{Ms_m'^{(1)}(0)}{Ms_m'^{(3)}(0)} \tag{3-19}$$

because

$$Mc_m'^{(1)}(0) \equiv 0 \quad \text{for} \quad m = 0, 1, 2 \cdots . \tag{3-19a}$$

Furthermore

$$\frac{Ms_1'^{(i)}(0)}{Ms_1'^{(3)}(0)} = \frac{i\pi}{2} h^2 \left[1 + 0(h^2)\right] \tag{3-20a}$$

$$\frac{Ms_2'^{(1)}(0)}{Ms_2'^{(3)}(0)} = \frac{-i\pi}{16} h^4 \left[1 + 0(h^2)\right] \tag{3-20b}$$

$$se_1(\eta;h^2) = \sin\varphi - \frac{h^2}{2}\sin 3\varphi + 0(h^4) \qquad (3\text{-}20c)$$

$$se_2(\eta;h^2) = \sin 2\varphi - \frac{h^2}{12}\sin 4\varphi + 0(h^4) \quad . \qquad (3\text{-}20d)$$

With Eqs. (3-19), (3-20) and similar expressions for $m>2$ it can be shown that

$$g_m(\varphi,\varphi') = 0\left(\frac{ka}{2}\right)^m$$

The leading term has the form

$$g_1(\varphi,\varphi') = 4\pi h^2 \sin\varphi \sin\varphi' + 0(h^4) \; . \qquad (3\text{-}21)$$

The quantities φ,φ' and h^2 may be expressed in terms of θ,θ', a, etc. Rather than using the general Eqs. (2-6), (3-3), (3-5), (3-7) and (3-10a), one may obtain the result by inspection for the special case under discussion (see Fig. (5)):

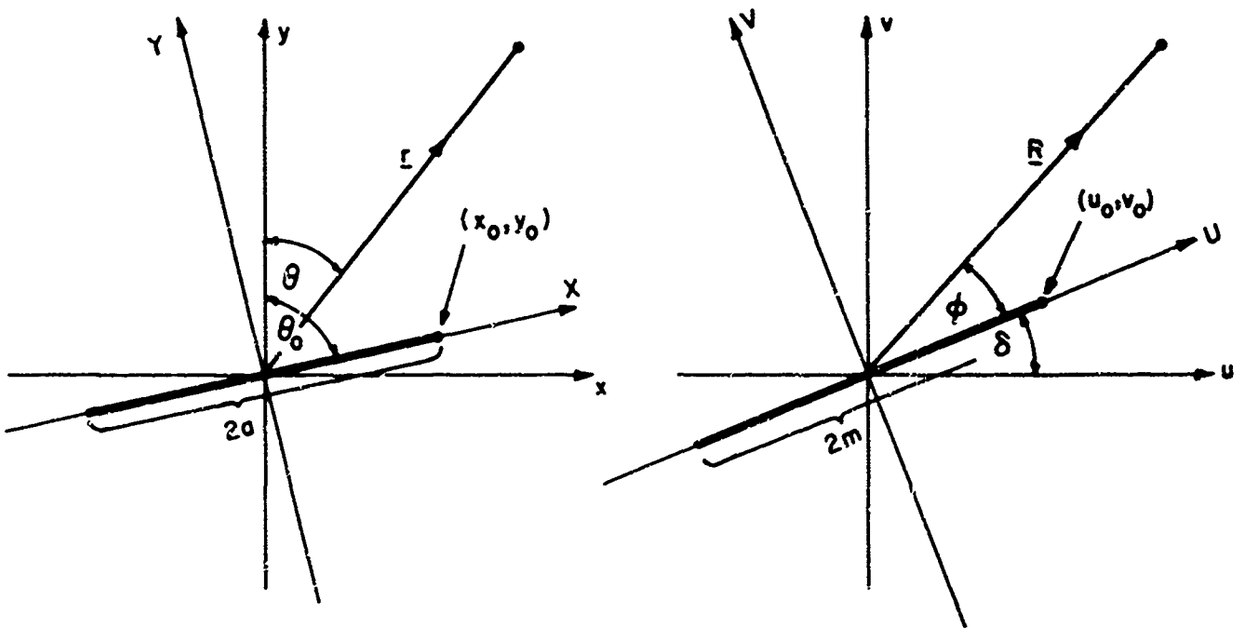

Fig. 5 The conducting strip in the real (x, y) and the transformed (u, v) space.

$$R = \sqrt{U^2 + V^2} = \sqrt{u^2 + v^2} = \sqrt{\frac{x^2}{\alpha} + \frac{y^2}{\epsilon}} = \frac{r\,N(\theta)}{\sqrt{\alpha\epsilon}} \tag{3-22a}$$

$$\sin\delta = \frac{v_o}{\sqrt{u_o^2 + v_o^2}} = \frac{\sqrt{\alpha}\,y_o}{r_o N(\theta_o)} = \frac{\sqrt{\alpha}\cos\theta_o}{N(\theta_o)} \tag{3-22b}$$

$$\cos\delta = \frac{u_o}{\sqrt{u_o^2 + v_o^2}} = \frac{\sqrt{\epsilon}\,x_o}{r_o N(\theta_o)} = \frac{\sqrt{\epsilon}\sin\theta_o}{N(\theta_o)} \tag{3-22c}$$

$$\sin\varphi = \frac{V}{R} = \frac{-u\sin\delta + v\cos\delta}{R} = \frac{-x\cos\theta_o + y\sin\theta_o}{r\,N(\theta)\,N(\theta_o)}\sqrt{\alpha\epsilon} =$$

$$= \frac{-\sin\theta\cos\theta_o + \cos\theta\sin\theta_o}{N(\theta)\,N(\theta_o)}\sqrt{\alpha\epsilon} = \sqrt{\alpha\epsilon}\,\frac{\sin(\theta_o - \theta)}{N(\theta)\,N(\theta_o)} \tag{3-22d}$$

Thus, Eqs. (3-17a), (3-21) and (3-22d) yield

$$g_1(\varphi,\varphi') = \hat{g}_1(\theta,\theta') = \pi(k_o a)^2\,\alpha\epsilon\,\frac{\sin(\theta_o-\theta')}{N(\theta')}\,\frac{\sin(\theta_o-\theta)}{N(\theta)} + O(k_o a)^4 \tag{3-23}$$

One may verify that Eq. (3-23) represents the radiation from an electric dipole line source and find therefrom the polarizability of the strip.

D. ELECTRIC DIPOLE LINE RADIATION, AND THE POLARIZABILITY OF A STRIP

Consider Maxwell's equations

$$\nabla \times \underline{E} = i\omega\mu_o \underline{H} \tag{3-24a}$$

$$\nabla \times \underline{H} = i\omega\,\underline{\underline{\epsilon}} \cdot \underline{E} + \underline{J} \tag{3-24b}$$

with $\underline{\underline{\epsilon}}$ given by Eq. (2-1a), $\underline{H}$ given by Eq. (2-3b) because there is no variation in the z-direction $\left(\frac{\partial}{\partial z} \equiv 0\right)$ and the source term given by

$$\underline{J} = \underline{p}\,\delta(\underline{r}) \tag{3-24c}$$

$$\underline{p} = (\underline{x}_o \sin\theta_o + \underline{y}_o \cos\theta_o)\, p \tag{3-24d}$$

This excitation describes a uniform line distribution of electric dipoles oriented perpendicular to the line axis. From Eqs. (3-24), one may derive the wave equation

$$\left[\alpha \frac{\partial^2}{\partial x^2} + \epsilon \frac{\partial^2}{\partial y^2} + k^2\right] H = \epsilon \frac{\partial J_x}{\partial y} - \alpha \frac{\partial J_y}{\partial x} = A\delta(\underline{r}) , \tag{3-25}$$

where $A = p\left[\epsilon \sin\theta_o \frac{\partial}{\partial y} - \alpha \cos\theta_o \frac{\partial}{\partial x}\right]$ (3-25a)

If we define $H = -AG$, then the equation for G reduces to

$$\alpha \frac{\partial^2 G}{\partial x^2} + \epsilon \frac{\partial^2 G}{\partial y^2} + k^2 G = -\delta(\underline{r}) \tag{3-26}$$

whose solution, subject to a radiation condition at infinity, has already been given by $G_d(\underline{r}, 0)$ in Eq. (3-14). Thus, the solution of Eq. (3-25) is

$$H(\underline{r}) = \frac{i}{4} p\left[\alpha \cos\theta_o \frac{\partial}{\partial x} - \epsilon \sin\theta_o \frac{\partial}{\partial y}\right] H_o^{(1)}\left[k_o\sqrt{\alpha y^2 + \epsilon x^2}\right] =$$

$$= \frac{i}{4} p\, k_o\, \alpha\epsilon \left[\cos\theta_o \frac{x}{\sqrt{\alpha y^2 + \epsilon x^2}} - \sin\theta_o \frac{y}{\sqrt{\alpha y^2 + \epsilon x^2}}\right] H_1^{(1)}\left[k_o\sqrt{\alpha y^2 + \epsilon x^2}\right] =$$

$$= \frac{i}{4} p\, k_o\, \alpha\epsilon \frac{\sin(\theta - \theta_o)}{N(\theta)} H_1^{(1)}\left[k_o\sqrt{\alpha y^2 + \epsilon x^2}\right]$$

For $k_o\sqrt{\alpha y^2 + \epsilon x^2} = k_o r N(\theta) \gg 1$ one may write

$$H_1^{(1)}\left[k_o r N(\theta)\right] \sim -i\, H_o^{(1)}\left[k_o r N(\theta)\right]$$

so that

$$H(\underline{r}) \sim p k_o \alpha \epsilon \frac{\sin(\theta - \theta_o)}{N(\theta)} \left\{ \frac{i}{4} H_o^{(1)} \left[k_o r N(\theta) \right] \right\}, \tag{3-27}$$

comparison of Eqs. (3-15), (3-27) and (3-23) yields

$$p = A_o \left[\pi \frac{(k_o a)^2}{k_o} \frac{\sin(\theta_o - \theta')}{N(\theta')} + O(k_o a)^4 \right] \tag{3-28}$$

where A_o is the intensity of the incident field at the location of the obstacle. Eq. (3-27) shows the leading term in the expansion of the scattered field as an electric dipole term, and Eq. (3-28) gives the intensity of the dipole induced in the strip by the incident field. The first order approximation of the scattering pattern as given by Eq. (3-23) is shown in Fig. 6. A calculation similar to the above for the determination of the quadrupole radiation is given in appendix B.

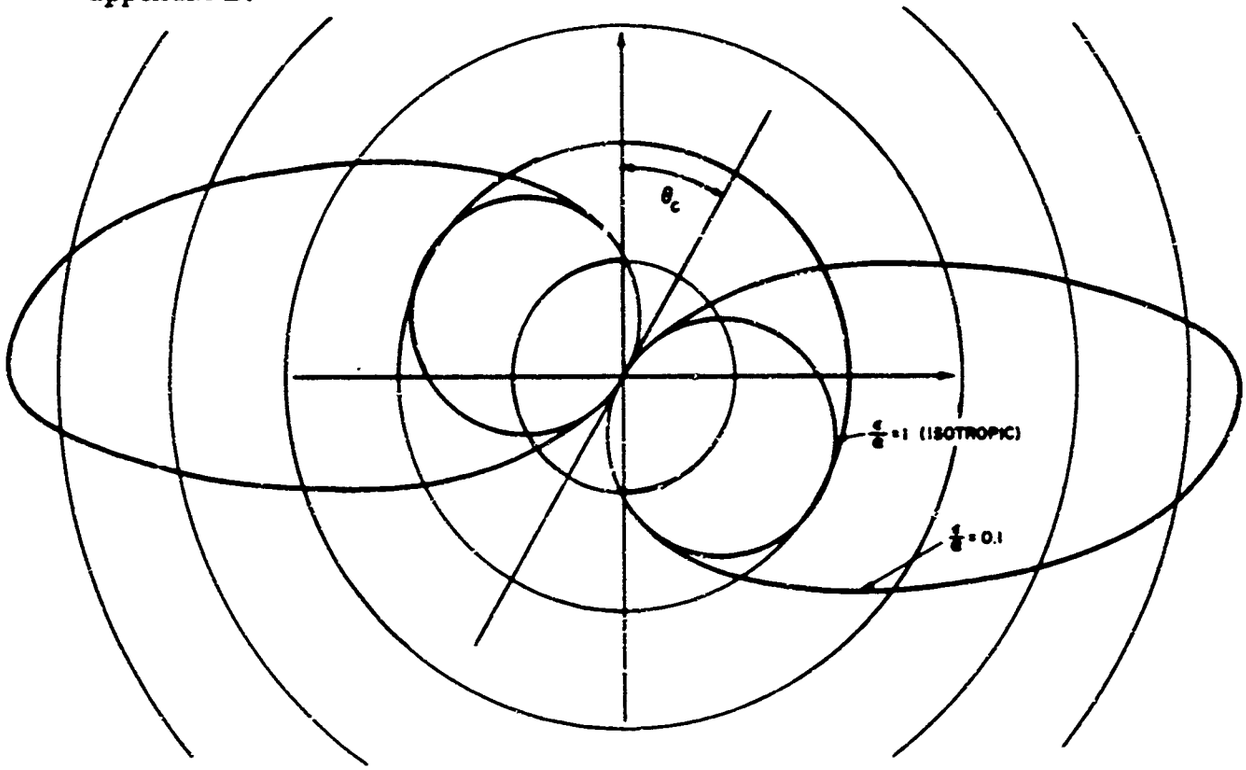

Fig. 6 Dipole radiation: first order approximations of the scattered field.

E. CONCLUDING REMARKS ON LONG-WAVE SCATTERING

The expansion of Eq. (3-19) can be carried out to higher powers of ka (or h). In the same manner as in the preceding section, one may show that the leading term in $g_2(\varphi,\varphi')$ is $O(k_o a)^4$ and its angular pattern is that of a linear electric quadrupole.

If one considers the problem of an elliptic cylindrical scatterer ($b \neq 0$), the leading term in the exapnsion of the scattered field is from the $m = 0$ term in Eq. (3-15a). This respresents an induced "monopole", i.e., an equivalent line source. There will also be two induced dipole terms, one along the major axis and one along the minor axis of the elliptic scatterer, and Eq. (3-28) will e written in dyadic form

$$\underline{p} = \underset{\sim}{P} \cdot \underline{E}$$

where $\underline{E}$ is the incident electric field. The expansion has been performed [12] up to $O(h^6)$. By properly transforming $\sin m\varphi$ and $\cos m\varphi$ (as has been done with $\sin\varphi$ in Eqs. (3-22)), one may find the scattering pattern in the anistropic medium.

For the case where the uniaxial medium represents a plasma in a strong constant magnetic field, a is real and positive, but ϵ may be positive or negative (in the lossless case) or complex with positive imaginary and positive or negative real part (in the lossy case). In the former instance, it is seen from Eq. (2-11) that if $\epsilon < 0$, $N(\theta)$ will be imaginary in that part of space for which

$$\tan\theta > \tan\theta_c = \sqrt{\left|\frac{a}{\epsilon}\right|} \qquad (3\text{-}29)$$

Felsen [7] has shown that if $\mathrm{Im}\ N(\theta) \geq 0$ (for the $e^{-i\omega t}$ time dependence), the expression given by Eq. (3-13) for the field radiated by a line source in an infinite medium (which is identical with G_d of Eq. (3-11)) still satisfies the radiation condition. We may define the square root in Eq. (2-11) to be positive

when real and have a positive imaginary part when complex. This restricts the quotient $\frac{\varepsilon}{\alpha}$ to have a positive imaginary part,

$$\mathrm{Im}(\frac{\varepsilon}{\alpha}) \geq 0 \tag{3-30}$$

It is possible to show that the same condition on $\frac{\varepsilon}{\alpha}$ is necessary for the scattered part G_s of Eq. (3-11) to be convergent and to satisfy the radiation condition. From theorem 1 in section 1.3 of reference (8) one may deduce that the various Mathieu functions and their derivatives, which appear in Eq. (3-11), are analytic functions of h for fixed (possibly complex) arguments. Thus, for fixed $\underline{r}, \underline{r}'$ and ξ_o, G_s is an analytic function of h. It follows, that if the power series expansion of G converges within a certain real interval $-h_o \leq h \leq h_o$, it will converge within the circle $|h| \leq |h_o|$ for complex values of h*. Also (according to reference (8) p. 98) the various formulas for the Mathieu functions of which we make use in this chapter, are valid for arbitrary complex arguments and parameters. Thus Eq. (3-15) is valid even if R, R', φ and φ' are complex. However, in order to satisfy the radiation condition, the inequality (3-30) has to be satisfied, because in (3-15) G_s is seen to be asymptotically proportional to G_d (multiplied by the scattering pattern). The same singularities which appear along the direction θ_c (Eq. (3-29)) in the direct field will appear in the scattered field for negative real $\frac{\varepsilon}{\alpha}$. Eq. (3-28) also shows that the induced dipole (and higher multipoles) would be infinite if $\theta' = \theta_c$, because of the singularity of the incident field along that direction.

The scattering pattern function g (Eq. (3-15)) in isotropic media is a function of the geometry of the scatterer, and its orientation with respect to the directions of incidence θ', and observation θ. Eq. (3-23) shows, that the orientation with respect to the optic axis θ_o is an additional parameter in anisotropic media. Also the ray refractive index in the directions θ and θ' enters explicitly into the expansion of g. The ray refractive index is a property of the anisotropic medium[13], and may be found in more general anisotropic media as well. Therefore the results obtained indicate what properties of the medium enter the expression of the scattering pattern g or the scattering cross-section which is related thereto when the scatterer is embedded in an anisotropic medium.

*See for example chapter 9 in "Advanced Calculus" by W. Kaplan (Addison-Wesley, 1952) for proofs of these statements.

CHAPTER IV

DIFFRACTION IN THE SHORT WAVE RANGE

A. INTRODUCTION

Diffraction by objects of relatively arbitrary shape is known to arise from certain localized regions on the scatterer surface when the obstacle dimensions are large compared to the wave length of the incident radiation. The resulting phenomena are described conveniently in terms of rays which account for diffraction effects in addition to those of reflection and refraction in geometrical optics. For electromagnetic wave propagation in isotropic regions, Keller[3] has presented a ray theory for the construction of the geometric-optical as well as the diffracted field. The theory is based on certain postulates which have been verified in special but representative cases by comparison with the asymptotic representation of rigorous solutions. The purpose of the present investigation is to furnish a similar interpretation when the medium surrounding the obstacle is anisotropic.

A significant difference between propagation in isotropic and anisotropic regions is the distinction in the latter between the directions of propagation of the phase fronts (wave normal direction) and of the energy (ray direction) in a plane wave. Since the fields along a ray are locally those of a plane wave, the laws of reflection of a ray may be deduced from a solution of the corresponding plane wave boundary value problem. Alternatively, these laws may be derived by applying Fermat's principle in a form suited to propagation in anisotropic regions, and this approach is adopted here. The field amplitudes along a reflected ray may be determined from the principle of conservation of energy in a ray tube, thereby permitting the construction of the reflected field by arguments of geometrical optics. Diffraction effects may arise from surface singularities or from the vicinity of the shadow boundary on the obstacle. Two types of representative problems are investigated in this connection: diffraction

by a perfectly conducting half plane, and diffraction by smoothly curved surfaces. In each case, the solution is obtained from the asymptotic evaluation of a rigorous formula and its subsequent interpretation in general ray-optical terms, thereby permitting a generalization to anisotropic regions of the geometrical theory of diffraction[3]. The formulation exhibits explicitly the dependence on the local properties of the medium and the scatterer surface.

As mentioned in Chapter II, the present investigation is restricted to perfectly conducting cylindrical structures excited by axially independent incident fields, and most of the phenomena described pertain to uniaxial anisotropy, with the optic axis of the medium perpendicular to that of the scatterer. The diffraction problem may be reduced by Felsen's method of scaling to an equivalent one in an isotropic region[2], thereby permitting the direct construction of rigorous asymptotic solutions and their ray-optical interpretation. The analytic continuation of the solution from $\arg \epsilon = 0$ to $0 < \arg \epsilon \leq \pi$ is given specific attention. The continuation is justified in detail for the half plane problem and the parabolic cylinder problem, thereby lending an extended range of validity to the results derived by the scaling technique.

B. GEOMETRICAL OPTICS

It is well known that geometrical optics predicts correctly the dominant effects of the electromagnetic field when the wave length tends to zero. The geometric optical field is comprised of the incident (direct), reflected and refracted constituents and its properties are described conveniently in terms of rays. Since the geometric optical field is locally a plane wave field, the reflection and refraction properties of the rays are deducible from those of the corresponding plane waves. Moreover, the local reflection and refraction characteristics of slowly curved interfaces are, in the geometric-optical approximation, the same as for a plane interface tangent at the point of impact of the ray, so that the information extracted from the analysis of plane wave reflection and refraction by a plane interface separating two media suffices for a determination of the initial direction and amplitude along a reflected or

refracted ray. It must be kept in mind that in an anisotropic medium, the ray direction (direction of local energy transport) differs from that of the wave normal (direction of progressing phase fronts), with the relative orientation of the ray and wave normal vectors determined by the medium constants. The utility of the refractive index surfaces for the anisotropic medium in predicting the plane wave (and therefore the ray) propagation, reflection and refraction characteristics has been emphasized elsewhere[2][5][6]. In the present analysis, the ray trajectories are derived from purely ray-optical considerations via Fermat's principle of stationary propagation time, and it is shown that the results so obtained agree with those derived from the previously mentioned plane wave considerations. Since only perfectly conducting surfaces are considered, the analysis involves the direct and reflected rays only.

The pertinent form of Fermat's principle for propagation along a ray path s in an anisotropic medium is (reference 6, p. 289),

$$\delta \int_s N \, dl = 0 \tag{4-1}$$

where N, the ray refractive index, is related to the ordinary refractive index n via $N = n \cos \gamma$, with γ denoting the angle between the ray and the wave normal. Since the ray refractive index determines the propagation speed of the phase front along the direction of the ray, the "stationary time" in Fermat's principle refers to the latter and not to the time of energy transport. The dependence of N on n may also be expressed as (reference 6, p. 253)

$$N = n \cos \gamma \, , \tag{4-2a}$$

$$\tan \gamma = \frac{1}{n(\varphi)} \frac{\partial n(\varphi)}{\partial \varphi} \, , \tag{4-2b}$$

$$\varphi = \theta - \gamma \, , \tag{4-2c}$$

where the presence of a variation of n with direction is indicative of the medium anisotropy. The angles θ and φ measured from the y-axis identify the directions of the ray and wave normal, respectively. (Fig. 7)

For the class of problems considered here the refractive index may be calculated by assuming a plane wave solution of the form

$$H(x,y) = Ae^{i(\zeta x + \varkappa y)} = Ae^{i\underline{k}\cdot\underline{r}} = Ae^{ik_o n\hat{\underline{k}}\cdot\underline{r}}, \tag{4-3}$$

substituting into the homogeneous Eq. (2-4), and determining thereby the plane wave dispersion relation which connects the wave numbers ζ and $\varkappa$:

$$\varkappa^2 = \frac{1}{\epsilon}(k_o^2\Delta - \alpha\zeta^2) \tag{4-4}$$

with Δ defined by Eq. (2-4b). In Eq. (4-3),

$$\underline{k} = \underline{x}_o\zeta + \underline{y}_o\varkappa = k_o n\hat{\underline{k}} \tag{4-5}$$

is the wave normal vector defining the direction of propagation of the phase fronts, $\hat{\underline{k}} = \underline{k}/k$ is a unit vector in the direction of $\underline{k}$, and $\underline{r} = \underline{x}_o x + \underline{y}_o y$ is the position vector. As noted previously, the energy flux vector $\underline{S}$ (which, in a lossless medium, is the time-averaged Poynting vector $\mathrm{Re}\,\underline{E} \times \underline{H}^*$) is inclined with respect to $\underline{k}$ by the angle γ, and the various angles employed subsequently are schematized in Fig. 7. From Eqs. (4-4) and (4-5),

$$n(\varphi) = \frac{\sqrt{\Delta}}{\sqrt{\epsilon\cos^2\varphi + \alpha\sin^2\varphi}} \tag{4-6}$$

and the above-mentioned refractive index diagram is obtained by plotting $n(\varphi)$ vs. φ. If the ray progresses along the θ-direction, with $\tan\theta = x/y$, then $(\zeta x + \varkappa y) = k_o n(\varphi)\hat{\underline{k}}\cdot\underline{r} = k_o r N(\theta)$, and it is not difficult to show from these considerations or from Eqs. (4-2) that

$$N(\theta) = \sqrt{\Delta\left(\frac{1}{\epsilon}\cos^2\theta + \frac{1}{\alpha}\sin^2\theta\right)} \tag{4-7}$$

which reduces to the expression given by Eq. (2-11) when $\theta=0$ in Eq. (2-1b).

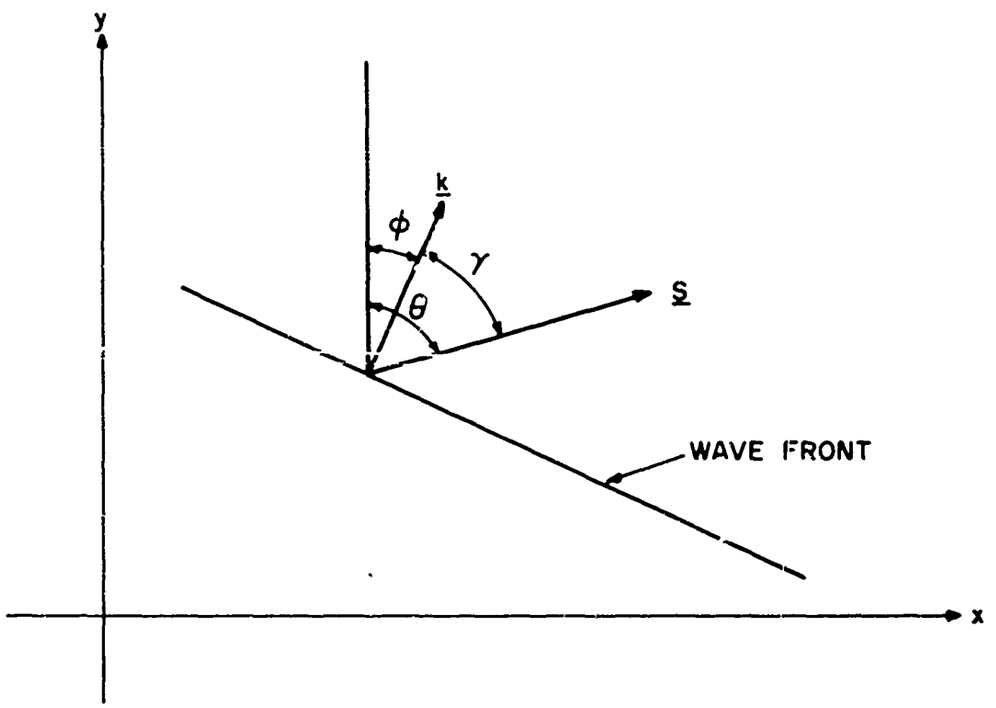

Fig. 7: Plane wave propagation in an anisotropic medium.

It has been mentioned in Chapter II that two special cases arise which are of interest in connection with plasma media subjected to an external steady magnetic field. If the magnetic field is parallel to the z-axis, then $\alpha = \epsilon^{(1)}$ so that both $n(\omega)$ and $N(\vartheta)$ are constant and equal to Δ. The wave equation (2-4) then reduces to the one for an isotropic medium, and the anisotropy manifests itself only through the relations (2-5 a, b) which differ from the isotropic case in view of the non-vanishing ϑ. Since the anisotropic features are caused in this instance primarily by the presence of boundaries rather than by the medium itself, this case is not considered further. Instead, we specialize to the uniaxial situation $\vartheta = 0$, $\alpha = 1$, $\epsilon = 1 - (\omega_p/\omega)^2$, which arises when the external magnetic field is very strong and is oriented along one of the coordinate axes perpendicular to z, say y (ω_p denotes the plasma frequency based on the motion of electrons only, and ω is the frequency of the electromagnetic field). Eq. (4-7) then reduces to

$$N(\theta) = \sqrt{\cos^2\theta + \varepsilon \sin^2\theta} \quad , \quad \theta = 0, \ \alpha = 1 \quad . \tag{4-8}$$

With the ray refractive index specified, the ray trajectories may be calculated from Eq. (4-1). Since the medium is assumed to be homogeneous, the rays proceed along straight lines and it is trivial to determine the direct path from the source to the observation point. If a plane reflecting surface is present as in Fig. 8 inclined at an angle θ_o to the "optic axis" y, then the optical path from point $P(x_1, y_1)$ to point $Q(x_2, y_2)$,

$$L = \int_P^Q N\,dl = \sqrt{(y_1-y)^2 + \varepsilon(x_1-x)^2} + \sqrt{(y-y_2)^2 + \varepsilon(x-x_2)^2} \tag{4-9}$$

must be extremized subject to the constraint that point C on the trajectory lies on the plane.

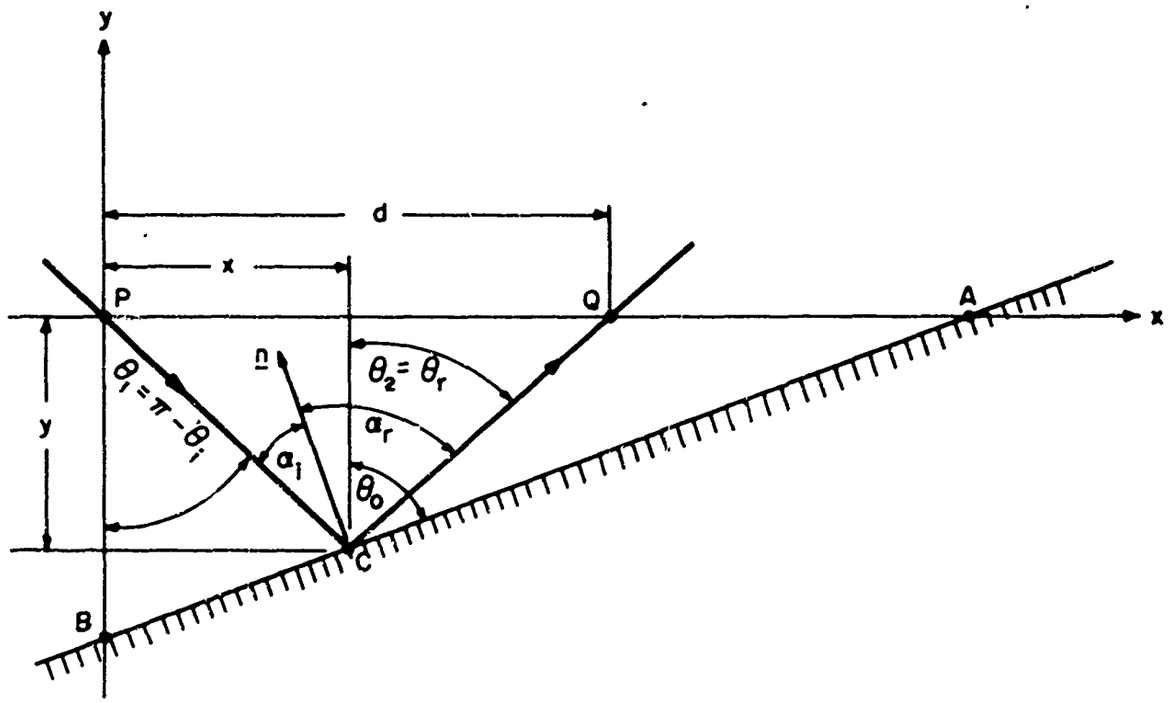

Fig. 8: Reflection of a ray from a perfectly conducting plane in an anisotropic medium.

The details of the calculation are given in Appendix C and the result furnishes a relation between the reflected ray direction θ_r, the incident ray direction θ_i, and the angle θ_o, all angles being measured in the clockwise sense from the y-axis:

$$\tan\theta_r = \frac{-(1-\epsilon\tan^2\theta_o)\tan\theta_i + 2\tan\theta_o}{(1-\epsilon\tan^2\theta_o) + 2\epsilon\tan\theta_o\tan\theta_i} \qquad (4\text{-}10)$$

This formula may be shown to agree with Eq. (10) of reference 15 which was obtained from a solution of the boundary value problem. If all angles are measured from the normal to the plane, the formula becomes instead

$$\tan\alpha_r = \tan\alpha_i + \frac{2A_3(\theta_o)}{A_2(\theta_o)} \qquad (4\text{-}10a)$$

where $A_3(\theta_o)$ and $A_2(\theta_o)$ are defined by Eqs. (4-24), θ_o being the angle between the conducting surface and the optic axis, measured clockwise from this axis. In the isotropic limit $\epsilon = 1$, this expression yields correctly the specular condition $\tan\alpha_r = \tan\alpha_i$. The preceding results may also be applied to a smoothly curved surface since reflection takes place locally as on an infinite tangent plane. With the ray trajectories known, it follows from the definition of the ray refractive index that the phase change over a distance d along a ray directed at an angle ϑ with the y-axis is $k_o\, d\, N(\theta)$. Referring to Fig. 8, for example, the phase increment along the incident ray over the distance $\overline{PC}$ between points P and C is $k_o \overline{PC}\, N(\theta_1)$, while the corresponding quantity along the reflected ray between points C and Q is $k_o \overline{CQ}\, N(\theta_2)$.

Attention may now be given to the field amplitudes along the direct and reflected rays. If the excitation is in the form of a line source of magnetic current located at the point (x', y'), the magnetic field $H(x, y)$ is given by the solution of Eq. (2-4) subject to a radiation condition at infinity. The solution may be constructed by Felsen's method which reduces the differential operator in

Eq. (2-4) to the ordinary Laplacian in the u-v space. The corresponding Green's function is known and may then be transformed back into the x-y frame, with the result (reference 2, Eq. (28):

$$H(x,y) = -\frac{\omega \varepsilon_o \Delta}{4\sqrt{\alpha\varepsilon}} H_o^{(1)}\left\{k_o\sqrt{\Delta\left[\frac{(x-x')^2}{\alpha}+\frac{(y-y')^2}{\varepsilon}\right]}\right\} =$$

$$= -\frac{\omega\varepsilon_o \Delta}{4\sqrt{\alpha\varepsilon}} H_o^{(1)}\left[k_o N(\theta)\,|\underline{r}-\underline{r}'|\right] \qquad (4\text{-}11)$$

which agrees with Eq. (3-13). The energy flux $\underline{S} = \mathrm{Re}(\underline{E} \times \underline{H}^*)$ is calculated from Eqs. (2-5) and (4-11) and yields the asymptotic result (when $k_o N(\theta)\,|\underline{r}-\underline{r}'| \gg 1$),

$$\underline{S} \sim \underline{r}_o \frac{\eta_o}{N(\theta)} |H(x,y)|^2 \quad , \quad \eta_o = \sqrt{\frac{u_o}{\varepsilon_o}} \quad , \qquad (4\text{-}12)$$

thereby confirming the straight-line character of the rays, and showing, in addition, that the rays emanate radially from the source.

While Eqs. (4-11) and (4-12) have been derived here on the assumption that α and ε are positive, it has been shown[2] (for the uniaxial case $\theta=0, \alpha=1,$) that Eq. (4-11) remains valid also for $0 \leq \arg\varepsilon \leq \pi$ provided that the resulting $N(\theta)$ is defined to have a positive imaginary part. The latter requirement is in accord with the radiation condition and assures the decay of the fields at infinity, either due to the presence of dissipation when ε is complex or due to shadow effects when ε is negative real. When $\varepsilon<0$, (for the uniaxial plasma, this occurs when $\omega<\omega_p$) $\underline{S}$ in Eq. (4-12) differs from zero only in those angular regions wherein $N(\theta) = (\cos^2\theta + \varepsilon\sin^2\theta)^{1/2}$ is real. Illumination is therefore confined to a wedge-shaped region centered at the source and surrounding the optic axis. A simple ray-optical description obtains when the Hankel function in Eq. (4-11) can be replaced by its asymptotic form, i.e., when $k_o N(\theta)\,|\underline{r}-\underline{r}'| \gg 1$. While this condition can always be realized for sufficiently large k_o when $N(\theta) \neq 0$, it fails on the shadow boundary $(N(\theta_c) = 0)$. In the transition region surrounding $\theta_c = \tan^{-1}(1/\sqrt{|\varepsilon|})$, one must emploiy the exact formula (4-11).

Away from the transition region surrounding θ_c, the asymptotic form of Eq. (4-11) may be employed to furnish the magnitude of H at a distance R_1 from the source, and the corresponding flux density $\underline{S}_1$ at (x_1, y_1) is then obtained from Eq. (4-12). One may now apply the principle of conservation of energy to a narrow tube of rays to deduce that $\underline{S}_1\, dA_1 = \underline{S}_2\, dA_2$, where dA_1 is the cross-sectional area of the tube at R_1, and dA_2 is the analogous quantity at a distance $R_2 > R_1$ along the ray. For this two-dimensional configuration, $dA_1 = R_1\, d\theta$, $dA_2 = R_2\, d\theta$, so that

$$|H(x_2, y_2)| = |H(x_1, y_1)| \sqrt{\frac{R_1}{R_2}} \quad . \tag{4-13}$$

When an incident ray strikes a smoothly curved surface as in Fig. 9, it gives rise to a reflected ray whose direction may be inferred from the reflection law in Eq. (4-10), with θ_o representing the angle between the optic (y) axis and the tangent to the surface at the point of reflection.

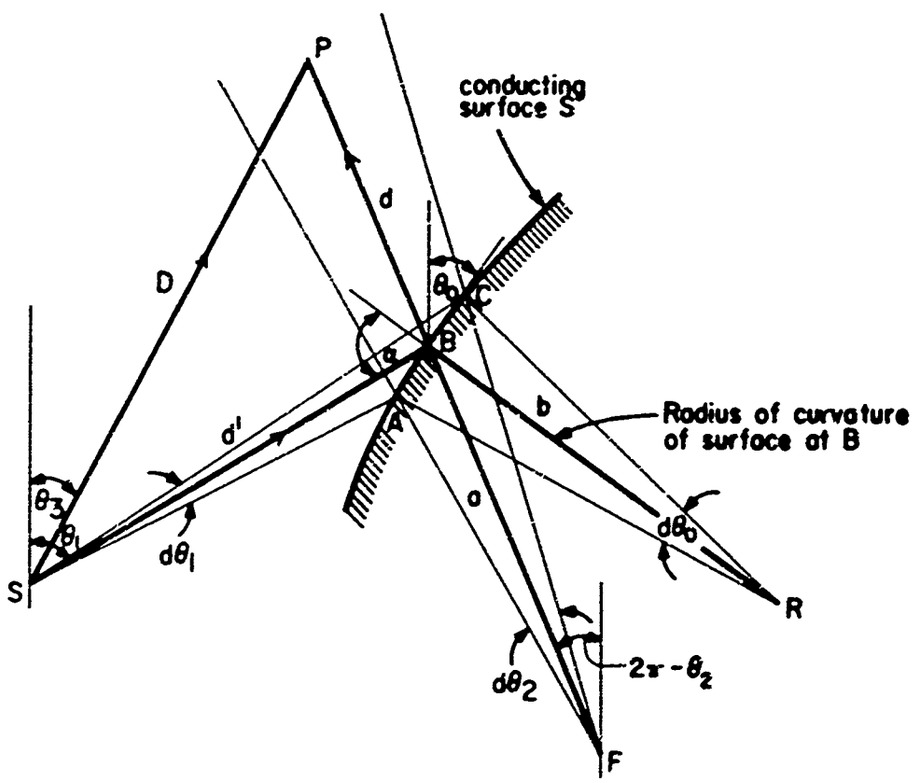

Fig. 9: Geometric-optical construction of the field due to a line source in the presence of a smoothly curved perfectly conducting cylinder.

To determine the reflected ray amplitude, the conservation of energy argument is applied to a narrow tube of reflected rays which appears to emanate from a focus F located at a distance "a" behind the reflecting surface. Upon applying the sine law to the three triangles SAC, FAC and RAC in Fig. 9 one obtains the relations

$$\frac{ds}{d\theta_o} = b \tag{4-14a}$$

$$\frac{ds}{d\theta_1} = \frac{d'}{\sin(\theta_1 - \theta_o)} \tag{4-14b}$$

$$\frac{ds}{d\theta_2} = \frac{ds}{m\,d\theta_1 + n\,d\theta_o} = \frac{a}{\sin(\theta_o - \theta_2)} \tag{4-14c}$$

where we have utilized

$$d\theta_2 = m\,d\theta_1 + n\,d\theta_o \ , \tag{4-14d}$$

and the partial derivatives $m = (\partial\theta_2/\partial\theta_1)$ and $n = (\partial\theta_2/\partial\theta_o)$ can be evaluated from Eq. (4-10); b is the radius of curvature of the cylinder at the reflection point; "a" can now be found as follows:

$$\frac{1}{a} = \frac{m}{d'}\,\frac{\sin(\theta_1 - \theta_o)}{\sin(\theta_o - \theta_2)} + \frac{n}{b}\,\frac{1}{\sin(\theta_o - \theta_2)} \ . \tag{4-15}$$

For the special case of an isotropic medium, $\theta_2 = 2\theta_o - \theta_1$ and Eq. (4-15) reduces tc the known formula (of reference 16, Eq. (3))

$$\frac{1}{a} = \frac{1}{d'} + \frac{2}{b\cos\alpha} \ . \tag{4-15a}$$

(see Fig. 9)

The required geometrical quantities are now determined and we may proceed to the consideration of the power flow in the incident and reflected ray tubes. If

$$H_o = \frac{-\omega \varepsilon_o \sqrt{\varepsilon}}{4} \sqrt{\frac{2}{\pi k_o N(\theta_1)}}\, e^{-i\pi/4} \tag{4-16}$$

denotes the incident field at unit distance from the source (see Eq. (4-11), then the incident field H_i' at the reflection point B in Fig. 9 is given via Eq. (4-13) and the inclusion of the phase change as $H_i' = H_o(d')^{-1/2} \exp(ik_o d' N(\theta_1))$; the associated energy flux in the incident ray tube is

$$S_i\, dA_i = \eta_o |H_o|^2 \left[d' N(\theta_1)\right]^{-1} d' d\theta_1$$

(see Eq. (4-12)). Similarly, if H_r' denotes the reflected magnetic field at B, then the flux in the reflected ray tube at the surface is

$$S_r\, dA_r = \eta_o |H_r'|^2 \left[N(\theta_2)\right]^{-1} a\, d\theta_2 \quad .$$

By conservation of power, $S_r\, dA_r = S_i\, dA_i$, thereby permitting the determination of $|H_r'|$ in terms of $|H_i'|$ and the derivative $(d\theta_1/d\theta_2)$ in Eqs. (4-14 b, c). $|H_r|$ at the observation point P in Fig. 8 is then given by

$$|H_r| = |H_r'| \sqrt{\frac{a}{a+d}}$$

and the phase of H_r differs from that of H_r' by $k_o d N(\theta_2)$. Since the plane wave reflection coefficient for the magnetic field is easily shown to be equal to (+1), no phase change occurs upon reflection, and one finds by combining the various expressions that the reflected field H_r at P due to excitation by a line source at S is given by:

$$H_r = -\frac{\omega \varepsilon_o \sqrt{\varepsilon}}{2\sqrt{2\pi}} \sqrt{\frac{N(\theta_2)\sin(\theta_1 - \theta_o)}{N^2(\theta_1)\sin(\theta_o - \theta_2)}} \cdot$$

$$\cdot \frac{e^{ik_o\left[d_1' N(\theta_1) + d N(\theta_2)\right] - i\pi/4}}{\sqrt{k_o\left[d' + \frac{d m \sin(\theta_1 - \theta_o)}{\sin(\theta_o - \theta_2)} + \frac{d' d n}{b} \frac{1}{\sin(\theta_o - \theta_2)}\right]}} \qquad (4\text{-}17)$$

The incident field H_i over the direct path D from S to P is found from Eqs. (4-16) and (4-13) as:

$$H_i = \frac{-\omega \varepsilon_o \sqrt{\varepsilon}}{2\sqrt{2\pi N(\theta_3) k_o D}} e^{ik_o D N(\theta_3) - i\pi/4} . \qquad (4\text{-}18)$$

The geometric-optical field $H = H_i + H_r$ may be expected to furnish good approximation to the actual high-frequency field in the illuminated region of the smoothly curved scatterer. This statement is verified subsequently from a study of the asymptotic field solution for the special case of a parabolic cylinder.

It may also be shown that the geometrical optics formula in Eq. (4-17) yields the correct result when the medium is taken as isotropic $(N(\theta) = 1)$, or when the reflecting surface is planar $(b = \infty)$. In the former case, the relation between θ_2, θ_1 and θ_o simplifies to $\theta_2 = 2\theta_o - \theta_1$. Upon introducing the angle $\alpha = (\pi/2) - (\theta_1 - \theta_o)$ between the incident ray and the surface normal (see Fig. 9) one may reduce Eq. (4-17) to the known formula [16], [17]

$$H_r = -\frac{\omega \varepsilon_o}{2\sqrt{2\pi}} \frac{e^{ik_o(d' + d) - i\pi/4}}{\sqrt{k_o\left[d + d' + \frac{2d d'}{b \cos\alpha}\right]}} \qquad (4\text{-}19)$$

Alternatively, when $b = \infty$, Eq. (4-17) agrees with the expression for reflection of a cylindrical wave from an infinite plane, which was obtained from a solution

of the wave equation[15]. This statement is verified in Appendix D. Since the latter result was shown to apply as well when $0 \leq \arg \epsilon \leq \pi$, the same range of applicability may be expected from Eq. (4-17) provided that the imaginary part of $N(\theta)$ is restricted to be positive. If $\epsilon < 0$, the radiation emanating from the line source is confined to a wedge shaped region $|\tan \theta_1| < |\tan \theta_c|$ and the simple ray-optical description fails at the shadow boundaries $|\tan \theta_1| = \tan \theta_c$, thereby necessitating use of the exact formula (4-11). Analogous considerations are valid for the reflected field which is also confined to the angular interval $|\tan \theta_2| < |\tan \theta_c|$; since the reflected field appears to come from an image source, it is to be expected that its value near the shadow boundary $|\tan \theta_2| = \tan \theta_c$ may be obtained by retention of the Hankel function in (4-11) with the appropriate argument.

C. DIFFRACTION BY A STRAIGHT EDGE

The geometric-optical solution constructed in the preceding section may be expected to yield the dominant contribution in the illuminated region of the obstacle, but it yields no information about diffraction effects which modify the field in this region and also account for field penetration into the shadow zone. Diffraction phenomena arise when the surface contains singularities such as edges or corners, and also from the vicinity of the shadow boundary on a smoothly curved object. A prototype structure for the study of edge effects, a perfectly conducting half plane, is investigated in this Section. When the medium is uniaxial ($\beta = 0$, $\alpha = 1$ in Eq. (2-1b)), the previously mentioned method of scaling may be employed to reduce the problem of scattering by perfectly conducting cylindrical surfaces in the anisotropic medium to equivalent conventional problems in an isotropic region.[2] The latter configuration is a real one when ϵ is positive real, but loses its physical significance for other values of ϵ. In utilizing the auxiliary isotropic space, it is therefore necessary to construct the solution for $\epsilon > 0$ and to seek an extended range of validity by analytic continuation.

The problem of diffraction by a perfectly conducting half plane in a

uniaxially anisotropic region has already been treated from this viewpoint[2] and the solution has been given in a form analogous to that derived first by MacDonald.[18] In this representation, it is convenient to employ angles which delimit the various ray-optical domains; while the interpretation is unambiguous when $\epsilon > 0$, it is not clear how to effect the continuation into the range of complex or negative real ϵ since the angles then become complex.

To clarify the picture, an alternative analysis has been carried out wherein distances rather than angles are employed throughout. The problem has been solved directly by the Wiener-Hopf technique without the intervention of the scaling argument, and the solution cast into a form which facilitates the analytic continuation. The same basic representation may also be obtained when Felsen's method is applied judiciously to the Wiener-Hopf solution in an isotropic medium[4]. This approach has been adopted elsewhere[19], and serves as a check on the correctness of the direct approach.

The physical configuration is shown in Fig. 10, with the half plane occupying the negative X axis, and the optic axis in the medium oriented along y.

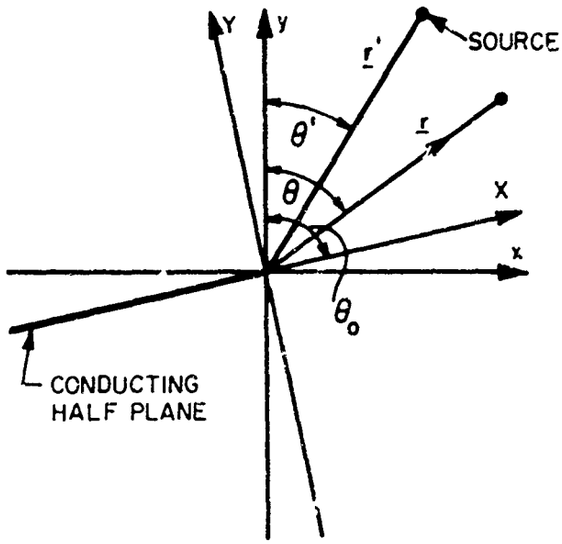

Fig. 10: Coordinate designation for the half-plane diffraction problem.

Since $\alpha = 1$, $\beta = 0$, Eq. (2-4) reduces to

$$\left(\frac{\partial^2}{\partial x^2} + \varepsilon \frac{\partial^2}{\partial y^2} + k_o^2 \varepsilon\right) H(x, y) = - i\omega\varepsilon_o \varepsilon \, \delta(x-x') \, \delta(y-y') \qquad (4\text{-}20a)$$

The boundary conditions are:

$$|\underline{n} \times \underline{E}| = \frac{\partial H}{\partial x} \cos\theta_o - \frac{\partial H}{\partial y} \varepsilon \sin\theta_o = 0 \quad \text{on } S \qquad (4\text{-}20b)$$

Radiation condition at $r \to \infty$ (4-20c)

Edge condition* at $r \to 0$ (4-20d)

The physical configuration indicates that a transformation to the X-Y coordinate system will simplify the task of solving Eqs. (4-20). Applying the transformation

$$\begin{pmatrix} x \\ y \end{pmatrix} = \begin{pmatrix} \sin\theta_o & -\cos\theta_o \\ \cos\theta_o & \sin\theta_o \end{pmatrix} \begin{pmatrix} X \\ Y \end{pmatrix} \qquad (4\text{-}21)$$

to Eqs. (4-20 a, b) yields:

$$\left[A_1(\theta_o)\frac{\partial^2}{\partial x^2} + A_2(\theta_o)\frac{\partial^2}{\partial Y^2} + 2A_3(\theta_o)\frac{\partial^2}{\partial X \partial Y} + k^2\right] H(X, Y) \equiv L^{(2)} H =$$

$$= - i\omega\varepsilon_o\varepsilon \, \delta(X-X') \, \delta(Y-Y') \qquad (4\text{-}22a)$$

*The edge condition, which is necessary for making the solution unique, is a limit on the allowable singularities of the field components near the edge. The singularities must be such that the average stored electromagnetic energy in a finite volume surrounding the edge will be finite. In our case, the energy density is $W = \frac{1}{4}\left[\underline{E}^* \cdot \frac{\partial}{\partial\omega}(\omega\underline{\varepsilon}) \cdot \underline{E} + \mu_o |H|^2\right]$. The components of $\underline{E}$ are derivable from H via Eqs. (2-5), thus the condition $\int_0^{2\pi}\int_0^{R} W(r, \theta) dr \, d\theta < \infty$ sets an upper limit on the growth of H as $r \to 0$. In the process of solving the problem (Appendix E) this is a crucial point.

$$\left[A_2(\theta_o)\frac{\partial}{\partial Y} + A_3(\theta_o)\frac{\partial}{\partial X}\right] H(X,Y) \equiv L^{(1)} H = 0 \quad \text{on} \quad \begin{cases} Y = 0 \\ -\infty < X \leq \infty \end{cases} \tag{4-22b}$$

The radiation and edge conditions remain unchanged, because

$$r = \sqrt{x^2 + y^2} = \sqrt{X^2 + Y^2} \ . \tag{4-23}$$

In Eqs. (4-22)

$$A_1(w) = \sin^2 w + \epsilon \cos^2 w \tag{4-24a}$$

$$A_2(w) = \cos^2 w + \epsilon \sin^2 w = \left[N(w)\right]^2 \tag{4-24b}$$

$$A_3(w) = (\epsilon - 1) \sin w \cos w \tag{4-24c}$$

$$k^2 = k_o^2 \epsilon \tag{4-24d}$$

The solution of Eqs. (4-22) proceeds in two steps. First, plane wave excitation is considered, i.e. $X' \to \infty$, $Y' \to \infty$ and $X'/Y' = \tan\theta'$. From the solution of that problem, the solution for line source excitation (finite X' and Y') may be synthesized. In both cases the total field H is decomposed into incident and scattered parts (H_i and H_s respectively)

$$H = H_i + H_s \tag{4-25a}$$

or

$$\varphi = \frac{H}{i\omega\epsilon_o\epsilon} = \varphi_i + \varphi_s \quad * \tag{4-25b}$$

In the case of line source excitation, φ_i is a cylindrical wave (Eqs. (3-13) and (4-11)). By letting $\underline{r}' \to \infty$ along a direction θ', while normalizing the amplitude to unity, the cylindrical wave becomes a plane wave whose ray (energy transport) direction is along θ':

---

* φ here denotes a wave function and should not be confused with the same symbol employed for angles in other Chapters.

$$\varphi_i = \exp\left[-ik_o(B_2 X + B_3 Y)\right] \tag{4-26}$$

with

$$B_2 = \frac{1}{N(\theta')}\left[\varepsilon \sin\theta_o \sin\theta' + \cos\theta_o \cos\theta'\right] \tag{4-26a}$$

$$B_3 = \frac{1}{N(\theta')}\left[\sin\theta_o \cos\theta' - \varepsilon \cos\theta_o \sin\theta'\right] \quad . \tag{4-26b}$$

In this case, φ must satisfy Eq. (4-22a) with the inhomogeneous term set equal to zero, and the boundary conditions Eqs. (4-22b) and (4-20 c, d). From Eqs. (4-22) and (4-25) one may formulate the boundary value problem for the scattered part of the field φ_s:

$$L^{(2)}\varphi_s = 0 \tag{4-27a}$$

$$L^{(1)}\varphi_s = -L^{(1)}\varphi_i \quad \text{on} \quad S \tag{4-27b}$$

By using Eqs. (4-24) and (4-26), Eq. (4-27b) may be written explicitly as:

$$L^{(1)}\varphi_s = ik_o\left[A_3(\theta_o)B_2 + A_2(\theta_o)B_3\right]\exp\left[-ik_o B_2 X\right] =$$

$$= \frac{ik_o \varepsilon \sin(\theta_o - \theta')}{N(\theta')} \exp\left[-ik_o B_2 X\right] \text{ on } \begin{cases} Y = 0 \\ -\infty < X \leq 0 \end{cases} \tag{4-27c}$$

The following Fourier transforms are now defined:

$$\Phi(\alpha, Y) = \Phi_+(\alpha, Y) + \Phi_-(\alpha, Y) = \frac{1}{\sqrt{2\pi}} \int_{-\infty}^{\infty} \varphi(X, Y)\, e^{i\alpha X}\, dX \tag{4-28a}$$

where

$$\Phi_+(\alpha, Y) = \frac{1}{\sqrt{2\pi}} \int_{0}^{\infty} \varphi(X, Y)\, e^{i\alpha X}\, dX \tag{4-28b}$$

$$\Phi_{-}(\alpha, Y) = \frac{1}{\sqrt{2\pi}} \int_{-\infty}^{0} \varphi(X, Y)\, e^{i\alpha X}\, dX \qquad (4\text{-}28c)$$

$$\varphi(X, Y) = \frac{1}{\sqrt{2\pi}} \int_{-\infty}^{\infty} \Phi(\alpha, Y)\, e^{-i\alpha X} d\alpha \qquad (4\text{-}28d)$$

Application of Eq. (4-28a) to Eq. (4-27a) yields*

$$A_2 \frac{d^2\Phi_s}{dY^2} - 2i\alpha A_3 \frac{d\Phi_s}{dY} + \left(k^2 - \alpha^2 A_1\right) \Phi_s = 0 \ . \qquad (4\text{-}29)$$

After assuming

$$\Phi_s(\alpha, Y) = I(\alpha)\, e^{iqY} \ , \qquad (4\text{-}30)$$

substitution into Eq. (4-29) leads to the quadratic equation

$$q^2 - 2\alpha \frac{A_3}{A_2} q + \frac{\alpha^2 A_1 - k^2}{A_2} = 0 \ , \qquad (4\text{-}31)$$

the solutions of which yield the dispersion relation

$$q_{1,2}(\alpha) = \alpha \frac{A_3}{A_2} \pm \sqrt{\frac{\epsilon}{A_2}\left(k_o^2 - \frac{\alpha^2}{A_2}\right)} \qquad (4\text{-}32)$$

The function $\sqrt{\frac{\epsilon}{A_2}\left(k_o^2 - \frac{\alpha^2}{A_2}\right)}$ is double valued. We choose that value for which the square root is positive when real, and has a positive imaginary part when complex.

*In the following discussion $A_1(\theta_o)$, $A_2(\theta_o)$ and $A_3(\theta_o)$ will be written simply as A_1, A_2 and A_3 respectively. The argument will be written explicitly only when it is different from θ_o.

The corresponding choice of q_1 (upper sign) or q_2 (lower sign) is discussed in reference (15)*. In order that φ_s satisfy the radiation condition, it is shown that one has to choose

$$\phi_s(\alpha, Y) = I_1(\alpha)\, e^{iq_1 Y} \qquad \text{for } Y > 0 \ , \tag{4-33a}$$

$$\phi_s(\alpha, Y) = I_2(\alpha)\, e^{iq_2 Y} \qquad \text{for } Y < 0 \ , \tag{4-33b}$$

the relation between $I_1(\alpha)$ and $I_2(\alpha)$ is determined from the fact that along $Y = 0$, the tangential component of the electric field is continuous: i.e. both $L^{(1)}\varphi$ and $L^{(1)}\varphi_i$ are continuous at $Y = 0$, which implies that $L^{(1)}\varphi_s$ is continuous along $Y = 0$. Thus, from Eqs. (4-33) and (4-28d) one gets

$$\left[A_2 q_1(\alpha) - A_3 \alpha\right] I_1(\alpha) = \left[A_2 q_2(\alpha) - A_3 \alpha\right] I_2(\alpha)$$

which, upon use of Eq. (4-32), yields the relation

$$I_1(\alpha) = - I_2(\alpha) \ .$$

Therefore

$$\phi_s(\alpha, Y) = \pm\, I(\alpha)\, e^{iq_{1,2}(\alpha) Y} \qquad \text{for } Y \lesseqgtr 0 \tag{4-34}$$

The determination of $I(\alpha)$ by means of the Wiener-Hopf technique proceeds as in reference (4). (Details are given in Appendix E). The result is

$$I(\alpha) = \sqrt{\frac{k_o}{2}\left[1 - \frac{B_2}{N(\theta_o)}\right]}\ \frac{1}{(\alpha - k_o B_2)\sqrt{\frac{\alpha}{N(\theta_o)} - k_o}} \tag{4-35}$$

* The reader is cautioned to note the slightly different definitions of A_1, A_2, A_3 and $q_{1,2}$ in reference (15).

from which, via Eq. (4-28d),

$$\varphi_s(X,Y) = \frac{\pm 1}{2\pi}\sqrt{k_o\left[1-\frac{B_2}{N(\theta_o)}\right]}\int_{-\infty}^{\infty}\frac{d\alpha\exp\left[-i\alpha X+iq_{1,2}(\alpha)Y\right]}{(\alpha-k_oB_2)\sqrt{\frac{\alpha}{N(\theta_o)}-k_o}}\,,\ Y\gtrless 0\,. \quad (4\text{-}36)$$

Eq. (4-36) is an exact solution to our diffraction problem. It should be noted that it has been derived by assuming ϵ to be real and positive. Next, we investigate the behavior of the integral in Eq. (4-36) when ϵ is complex.

The integrand in Eq. (4-36) has branch points at $\alpha = \pm k_o N(\theta_o)$ which, for real and positive ϵ, lie on the real axis of the complex α plane. The branch cuts are chosen in such a way that on the entire upper Riemann sheet of the double valued function $\sqrt{\frac{\epsilon}{A_2}\left(k_o^2-\frac{\alpha^2}{A_2}\right)}$, the imaginary part of the square root is positive. The integration path shown in Fig. 11 lies entirely on the upper Riemann sheet.

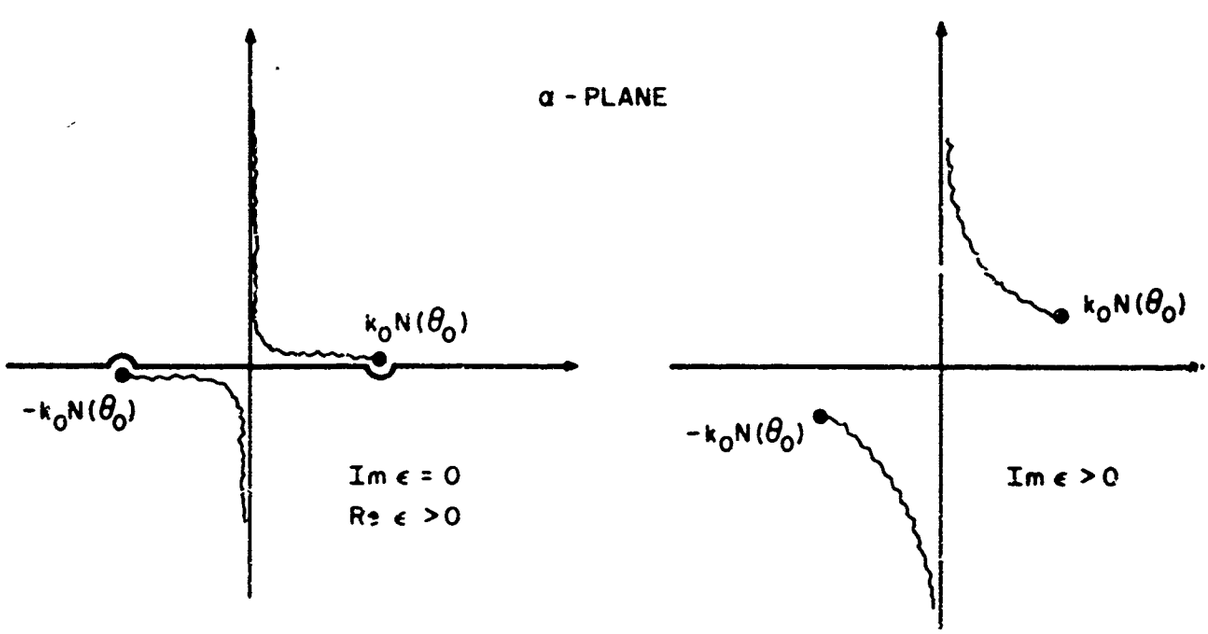

Fig. 11: The path of integration in the complex α plane
a) ϵ real and positive
b) ϵ complex, Im $\epsilon > 0$

When ε is complex, $N(\vartheta_o)$ will be complex. In Chapter III, it was shown that in order to satisfy the radiation condition, N has to be positive when real and Im N positive when N is complex. This condition is satisfied when

$$0 \leq \arg \varepsilon \leq \pi \tag{4-37}$$

(see Eq. (3-30)). The branch points then move into the first and third quadrant as in Fig. 11(b), and will not interfere with the integration path. Uniform convergence of the integral in Eq. (4-36) is assured if as $\alpha \to \pm\infty$,

$$\mathrm{Re}\left[i q_{1,2}(\alpha) Y \right] \leq 0 , \quad Y \gtrless 0 , \tag{4-38}$$

which condition is seen to be equivalent to

$$\mathrm{Im} \frac{i\sqrt{\varepsilon} \pm A_3(\vartheta_o)}{A_2(\vartheta_o)} \geq 0 . \tag{4-39}$$

With

$$\varepsilon = |\varepsilon| e^{i\psi} , \tag{4-40}$$

and using Eqs. (4-24), condition (4-39) becomes

$$\sqrt{|\varepsilon|} \cos\frac{\psi}{2}\left(\cos^2\vartheta_o + |\varepsilon| \sin^2\vartheta_o \pm 2\sqrt{|\varepsilon|}\cos\theta_o \sin\theta_o \sin\frac{\psi}{2}\right) \geq 0 \tag{4-41}$$

which inequality is satisfied for any ϑ_o and ε satisfying Eq. (4-37). One may check independently that the individual plane waves, and therefore the total solution, satisfy the power radiation condition when $\varepsilon < 0$ (see reference 15). Since the other characteristics of the solution are not affected by letting ε take on the range of values mentioned above, Eq. (4-36) remains valid when $\varepsilon < 0$.

The ray-optical feature of this result may now be determined from an asymptotic evaluation, the details of which are given in Appendix F, for positive or negative real ε. The method of steepest descent is used, and it is shown that there are two contributions to the asymptotic result, one from a saddle point which we denote by ϑ_c and one from a pole which we denote by ϑ_g:

$$\varphi_s = \varphi_c + \varphi_g \tag{4-42}$$

It is also shown that φ_g exists only in certain regions of space which are determined by the relative position of the pole and the saddle point. One finds that φ_g is that part of the solution which could have been found by geometrical optics; it consists of the geometrically reflected field (obeying the reflection law in Eq. (4-10)) and another part which cancels the incident field in the region of the geometrical shadow. φ_c exists throughout space, and is given by

$$\varphi_c \sim f(w_s)\sqrt{\frac{2}{\pi k_o r N(\vartheta)}}\, e^{i k_o r N(\vartheta) - i\frac{\pi}{4}} \tag{4-43a}$$

where

$$f(w_s) = \frac{1}{2}\,\frac{\sqrt{1-\dfrac{\varepsilon \sin\theta_o \sin\theta' + \cos\theta_o \cos\theta'}{N(\theta_o)\,N(\theta')}}\sqrt{1-\dfrac{\varepsilon \sin\theta_o \sin\theta + \cos\theta_o \cos\theta}{N(\theta_o)\,N(\theta)}}}{\dfrac{\varepsilon \sin\theta_o \sin\theta' + \cos\theta_o \cos\theta'}{N(\theta_o)\,N(\theta')} + \dfrac{\varepsilon \sin\theta_o \sin\theta + \cos\theta_o \cos\theta}{N(\theta_o)\,N(\theta)}} \tag{4-43b}$$

For $\varepsilon = 1$ (isotropic medium) this formula reduces to that of Sommerfeld[20]

$$f(w_s)\Big|_{\varepsilon = 1} = \frac{2 \sin\dfrac{\vartheta_o - \theta'}{2}\, \sin\dfrac{\vartheta_o - \vartheta}{2}}{\cos(\vartheta_o - \vartheta') + \cos(\vartheta_o - \vartheta)} \tag{4-43c}$$

Eq. (4-43a) is not valid in the neighborhood of the poles of $f(w_s)$. Physically these poles correspond to observation point locations on a boundary between geometrically illuminated and shadow regions (see Fig. 12). For evaluating the field in these transition zones, a more elaborate calculation of (4-36) is necessary[20] which yields a result in terms of Fresnel integrals. It is found that the denominator of $f(w_s)$, Eq. (4-43b), vanishes at two angles:

$$\theta_1 = \theta' \pm \pi \tag{4-44a}$$

$$\theta_2 = \tan^{-1}\left[\frac{-(1-\varepsilon\tan^2\theta_o)\tan\theta' + 2\tan\theta_o}{(1-\varepsilon\tan^2\theta_o) + 2\varepsilon\tan\theta_o\tan\theta'}\right] \qquad (4\text{-}44b)$$

A comparison of Eqs. (4-44b) and (4-10) discloses that θ_2 is precisely the angle of the limiting reflected ray corresponding to rays incident from the direction θ' (Fig. 12), while θ_1 describes the geometrical shadow boundary. It has therefore been confirmed that the asymptotic field solution in the exterior of transition regions may be represented in simple ray-optical terms. The geometrical optics field is constructed in accord with the discussion in Section B of this chapter, whereas the edge gives rise to a diffracted field which may be interpreted in terms of diffracted rays (cf. reference 3). The diffracted rays progress radially outward from the edge and therefore have a radial dependence as given by the factors multiplying $f(w_s)$ in Eq. (4-43a)(see also Eq. (4-16) et. seq.), while $f(w_s)$ represents the "diffraction coefficient" which yields the starting amplitude of the ray.

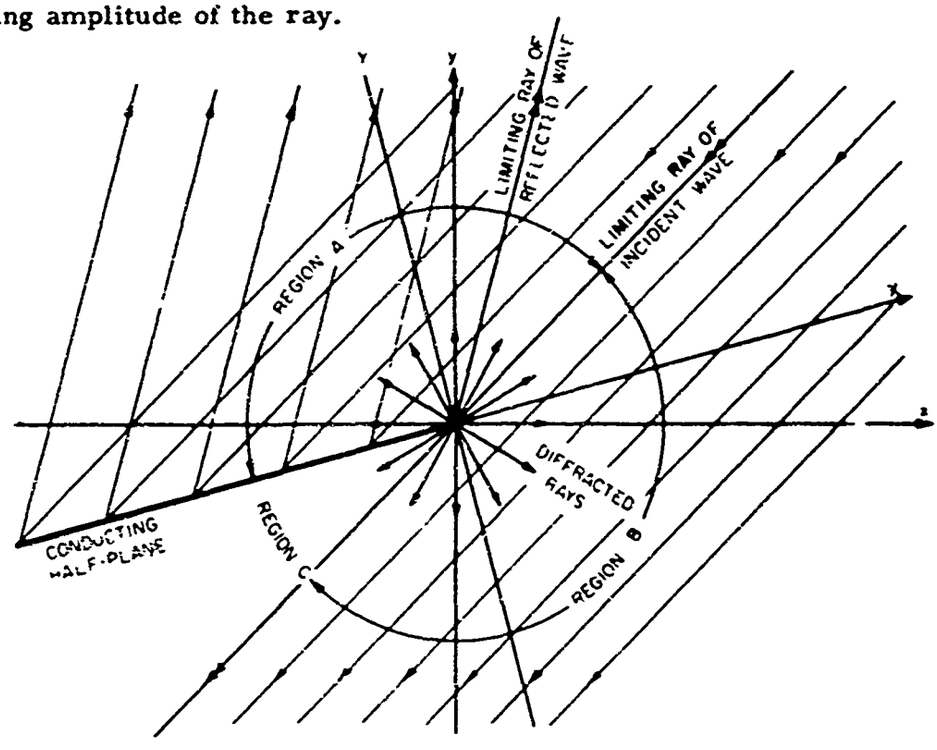

Fig. 12: The field constituents in the half-plane diffraction problem.

The plots of $f(w_s)$ in Figs. 13a, b, c, d show the influence of the anisotropic medium on the diffraction coefficient. Whereas the diffraction pattern is symmetrical in the isotropic medium (Fig. 13a), the presence of anisotropy may introduce substantial distortion. When ϵ is chosen negative, propagating fields are confined to certain angular directions so that the diffracted field emanating from the edge creates its own region of illumination; the pattern function in the shadow zone describes the angular dependence of the evanescent diffracted fields ("evanescent rays"). (It is to be kept in mind that the last mentioned regions of illumination and shadow are consequences of the medium properties when $\epsilon < 0$ and should not be confused with illumination or shadow zones caused by the obstacle). In Fig. 13d, the incident field is itself evanescent but gives rise to a propagating diffracted field. This aspect is of importance in connection with excitation by a line source, to be considered next.

In view of the local nature of high-frequency (or far field) diffraction, it is to be expected that the amplitude of the diffracted field is proportional to that of the incident field at the edge. Since the incident radiation is locally that of a plane wave, it should be possible to construct the diffraction field due to arbitrary excitation from the canonical solution (4-43a) for a plane wave. This argument has been employed in the geometrical theory of diffraction[3] for electromagnetic wave propagation in isotropic regions, and we show that it remains valid also in the anisotropic case. To demonstrate this fact, we consider the case of a cylindrical wave incident on the half-plane, the rigorous solution for which can be derived from that of plane wave diffraction. The details of the calculation are given in appendix G. We assume that x' and y' in Eq. (4-20a) are finite and $(x'/y') = \tan\theta'$. The incident field φ_i is now in the form of a cylindrical wave as in Eq. (4-11), and the rigorous solution for the secondary field φ_s is shown to be (see Appendix G):

$$\varphi_s = \frac{\pm 1}{8\pi^2} \int_{-\infty}^{\infty} d\xi \frac{\exp\left[-i\xi X' + i q_1(\xi) Y'\right]}{\sqrt{k_o N(\theta_o) - \xi}} \int_{-\infty}^{\infty} d\alpha \frac{\exp\left[-i\alpha X + i q_1(\alpha) Y\right]}{\sqrt{k_o N(\theta_o) - \alpha}\,(\alpha + \xi)} \tag{4-45}$$

for $Y'>0$ and $Y\gtrless 0$. After carrying out an asymptotic evaluation of Eq. (4-45) for $k_o r N(\theta) >> 1$ (Appendix F), one finds again that the solution is in the form of Eq. (4-42), with φ_g representing a part which can be derived by geometrical optics (see Appendix C), while φ_c - the diffracted part- is given by

$$\varphi_c \sim f(w_s)\sqrt{\frac{2}{\pi k_o r' N(\theta')}}\, e^{i k_o r' N(\theta') - i\frac{\pi}{4}} \sqrt{\frac{2}{\pi k_o r N(\theta)}}\, e^{i k_o r N(\theta) - i\frac{\pi}{4}} \qquad (4\text{-}46)$$

Since $f(w_s)$ is the same coefficient as in Eq. (4-43b), and the factor distinguishing Eq. (4-46) from Eq. (4-43a) is precisely the incident ray amplitude at the edge (see Eq. (4-16)), this result confirms the local character of the diffraction process and the validity of the geometrical theory of diffraction. The preceding solution, valid for positive or negative ε, has also shown that the boundary of the geometrical shadow (i.e., the boundary of the domain of existence of the incident wave) is given by the ray from the source which grazes the edge, regardless of whether this ray is propagating or evanescent. Similarly, the reflected ray boundary is the one predicted from geometric optical considerations since the reflection law in Eq. (4-10) remains valid even when both the incident and reflected rays are non-propagating (see reference 15); in the latter case, the field is obtained by analytic continuation of the real ray solution to imaginary values of $N(\theta)$. The Wiener-Hopf representation has therefore furnished a simple interpretation of the "geometric-optical" (better, the direct and reflected) field when $\varepsilon<0$, and it has shown that this part of the solution (and its spatial domain of existence) may be determined from direct ray-optical considerations. This clarification did not emerge as easily from the alternative representation mentioned at the beginning of this section. The diffraction field in Eq. (4-46) is also seen to be in a form which is readily interpretable for positive, negative, or even complex ε. It is therefore to be expected that the direct and reflected field contributions in the presence of obstacles of more general shape may be constructed by the techniques of geometrical optics even when ε is non-positive. The diffraction field for a variety of structures may be determined from known isotropic results by Felsen's method[2] when ε is

positive, and analytic continuation should then provide the correct behavior when $0 \leq \arg \varepsilon \leq \pi$. These conclusions, valid for the half plane, remain to be confirmed for other configurations.

Depending on the location of the half plane with respect to the line source, a number of interesting situations may arise when $\varepsilon < 0$ so that ray propagation is limited to angles θ such that $|\tan\theta| < \tan\theta_c = 1/\sqrt{|\varepsilon|}$. Various cases are depicted in Figs. 14 (a-d). In Fig. 14 (a), the half plane is in the shadow of the source and the incident field near the surface is evanescent. As mentioned in connection with Fig. 13, the edge nevertheless creates its zone of illumination so that the diffracted field in this case dominates the evanescent reflected field. In Fig. 14 (b), a portion of the plane is illuminated and the edge is in the shadow. The reflected field is now the same as from an infinite plane and the diffraction effect is small since it is caused by an evanescent incident wave. When the edge is in the illuminated region of the source but the plane is mostly confined to the shadow (Fig. 14 (c)), both the reflected and diffracted fields may be significant, with special importance assigned to the diffracted wave in that region of space wherein the incident and reflected waves are evanescent. Analogous considerations apply to the final case wherein the entire plane is illuminated (Fig. 14 (d)).

D. DIFFRACTION BY A SMOOTH CONVEX CYLINDER: POSTULATIVE APPROACH

The present section deals with diffraction phenomena caused by surface curvature. It is known from studies in isotropic media, that such effects arise from the vicinity of the shadow boundary on the scatterer, and the diffracted fields may be associated with waves which are launched at the shadow boundary, travel along the surface into the shadow region, and leak energy continuously during their progress ("creeping waves")[21]-[24]. From a ray-optical viewpoint, the creeping waves are interpretable in terms of diffracted rays which are excited by an incident ray tangent to the obstacle. These creeping rays also satisfy a generalized form of Fermat's principle, and the mechanism of

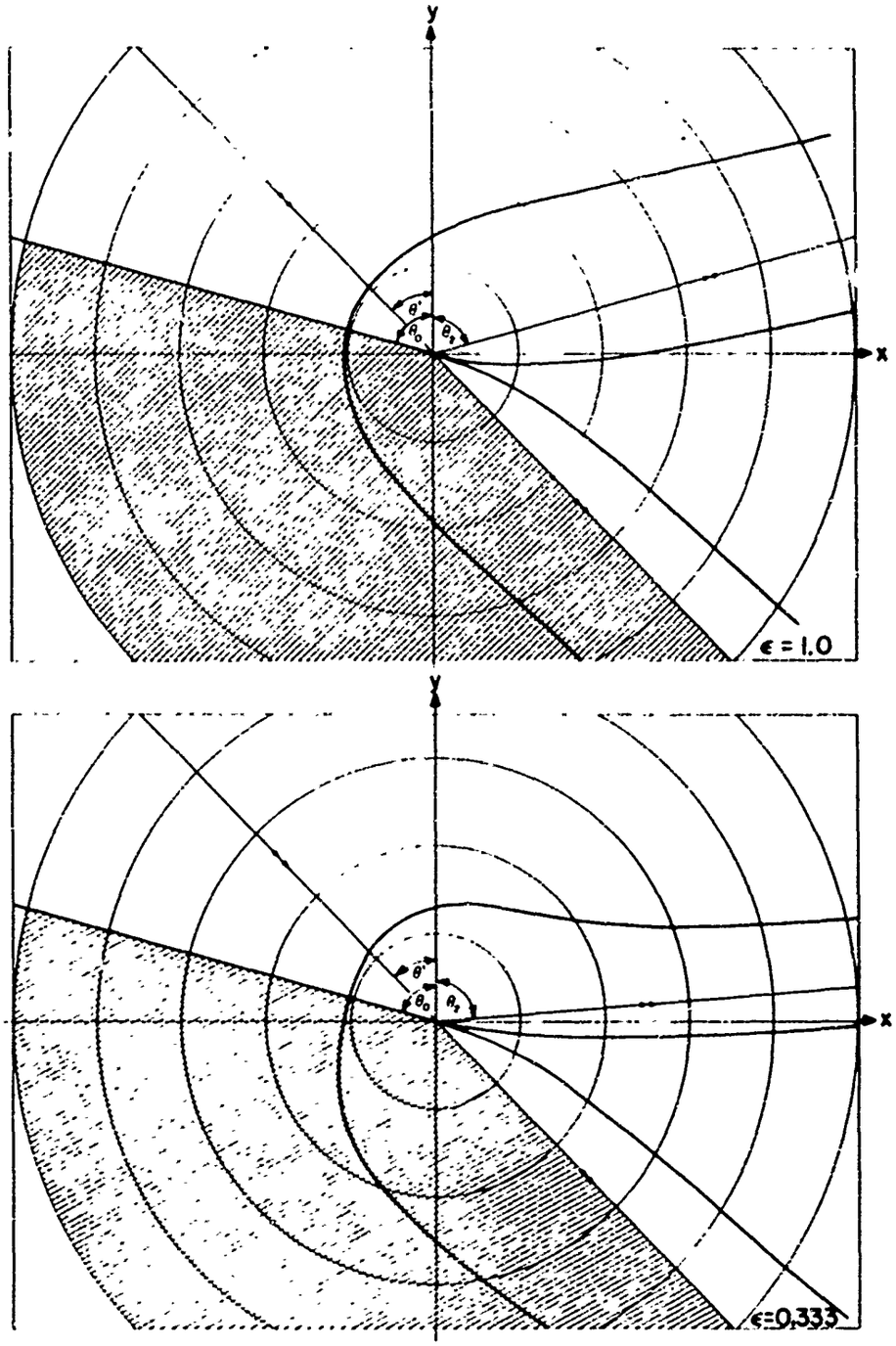

Fig. 13: The diffraction coefficient $f(w_s)$

a) $\epsilon=1$ (isotropic medium) $\theta_o=-75^o$ $\theta'=-45^o$

b) $\epsilon=0.333$ $\theta_o=-75^o$ $\theta'=-45^o$

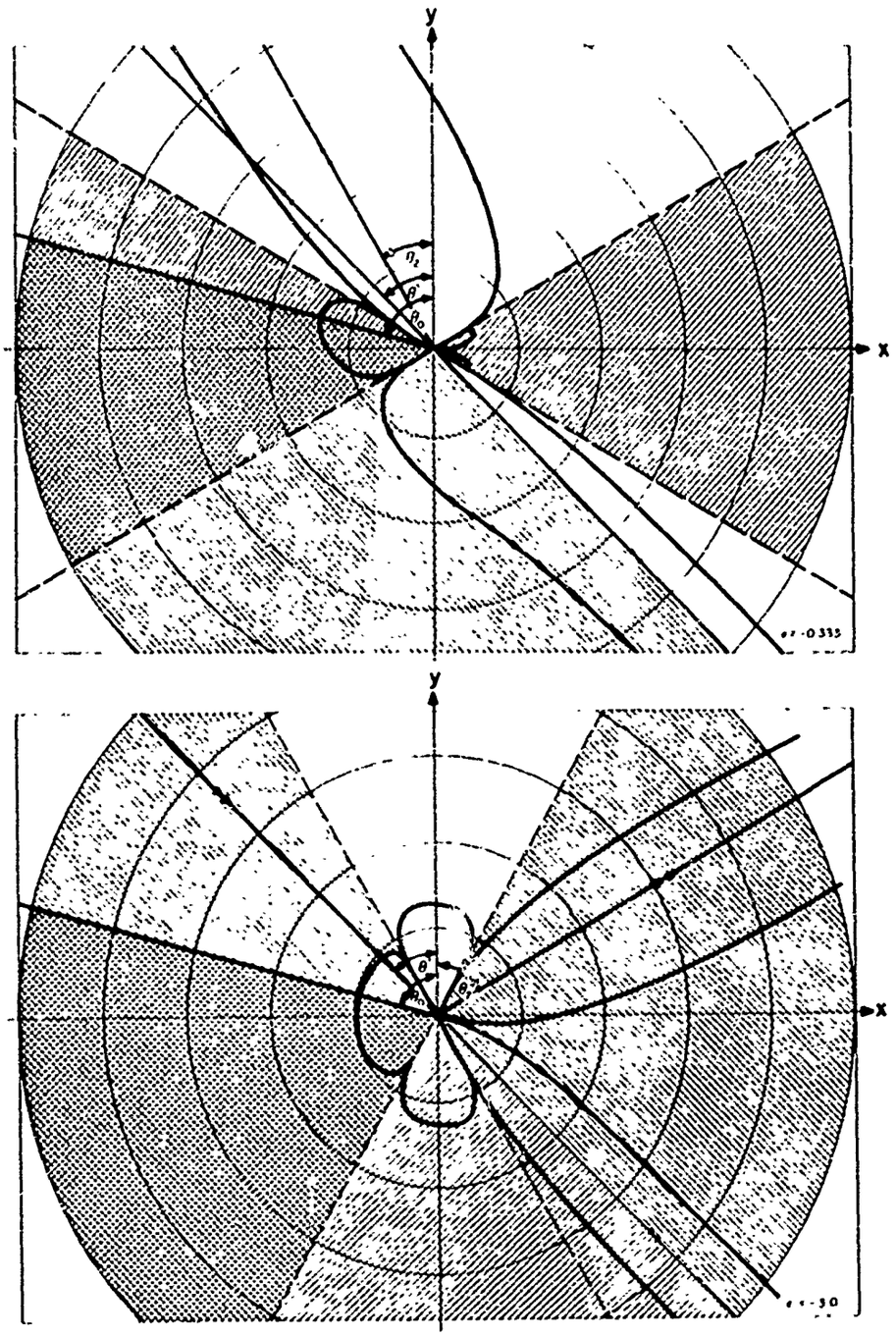

Fig. 13: The diffraction coefficient $f(w_s)$

c) $\varepsilon=-0.333 \quad \theta_c=60^o \quad \theta_o=-75^o \quad \theta'=-45^o$

d) $\varepsilon=-3.0 \quad \theta_c=30^o \quad \theta_o=-75^o \quad \theta'=-45^o$

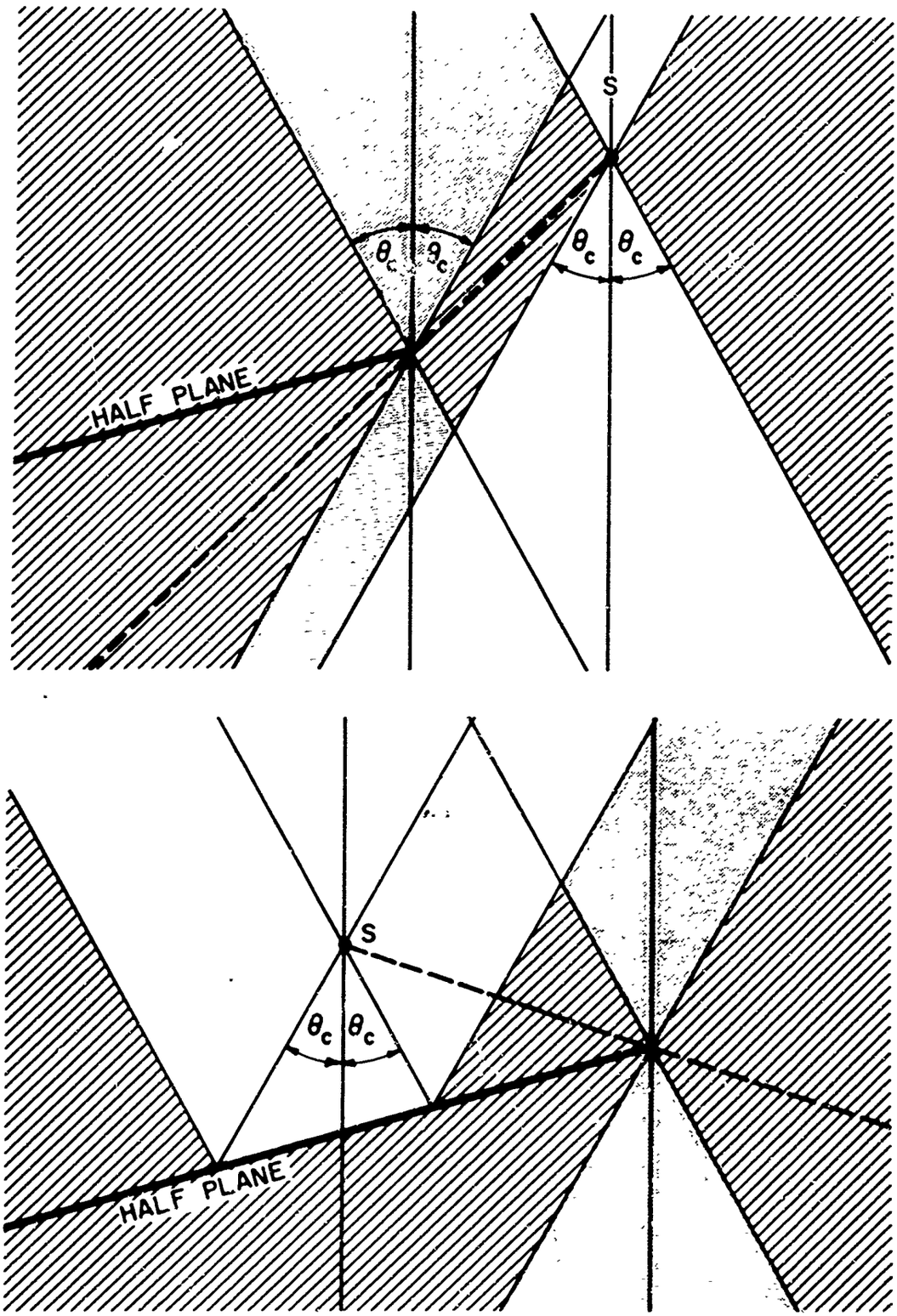

Fig. 14: Diffraction of a cylindrical wave by a half-plane.

a) half-plane totally in shadow region
b) edge in shadow region, but portion of half-plane illuminated

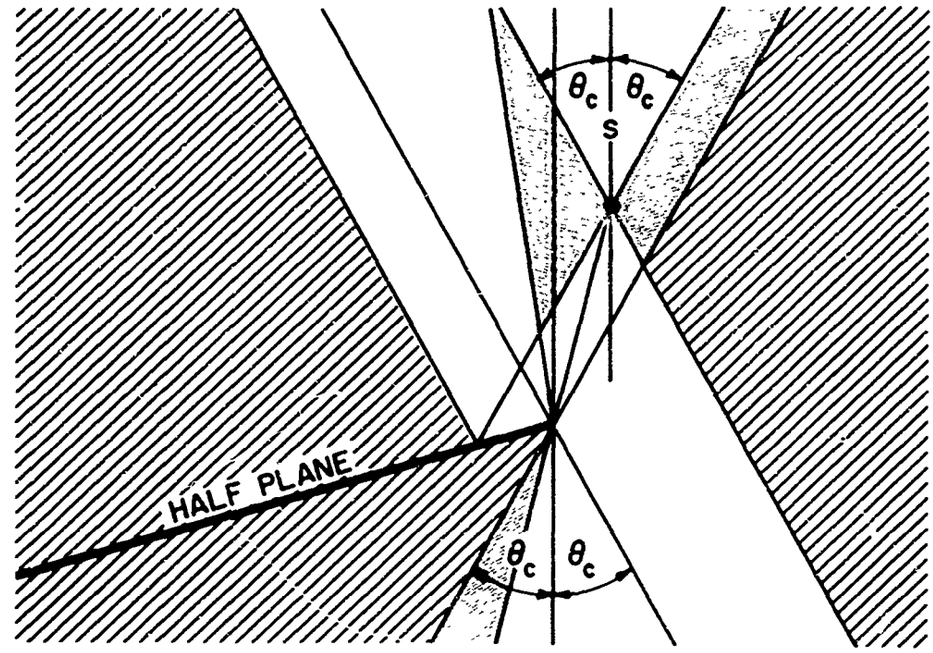

(c)

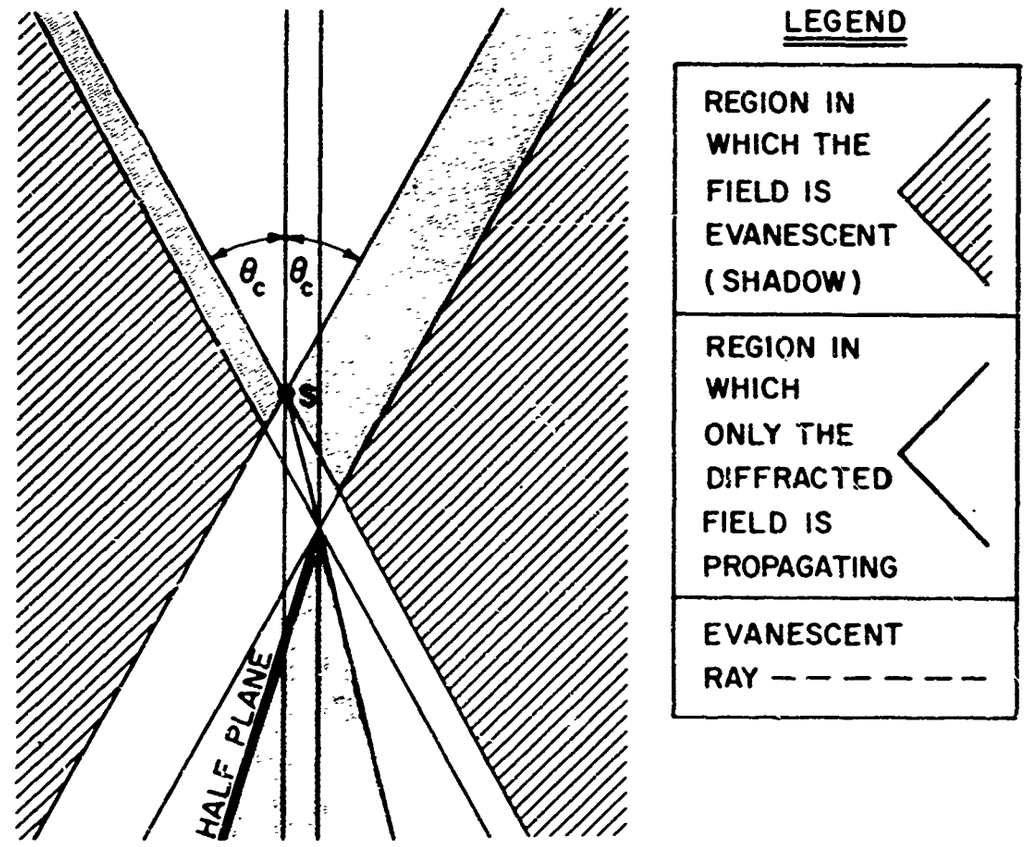

(d)

Fig. 14: Diffraction of a cylindrical wave by a half-plane.

c) edge in illuminated region, but most of the half-plane in shadow region
d) half-plane entirely in illuminated region

energy transport from a source point Q to a point P in the shadow region may be understood from the ray trajectories sketched in Figure 15. For a ray path $QQ_1 P_1 P$, QQ_1 is measured along the incident tangent ray, while $Q_1 P_1$ is the distance traveled by the diffracted ray along the surface (with an associated leakage of energy). Since the leakage may be represented by rays which leave the surface tangentially, the path segment $P_1 P$ is the associated trajectory. If the scatterer is a closed cylindrical structure as in Fig. 15(b), analogous considerations apply to the alternate path $QQ_2 P_2 P$. In that case there are additional field constituents at P, arising from rays which have encircled the cylinder one or more times before shedding. In view of the exponential decay of a diffracted ray during its travel along the surface, these latter contributions are frequently negligible.

The preceding features have been incorporated by Keller[16] into a prescription which allows the quantitative construction of the diffracted field in isotropic regions. While the validity of these postulates has not yet been established in general, the successful verification for various special cases[16][25] lends strong support for their applicability to smooth convex surfaces of relatively arbitrary shape. We shall therefore follow similar arguments to obtain representations for the diffracted field when the scatterer is embedded in an anisotropic medium. Referring again to Fig. 15, the incident field at Q_1 caused by a line source at Q is given by:

$$A_i(Q_1) = \frac{A_o'}{\sqrt{d_1'}} \tag{4-47}$$

where A_o' is the reference amplitude

$$A_o' = \sqrt{\frac{-2i}{\pi k_c N(\vartheta_1')}} \tag{4-47a}$$

We denote the field amplitude associated with the diffracted ray near the cylinder surface by $A_d(s)$, where s is the arc length measured from Q_1. To relate A_d to A_i, assume

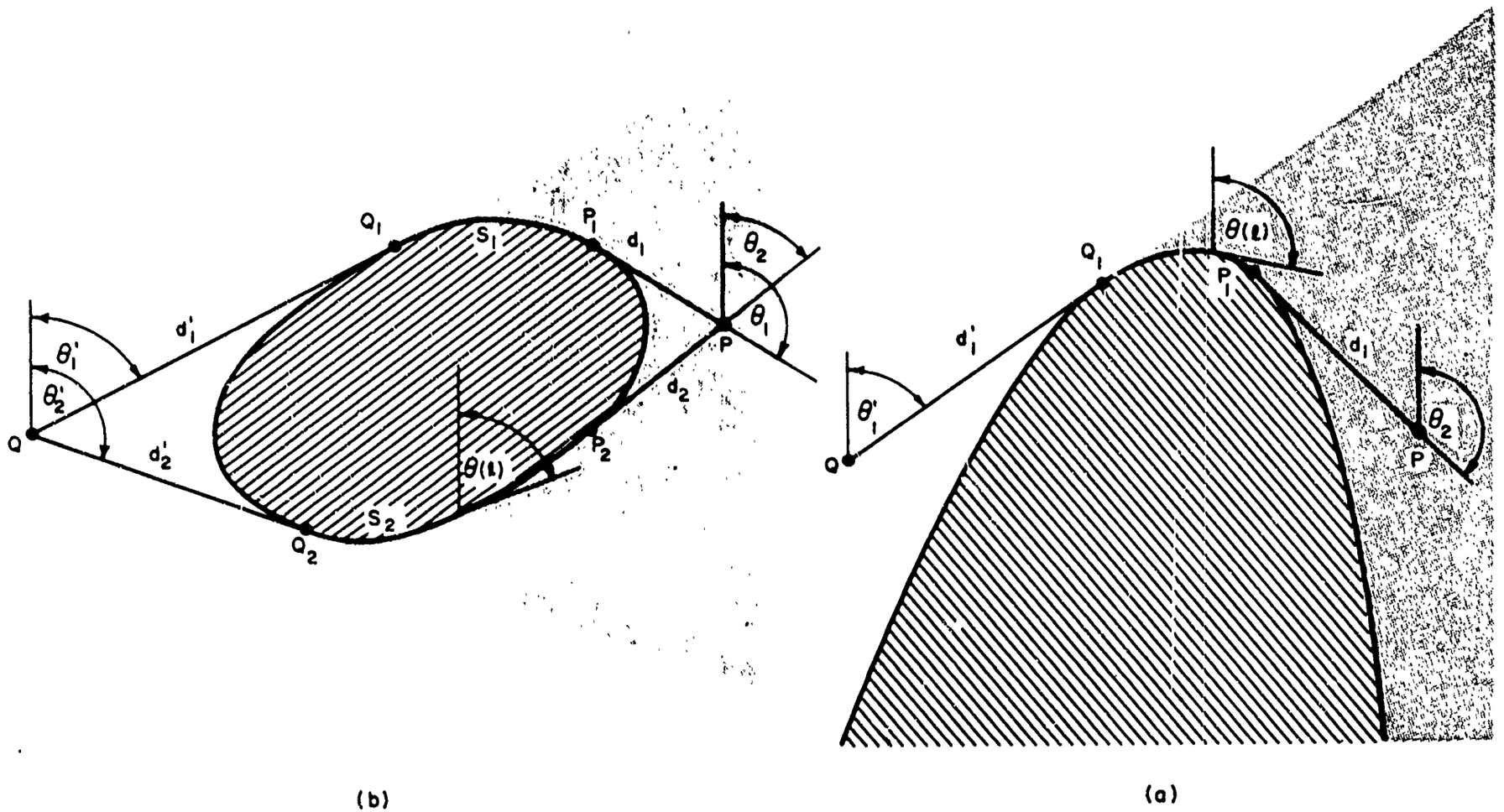

Fig. 15 Geometry for diffraction by a smooth cylinder
(a) Cylinder with open cross section
(b) Cylinder with closed cross section

$$A_d(0) = D(Q_1)\, A_i(Q_1)\,, \tag{4-48}$$

where $D(Q_1)$ is a diffraction coefficient which is a function of the properties of the surface and the medium at Q_1. Because of the continuous leakage of energy from the surface, it will be further assumed that

$$A_d(\ell) = A_d(0)\, \exp\left[-\int_0^{\ell} \hat{\alpha}\, d\ell\right]\,, \tag{4-49}$$

where $\hat{\alpha}$ is a decay coefficient which also is a function of the local properties of the surface and the medium. If $A(d)$ denotes the field amplitude along the ray which leaves the surface tangentially at P_1, then we assume that

$$A(0) = D(P_1)\, A_d(0)\, \exp\left[-\int_{Q_1}^{P_1} \hat{\alpha}\, d\ell\right], \tag{4-50}$$

where $D(P_1)$ is again a diffraction coefficient. As long as the field satisfies conventional reciprocity conditions (which is true for the uniaxial case), we may assume that $D(Q_1)$ and $D(P_1)$ have the same dependence on the surface and medium properties at Q_1 and P_1, respectively. In cases of more general anisotropy, this point has to be reexamined, and more general assumptions have to be made in accord with the reciprocity relations satisfied by the medium. Also,

$$A(P) = A(d) = A(0)\, \frac{A_o}{\sqrt{d_1}} \tag{4-51}$$

where

$$A_o = \sqrt{\frac{-2i}{\pi k_o N(\theta_1)}} \tag{4-51a}$$

The field at P due to one ray is therefore given by

$$A(P) = \frac{A_o A_o'}{\sqrt{d_1 d_1'}}\, D(Q_1)\, D(P_1)\, \exp\left[-\int_{Q_1}^{P_1} \hat{\alpha}\, d\ell + \Psi(P)\right], \tag{4-52}$$

where $\Psi(P)$ is the phase change along the trajectory:

$$\Psi(P) = ik_o\left\{d_1' N(\theta_1') + d_1 N(\theta_1) + \int_{Q_1}^{P_1} N\left[\theta(\ell)\right] d\ell\right\} \tag{4-52a}$$

By analogy to the isotropic case, we may expect the possible existence of different "modes" having different decay exponents $\hat{\alpha}_p$ and diffraction coefficient D_p, $p = 1, 2, \ldots$. The total field at the point P in Fig. 15(a) is therefore assumed to be given by a sum of all of these modes,

$$H_d(P) = \frac{i\omega\epsilon_o\epsilon}{4}\sqrt{\frac{-2i}{\pi k_o d_1' N(\theta_1')}}\sqrt{\frac{-2i}{\pi k_o d_1 N(\theta_1)}}\exp\left[ik_o\left\{d_1' N(\theta_1') + d_1 N(\theta_1) + \int_{Q_1}^{P_1} N\left[\theta(\ell)\right] d\ell\right\}\right]$$

$$\times \sum_{p=1}^{\infty} D_p(Q_1)\, D_p(P_1) \exp\left[-\int_{Q_1}^{P_1} \hat{\alpha}_p\, d\ell\right] . \tag{4-53}$$

If the scatterer has a closed cross section (Fig. 15(b)), one has to add the contributions from rays which have encircled the cylinder m-times, $m = 1, 2, \ldots$. The formulas for the corresponding rays differ from that in Eqs. (4-52) in that the integration interval extends from Q_1 to $(P_1 + mL)$ and from Q_2 to $(P_2 + mL)$, where L is the circumference of the cylinder. Using the formula for summation of an infinite geometric progression, we can write the sum of all these rays in closed form:

$$\exp\int_{Q}^{P}\left[ik_o N - \hat{\alpha}_p\right] d\ell + \exp\int_{Q}^{P+L}\left[ik_o N - \hat{\alpha}_p\right] d\ell + \ldots$$

$$\ldots + \exp\int_{Q}^{P+ML}\left[ik_o N - \hat{\alpha}_p\right] d\ell + \ldots = \frac{\exp\int_{Q}^{P}\left[ik_o N - \hat{\alpha}_p\right] d\ell}{1 - \exp\oint_{L}\left[ik_o N - \hat{\alpha}_p\right] d\ell} \tag{4-54}$$

Thus, the formula analogous to Eq. (4-53), which gives the total diffracted field in the shadow region of a closed cylinder, is:

$$H_d(P) = \frac{i\omega\epsilon_o\epsilon}{4}\sqrt{\frac{-2i}{\pi k_o d_1' N(\theta_1')}}\sqrt{\frac{-2i}{\pi k_o d_1 N(\theta_1)}} \cdot$$

$$\cdot \exp\left\{ik_o\left[d_1'N(\theta_1') + d_1 N(\theta_1) + \int_{Q_1}^{P_1} N\, d\ell\right]\right\}\sum_{p=1}^{\infty} \frac{D_p(Q_1)D_p(P_1)\exp\left[-\int_{Q_1}^{P_1}\hat{\alpha}_p\, d\ell\right]}{1 - \exp\oint_L\left[ik_oN - \hat{\alpha}_p\right]d\ell} +$$

$$+ \frac{i\omega\epsilon_o\epsilon}{4}\sqrt{\frac{-2i}{\pi k_o d_2' N(\theta_2')}}\sqrt{\frac{-2i}{\pi k_o d_2 N(\theta_2)}} \cdot$$

$$\cdot \exp\left\{ik_o\left[d_2'N(\theta_2') + d_2 N(\theta_2) + \int_{Q_2}^{P_2} N\, d\ell\right]\right\}\sum_{p=1}^{\infty} \frac{D_p(Q_2)D_p(P_2)\exp\left[-\int_{Q_2}^{P_2}\hat{\alpha}_p\, d\ell\right]}{1 - \exp\oint_L\left[ik_oN - \hat{\alpha}_p\right]d\ell} \qquad (4\text{-}55)$$

In these detailed formulas (Eqs. (4-53) and (4-55)), it is often sufficient to retain only the p=1 mode (having the lowest decay exponent $\hat{\alpha}_1$) and to ignore the denominator term in the summand (i.e. to neglect the rays which have encircled the cylinder completely one or more times). This results in an expression comprising one diffracted ray for the field in the shadow of an open cylinder (as in Eq. (4-52)), and two diffracted rays for the field in the shadow of a closed cylinder.

While the preceding discussion constitutes in effect an application of the geometrical theory of diffraction[3][16] to an anisotropic medium, and is therefore based on a series of postulates similar to those in the isotropic case, confirmation of its validity may be obtained directly for special configurations, when the medium is uniaxial. When $\theta = 0$, with α and ϵ real and positive, the scattering problem in the uniaxially anisotropic region is reducible to an equivalent isotropic problem by the previously described method of coordinate scaling (Eq. (2-6)). Since the isotropic analogue of Eq. (4-53) and (4-55) has been confirmed for such obstacles as circular, elliptic and parabolic cylinders[16][25], an application of the scale transformation yields a corresponding asymptotic solution for the uniaxial case. It may be verified that the result derived in this manner furnishes not only the general form given in Eqs. (4-53) and (4-55) but also yields specific expressions for the coefficients D_p and $\hat{\alpha}_p$.

To illustrate these remarks, consider the equation for a single ray (Eq. (4-52)) in an isotropic medium (uv - coordinate space) with wave number $k = k_o\sqrt{\Delta} = k_o\sqrt{\alpha\varepsilon}$:

$$\overline{H}_d = \frac{i\omega\varepsilon_o}{4}\sqrt{\frac{-2i}{\pi k\,\overline{d}'}}\sqrt{\frac{-2i}{\pi k\,\overline{d}}}\;\overline{D}_p(\overline{Q}_1)\,\overline{D}_p(\overline{P}_1)\cdot$$

$$\cdot\exp\left\{ik\left[\overline{d}' + \overline{d} + \int_{\overline{Q}_1}^{\overline{P}_1}\overline{d\ell}\right] - \int_{\overline{Q}_1}^{\overline{P}_1}\hat{\alpha}_p\,\overline{d\ell}\right\}, \qquad (4\text{-}56)$$

with the quantities $\overline{d}, \overline{d}'$ and $\overline{d\ell}$ defined in Fig. 16.

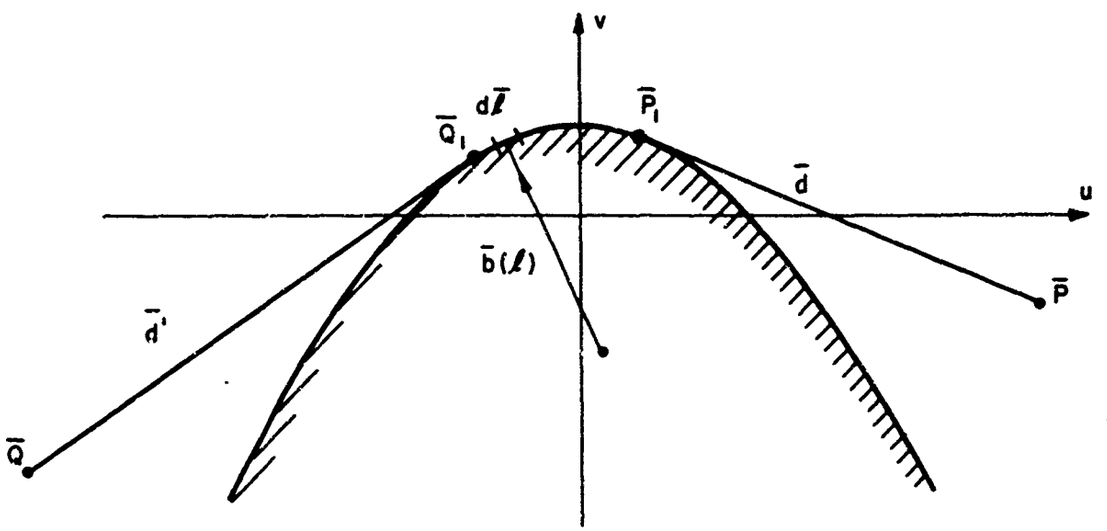

Fig. 16: The uv - coordinate space.

$\overline{D}_p$ and $\hat{\alpha}$ in the isotropic medium have been calculated by Keller[16]:

$$\overline{D}_p = \frac{\sqrt{\pi}}{2} \frac{e^{i\pi/12} \; k_o^{1/6} \; [\overline{b}(u,v)]^{1/6}}{\Delta^{1/12} \; 2^{1/4} \; 6^{1/6} [q_p A(q_p)]} \quad , \tag{4-56a}$$

$$\hat{\alpha}_p = -ik_o^{1/3} \Delta^{1/6} \tau_p [\overline{b}(u,v)]^{-2/3} \quad , \tag{4-56b}$$

where $\overline{b}(u,v)$ is the local radius of curvature of the perfectly conducting scatterer, and the numbers τ_p are defined by

$$\tau_p = q_p e^{i\pi/3} \; 6^{-1/3} \tag{4-56c}$$

with the numbers q_p denoting the roots of the equation

$$\frac{d}{dq} A(q) = \frac{d}{dq} \int_0^\infty \cos(w^3 - qw) dw = 0 \quad . \tag{4-56d}$$

By applying the transformation $x = u\sqrt{\alpha}$, $y = v\sqrt{\epsilon}$, the resulting solution in the x-y space is known to satisfy Eq. (2-4), the boundary condition $E_{tan} = 0$ on the trasformed obstacle, and the radiation conditon at infinity. Since

$$\frac{dv}{du} = \sqrt{\frac{\alpha}{\epsilon}} \frac{dy}{dx} = \sqrt{\frac{\alpha}{\epsilon}} \cot \theta,$$

where θ is measured from the positive y-axis, one obtains for the transformed length element

$$d\overline{\ell}(u,v) = \sqrt{du^2 + dv^2} = \sqrt{dx^2 + dy^2} \frac{\sqrt{\frac{1}{\alpha} dx^2 + \frac{1}{\epsilon} dy^2}}{\sqrt{dx^2 + dy^2}} = \frac{1}{\sqrt{\Delta}} N(\theta) \, d\ell(x,y)$$

(4-57a)

where $N(\theta)$ is the ray refractive index (see Eq. (4-8)) and $\Delta = \det|\underline{\varepsilon}| = \alpha\varepsilon$ (since $\beta = 0$). In the same way one can show that

$$k\bar{d}(u, v) = k_o N(\vartheta)\, d(x, y) \tag{4-57b}$$

$$k\bar{d}'(u, v) = k_o N(\theta')\, d'(x, y) \ . \tag{4-57c}$$

The phase function in Eq. (4-56) is seen to transform into the one given in Eq. (4-53), with due cognizance taken of the fact the $N(\vartheta)$ varies over the part of the trajectory on the obstacle surface. Similarly,

$$\left[\bar{b}(u, v)\right]^{-2/3} = \frac{\left(\frac{d^2 v}{du^2}\right)^{2/3}}{1 + \left(\frac{dv}{du}\right)^2} = \left(\frac{\alpha^2}{\varepsilon}\right)^{1/3} \frac{\left(\frac{d^2 y}{dx^2}\right)^{2/3}}{1 + \left(\frac{dy}{dx}\right)^2} \frac{1 + \left(\frac{dy}{dx}\right)^2}{1 + \frac{\alpha}{\varepsilon}\left(\frac{dy}{dx}\right)^2} =$$

$$= \frac{\Delta^{2/3}}{N^2(\vartheta)} \left[b(x\ y)\right]^{-2/3} \tag{4-58}$$

where $b(x, y)$ is the radius of curvature of the obstacle in the x-y space. The decay exponent in Eq. (4-56) is then converted into:

$$\int_{\bar{Q}_1}^{\bar{P}_1} \hat{\alpha}_p \, d\ell = -ik_o^{1/3} \Delta^{1/3} \tau_p \int_{Q_1}^{P_1} \frac{d\ell}{\left[b(\ell)\right]^{2/3} N\left[\vartheta(\ell)\right]}$$

from which one may identify

$$\hat{\alpha}_p = -\frac{ik_o^{1/3} \Delta^{1/3} \tau_p}{\left[b(\ell)\right]^{2/3} N\left[\vartheta(\ell)\right]} \ . \tag{4-59}$$

The diffraction coefficient D_p is obtained from $\bar{D}_p$ in Eq. (4-56a) upon inserting from Eq. (4-58).

Thus it has been shown that the field postulated in Eqs. (4-53) or (4-55), together with the results for $\hat{\alpha}_p$ and D_p from above, describes correctly the

diffracted rays on simple convex surfaces embedded in a uniaxially anisotropic medium characterized by real and positive α and ϵ. In the derivation of the result, it was assumed that the asymptotic field representation in the anisotropic medium may be derived by applying the scale transformation to the asymptotic field solution in the equivalent isotropic configuration. The validity of this procedure, not really in question when $\epsilon>0$, $\alpha>0$, is confirmed for two special cases treated in the next sections.

The series in Eqs. (4-53) and (4-55) remain convergent when $0 \leq \arg \epsilon \leq \pi$, as may be verified by examining the exponents in Eqs. (4-53) and (4-55), which retain a negative real part that increases with p for $0 \leq \arg N(\theta) \leq \pi/2$ (corresponding to $0 \leq \arg \epsilon \leq \pi$). It is plausible, therefore, to expect the preceding formulas to hold in this extended parameter range. A confirmation of this statement does not follow immediately from the previously utilized scaling technique since the scaled coordinates are non-real when ϵ is non-positive. By examining the problem of diffraction by a parabolic cylinder, however, the solution may be phrased in a form which validates the analytic continuation of the asymptotic formulas to non-real ϵ. The analysis, which establishes the validity of Eqs. (4-53) and (4-55) for $0 \leq \arg \epsilon \leq \pi$, is presented in the next Section.

E. DIFFRACTION BY A PARABOLIC CYLINDER: RIGOROUS ANALYSIS

In order to confirm the general results which were derived in the previous section in a postulative way, the rigorous solution to a special case is worked out in this section. Felsen's method[2] is used to obtain the expression for the field in presence of a perfectly conducting parabolic cylinder embedded in a uniaxially anisotropic medium ($\beta=0$, $\alpha=1$ in Eqs. (2-1)). The parabolic cylinder surface $S(x, y)$ is given by the equation

$$y = -\frac{x^2}{2b} \tag{4-60}$$

with the optic axis parallel to the y axis. This obstacle has a varying radius of curvature, with the smallest radius of curvature b at $x=0$. Also, the angle ψ between the surface normal and the optic axis varies continuously. A mag-

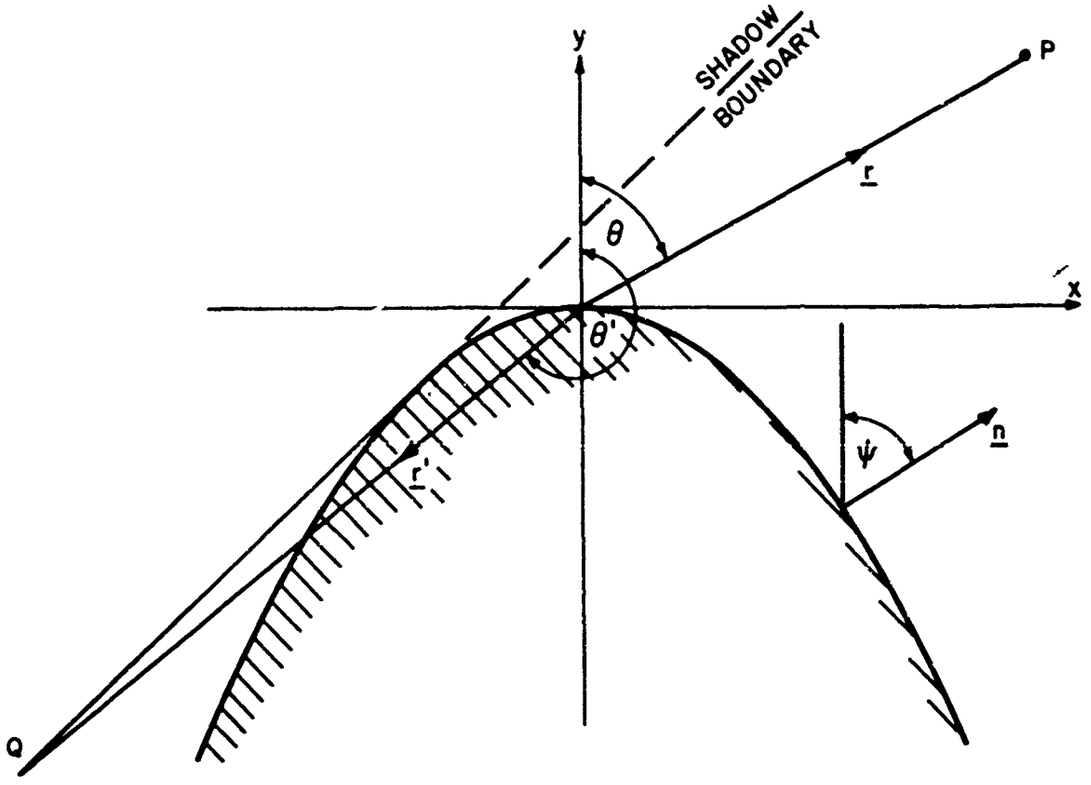

Fig. 17 Diffraction by a parabolic cylinder: The xy-space.

netic line current is located at the point Q to the left of the obstacle ($x<0$). As shown in Chapter II, Section A, the magnetic field has only a z-component $H(x, y)$ from which the two electric field components E_x and E_y may be derived. $H(x, y)$ is defined uniquely by the equations

$$\left(\frac{\partial^2}{\partial x^2} + \epsilon \frac{\partial^2}{\partial y^2} + k^2\right) H(x, y) = -i\omega\epsilon_o\epsilon \; \delta(x-x') \, \delta(y-y') \; , \tag{4-61a}$$

$$\frac{\partial H}{\partial x} \sin\psi + \frac{\partial H}{\partial y} \epsilon \cos\psi = 0 \qquad \text{on } S \; , \tag{4-61b}$$

Radiation condition at $r \to \infty$, (4-61c)

with $k=k_o\sqrt{\epsilon}$, and $\psi=\tan^{-1}\frac{dy}{dx}$ denoting the angle between the normal $\underline{n}$ and the optic axis.

It is convenient to define

$$\hat{y} = y+a \ , \tag{4-62a}$$

where a is an arbitrary (possibly complex) finite constant. The equation of the surface $\hat{S}(x,\hat{y})$ becomes

$$\hat{y} = a-\frac{x^2}{2b} \ . \tag{4-62b}$$

It is seen that the change of variable (4-62a) does not affect the quantities $\frac{\partial}{\partial y}$, $\frac{\partial^2}{\partial y^2}$, $\delta(y-y')$ and $\psi=\tan^{-1}\frac{dy}{dx}$ so that in Eqs. (4-61a) and (4-61b), y can be replaced by $\hat{y}$ and S by $\hat{S}$. The radiation condition requires outward flow of energy as $r=\sqrt{x^2+y^2}\to\infty$. As "a" is a finite quantity, the radiation condition Eq. (4-61c) also remains unchanged.

If we choose

$$a = {}^{e}/_{2b} \ , \tag{4-63}$$

then upon introduction of the transformation

$$x=u, \ \hat{y}=\sqrt{\epsilon}\ v \ , \tag{4-64a}$$

the equation for S becomes

$$v = \frac{\sqrt{\epsilon}\,b}{2} - \frac{u^2}{2\sqrt{\epsilon}\,b} \ , \tag{4-64b}$$

which is the equation of a constant coordinate surface in a parabolic coordinate system. Via Eq. (4-64a) the boundary value problem in the u-v coordinate system reads

$$\left(\frac{\partial^2}{\partial u^2}+\frac{\partial^2}{\partial u^2}+k^2\right) G(\underline{R},\underline{R}') = -\delta(u-u')\,\delta(v-v') \ , \tag{4-65a}$$

$$\frac{\partial G}{\partial \hat{n}} = \frac{\partial G}{\partial u} \sin \hat{\psi} - \frac{\partial G}{\partial v} \cos \hat{\psi} = 0 \text{ on } v = \frac{\sqrt{\epsilon}\, b}{2} - \frac{u^2}{2\sqrt{\epsilon}\, b} \tag{4-65b}$$

$$\text{Radiation condition at } R = \sqrt{u^2+v^2} \to \infty \ , \tag{4-65c}$$

where

$$G(\underline{R}, \underline{R}') = \frac{H}{i\omega \epsilon_o \sqrt{\epsilon}} \ , \tag{4-65d}$$

and

$$\hat{\psi} = \tan^{-1} \frac{dv}{du} = \tan^{-1} \frac{1}{\sqrt{\epsilon}} \frac{dy}{dx} \ . \tag{4-65e}$$

A set of parabolic cylinder coordinates is now introduced via

$$u = \eta \xi \ , \tag{4-66a}$$

$$v = \frac{1}{2}(\eta^2 - \xi^2) \ , \tag{4-66b}$$

the range of variation of η and ξ being

$$0 \leq \eta < +\infty \tag{4-66c}$$

$$-\infty < \xi < +\infty \tag{4-66d}$$

We assume ϵ to be real and positive at this stage. Thus $\hat{y}, u, v, \eta$ and ξ are all real. Later on we will let ϵ be complex and investigate analytic continuation of G in the complex ϵ plane. In the η-ξ space, Eqs. (4-65) become

$$\left[\frac{\partial^2}{\partial \eta^2} + \frac{\partial^2}{\partial \xi^2} + k^2(\eta^2+\xi^2)\right] G = -\delta(\eta-\eta')\,\delta(\xi-\xi') \ , \tag{4-67a}$$

$$\frac{\partial G}{\partial \eta} = 0 \quad \text{on } \eta = \eta_o = \sqrt{\sqrt{\epsilon}\, b} \ , \tag{4-67b}$$

$$\text{Radiation condition at } R = \frac{1}{2}(\eta^2+\xi^2) \to \infty \ . \tag{4-67c}$$

The surface $\eta = \eta_o$ is real only when ϵ is real and positive. For complex or negative real ϵ it cannot be drawn as in Fig. 18, but Eqs. (4-67) remain valid. The surface has a large radius of curvature if b is large with respect to wavelength. η_o is related to b via Eq. (4-67b), so we will assume

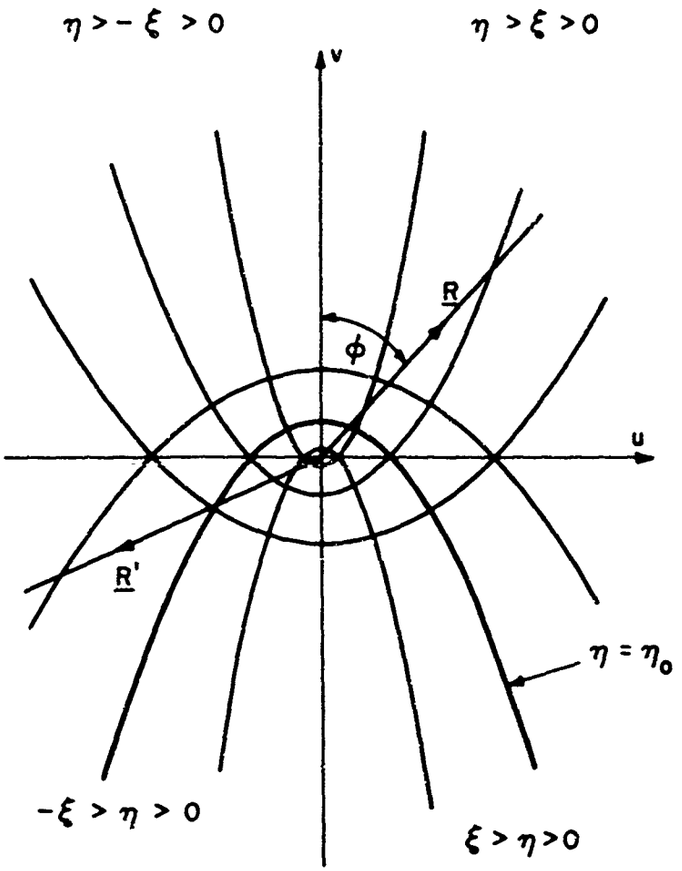

Fig. 18 Parabolic cylinder coordinates.

$$|k\eta_o^2| >> 1 \quad , \tag{4-68}$$

with the absolute value sign in Eq. (4-68) applying when ϵ is not real and positive. A representation of the Green's function G in terms of parabolic cylinder functions will now be found by means of the characteristic Green's function method[26]. According to that method G is given by

$$G(\underline{R}, \underline{R}') = \frac{1}{2\pi i} \oint g_\eta(\eta, \eta'; \lambda)\, g_\xi(\xi, \xi'; \lambda)\, d\lambda \tag{4-69}$$

where λ is the separation constant of the partial differential operator in Eq. (4-67a), and the functions g_η and g_ξ are solutions of the one-dimensional

equations

$$\left[\frac{d^2}{d\eta^2} + k^2\eta^2 - \lambda\right] g_\eta(\eta, \eta'; \lambda) = -\delta(\eta - \eta') \ , \tag{4-70a}$$

$$\left[\frac{d^2}{d\xi^2} + k^2\xi^2 + \lambda\right] g_\xi(\xi, \xi'; \lambda) = -\delta(\xi - \xi') \ . \tag{4-70b}$$

The contour of integration in Eq. (4-69) closes at infinity and surrounds all of the singularities of either g_η or g_ξ in the complex λ plane. The boundary conditions on g_η and g_ξ are identical with those satisfied by G in the η and ξ domains, respectively. Two linearly independent solutions of the homogeneous equation (4-70a) are given by [27][28]

$$f_1(\eta;\lambda) = D_{-\frac{1}{2} - \frac{i\lambda}{2k}}(\eta\sqrt{-2ik}) \ , \tag{4-71a}$$

$$f_2(\eta;\lambda) = D_{-\frac{1}{2} - \frac{i\lambda}{2k}}(-\eta\sqrt{-2ik}) \ , \tag{4-71b}$$

with $\sqrt{-i} = e^{-i\pi/4}$

where the parabolic cylinder function $D_\nu(z)$ satisfies the differential equation

$$\left[\frac{d^2}{dz^2} + (\nu + \frac{1}{2} - \frac{z^2}{4})\right] D_\nu(z) = 0 \ . \tag{4-71c}$$

To avoid ambiguity in the asymptotic expressions of f_1 and f_2 for $|\lambda| \to \infty$, it is necessary to define the relations between $\arg \nu$ and $\arg \lambda$

$$\begin{cases} \arg \nu = \arg \lambda - \frac{\pi}{2} & \text{when } |\nu| \to \infty \text{ and } \arg \nu < 0 \\ \arg \nu = \arg \lambda + \frac{3\pi}{2} & \text{when } |\nu| \to \infty \text{ and } \arg \nu > 0 \end{cases} \tag{4-71d}$$

Also, the Wronskian is given by

$$W\left[f_1, f_2\right] = f_1 f_2' - f_2 f_1' = \frac{2\sqrt{-i\pi k}}{\Gamma\left(\frac{1}{2}+\frac{i\lambda}{2k}\right)} \quad . \qquad (4\text{-}71e)$$

Only the function f_1 satisfies the radiation condition at $\eta \to \infty$. This may be seen from the asymptotic formulas for large values of $|z|$ which are

$$D_\nu(z) \sim z^\nu e^{-z^2/4}\left[1 + O(z^{-2})\right] , \qquad (4\text{-}72a)$$

$$|z| \gg |\nu| \text{ and } |\arg(z)| < \frac{3\pi}{4} ,$$

$$D_\nu(z) \sim z^\nu e^{-z^2/4}\left[1 + O(z^{-2})\right] - \frac{2\pi}{\Gamma(-\nu)} z^{-\nu-1} e^{i\pi\nu + z^2/4}\left[1+O(z^{-2})\right]$$

$$|z| \gg |\nu| \quad \text{and} \quad \frac{5\pi}{4} > \arg(z) > \frac{\pi}{4} . \qquad (4\text{-}72b)$$

Since η is real and positive, one finds from Eq. (4-72a)

$$D_{-\frac{1}{2}-\frac{i\lambda}{2k}}(\eta\sqrt{-2ik}) \sim (\eta\sqrt{-2ik})^{-\frac{1}{2}-\frac{i\lambda}{2k}} e^{ik\eta^2/2} , \qquad (4\text{-}72c)$$

which is proportional to e^{ikR} as $\eta \to \infty$. In view of Eq. (4-72b), the same relation is not obtained for f_2. A linear combination of f_1 and f_2 which satisfies condition (4-67b) is given by

$$f_3(\eta;\lambda) = \left[D_{-\frac{1}{2}-\frac{i\lambda}{2k}}(-\eta_< h)\right] + \left[D_{-\frac{1}{2}-\frac{i\lambda}{2k}}(\eta_< h)\frac{D'_{-\frac{1}{2}-\frac{i\lambda}{2k}}(-\eta_o h)}{D'_{-\frac{1}{2}-\frac{i\lambda}{2k}}(\eta_o h)}\right] \qquad (4\text{-}73)$$

with

$$h = \sqrt{-2ik} \qquad (4\text{-}73a)$$

and

$$D'_\nu(a x_o) \equiv \frac{\partial}{\partial x} D_\nu(a x)\Big|_{x=x_o} \qquad (4\text{-}73b)$$

It can be shown that the Wronskian of f_1 and f_3 is also given by Eq. (4-71e). The solution of Eq. (4-70a) subject to the proper boundary conditions at $\eta=\eta_o$ and $\eta\to\infty$ is now constructed from f_1 and f_3 is the usual way[29]:

$$g_\eta(\eta,\eta';\lambda) = \frac{f_1(\eta_>;\lambda)f_3(\eta_<;\lambda)}{W[f_1,f_3]} \tag{4-74}$$

where

$$\eta_> = \begin{cases} \eta\ , & \text{when } \eta>\eta' \\ \eta'\ , & \text{when } \eta'>\eta \end{cases} \tag{4-74a}$$

$$\eta_< = \begin{cases} \eta'\ , & \text{when } \eta'<\eta \\ \eta\ , & \text{when } \eta<\eta' \end{cases} \tag{4-74b}$$

Next we investigate the behavior of g_η as $|\lambda|\to\infty$. By expressing the solution of the homogeneous equation (4-70a) in terms of a uniform asymptotic approximation one finds

$$D_\nu(z)\sim\frac{1}{2}\left(\frac{\nu e^{\pm i\pi}}{e}\right)^{\nu/2} e^{\mp i\sqrt{\nu^2}z}\ ,\ |\nu|>>|z|^2,\ |\nu|\to\infty \tag{4-75a}$$

with the upper sign for $0>\arg\nu>-\frac{3\pi}{2}$,

and the lower sign for $0<\arg\nu<\frac{3\pi}{2}$.

Also,

$$\Gamma(\nu)\sim\sqrt{\frac{2\pi}{\nu}}\,\nu^\nu\, e^{-\nu} \tag{4-75b}$$

for $|\nu|\to\infty$ and $|\arg\nu|<\pi$.

According to the definitions (4-71d), we have $-\frac{3\pi}{2}<\arg\nu<0$, in the range $-\pi<\arg\lambda<\frac{\pi}{2}$. and the upper sign in Eq. (4-75a) is chosen. In the range

$-\frac{3\pi}{2}<\arg\lambda<-\pi$ we have $0<\arg\nu<\frac{\pi}{2}$, and the lower sign in Eq. (4-75a) is chosen. In this way Eqs. (4-74a, b) yield:

$$g_\eta(\eta,\eta';\lambda)\sim\frac{1}{2\sqrt{\lambda}}\left[e^{-\sqrt{\lambda}|\eta-\eta'|}-e^{-\sqrt{\lambda}\,(\eta+\eta'-2\eta_o)}\right],\ -\pi<\arg\lambda<\frac{\pi}{2} \tag{4-76a}$$

$$g_\eta(\eta,\eta';\lambda)\sim\frac{-1}{2\sqrt{\lambda}}\left[e^{\sqrt{\lambda}|\eta-\eta'|}-e^{\sqrt{\lambda}\,(\eta+\eta'-2\eta_o)}\right],\ -\frac{3\pi}{2}<\arg\lambda<-\pi \tag{4-76b}$$

which, in view of the fact that $\eta+\eta'>2\eta_o$, is exponentially small throughout the indicated region. Special care is needed in the interval $-\pi<\arg\lambda<-\frac{\pi}{2}$ which corresponds to $-\frac{3\pi}{2}<\arg\nu<-\pi$. In that range Eq. (4-75b) cannot be used directly. Nevertheless one can define $\nu'=|\nu'|e^{i(\psi-2\pi)}$, where $\psi=\arg\nu$ and find the asymptotic behavior of $\Gamma(\nu)$ from the definition of that function[30]. By doing so, Eq. (4-76a) is shown to hold over the whole region of $-\pi<\arg\lambda<\frac{\pi}{2}$. Similarly, two independent solutions of the homogeneous equation (4-70b) are given by

$$h_1(\xi;\lambda) = D_{-\frac{1}{2}+\frac{i\lambda}{2k}}(\xi\sqrt{-2ik}) \tag{4-77a}$$

$$h_2(\xi;\lambda) = D_{-\frac{1}{2}+\frac{i\lambda}{2k}}(-\xi\sqrt{-2ik}) \tag{4-77b}$$

with

$$W[h_1,h_2] = h_1h_2'-h_2h_1' = \frac{2\sqrt{-i\pi k}}{\Gamma\left(\frac{1}{2}-\frac{i\lambda}{2k}\right)}\ . \tag{4-77c}$$

From Eq. (4-72a) it is easy to see that h_1 is proportional to e^{ikR} as $\xi\to+\infty$, and h_2 is proportional to e^{ikR} as $\xi\to-\infty$, thus[29]

$$g_\xi(\xi,\xi';\lambda) = \frac{h_1(\xi_>;\lambda)h_2(\xi_<;\lambda)}{W[h_1,h_2]}\ , \tag{4-77d}$$

with $\xi_>$ and $\xi_<$ defined as in Eqs. (4-74). The exponential decay of g_ξ as

$|\lambda| \to \infty$ can be shown in a way similar to the one used for g_η.

The singularities of g_ξ in the complex λ plane arise from the poles of the Γ function. g_ξ has a series of poles at

$$\lambda_n = -ik(2n+1), \quad n = 0, 1, 2\ldots$$

g_η does not have poles at $\lambda_n = ik(2n+1)$, because at these points

$$D_{-\frac{1}{2}-\frac{i\lambda}{2k}}(-\eta_< h) + D_{-\frac{1}{2}-\frac{i\lambda}{2k}}(\eta_< h) \left.\frac{D'_{-\frac{1}{2}-\frac{i\lambda}{2k}}(-\eta_o h)}{D'_{-\frac{1}{2}-\frac{i\lambda}{2k}}(\eta_o h)}\right|_{\lambda=\lambda_n} = 0$$

This can be shown by using the relations[11]

$$D'_\nu(z) = \tfrac{z}{2} D_\nu(z) - D_{\nu+1}(z) \ ,$$

valid for any complex ν and z, and

$$D_\nu(-z) = (1)^\nu D_\nu(z), \quad \nu = 0, 1, 2\ldots$$

Nevertheless, g_η has poles in the complex λ plane at those points where

$$D_{-\frac{1}{2}-\frac{i\lambda_p}{2k}}(\eta_o h) = 0 \qquad (4\text{-}78a)$$

The values λ_p have been calculated by Keller and Levy[32]. Their asymptotic values for $k\eta_o^2 \gg 1$ are

$$\lambda_p \sim k^2\eta_o^2\left[1 + 2\tau_p(k\eta_o^2)^{-2/3}\right] \qquad (4\text{-}78b)$$

where τ_p is defined by Eqs. (4-56c, d). The path of integration runs along the real axis from $\lambda = -\infty + is$ to $\lambda = +\infty + is$ with $-k < s < 0$, and closes by a semicircle on either the left or the right. Due to the exponential decay of g_η and g_ξ as $|\lambda| \to \infty$, the semicircle does not contribute to the integral. Defining

$$\mu = -\frac{1}{2}+\frac{i\lambda}{2k} \tag{4-79a}$$

and using the relation

$$\Gamma(-\nu)\Gamma(1+\nu) = \frac{-\pi}{\sin\pi\nu} \tag{4-79b}$$

Eq. (4-69) yields explicitly

$$G = G_1+G_2 =$$

$$= \frac{1}{2}\int_{-\frac{1}{2}-i\infty}^{-\frac{1}{2}+i\infty} \frac{d\mu}{\sin\mu\pi} D_\mu(\xi_> h) D_\mu(-\xi_< h) D_{-\mu-1}(\eta_> h)\left[D_{-\mu-1}(-\eta_< h)+D_{-\mu-1}(\eta_< h)\frac{D'_{-\mu-1}(-\eta_o h)}{D'_{-\mu-1}(\eta_o h)}\right] \tag{4-80}$$

Eq. (4-80) is a rigorous solution of the problem formulated in Eqs. (4-65)*. The solution of the original anisotropic problem stated in Eqs. (4-61) is obtained by expressing the η, ξ variables in terms of x and y. From Eqs. (4-66), (4-64), (4-63) and (4-62) one finds

$$\eta\sqrt{k} = \sqrt{k(R+v)} = \sqrt{k\sqrt{x^2+\hat{y}^2/\epsilon}+\hat{y}/\epsilon} =$$

$$= \sqrt{k_o\left[\sqrt{y^2+\epsilon x^2+\frac{\epsilon y}{b}+\frac{\epsilon^2}{4b^2}}+y+\frac{\epsilon}{2b}\right]} \tag{4-81a}$$

$$\xi\sqrt{k} = \sqrt{k(R-v)} = \sqrt{k_o\left[\sqrt{y^2+\epsilon x^2+\frac{\epsilon y}{b}+\frac{\epsilon^2}{4b^2}}-y-\frac{\epsilon}{2b}\right]} \tag{4-81b}$$

If the square roots are defined as positive when real and having positive imaginary parts, then it can be shown that for $0 \le \arg\epsilon \le \pi$

$$-\frac{\pi}{4} \le \arg(\eta\sqrt{-2ik}) \le \frac{\pi}{4} \tag{4-82a}$$

$$-\frac{\pi}{4} \le \arg(\xi\sqrt{-2ik}) \le \frac{\pi}{4} \tag{4-82b}$$

*Rice[31] and Jones[24] have discussed the diffraction of plane waves by a parabolic cylinder. Eq. (4-80) can be shown to agree with their expressions when $|R'| \to \infty$. They did not use the characteristic Green's function method for deriving their results.

It can be verified by inspection that Eq. (4-82a) follows from Eq. (4-81a). The derivation of Eq. (4-82b) from Eq. (4-81b) is less obvious. One has to show that $\mathrm{Im}\sqrt{y^2+\epsilon x^2+\epsilon\frac{y}{b}+\frac{\epsilon^2}{4b}} \geq \mathrm{Im}\,\frac{\epsilon}{2b}$. This can be done by observing the fact the x and y are confined to the region exterior to the parabolic cylinder.

Up to this point ϵ has been taken as positive real, thereby implying positive real η, η' and η_o. For a source location as in Fig. 18, ξ' is negative real, whereas ξ may be positive or negative real. Also $\arg(\eta\sqrt{-2ik}) = -\frac{\pi}{4}$, $\arg(-\eta\sqrt{-2ik}) = \frac{3\pi}{4}$, and similarly for the ξ variable. For bounded ν and $|x|\to\infty$, $D_\nu(x)$ is exponentially small in $|\arg(x)| < \frac{\pi}{4}$ and exponentially large in $|\arg(-x)| < \frac{\pi}{4}$. It is seen from Eqs. (4-82) that if ϵ is complex and $\mathrm{Im}\,\epsilon \geq 0$, the asymptotic behavior of $D_\nu(x)$ does not change, and the considerations concerning the radiation condition, which lead to the solution in Eq. (4-80), remain valid. The convergence of the integral (4-80) can also be shown, by using Eqs. (4-82) and (4-75). Thus, since the solution (4-80) of Eqs. (4-67) remains equivalent to that of Eqs. (4-61) when ϵ is complex, use of Eqs. (4-62), (4-63) and (4-64) permits the construction of the solution in the anisotropic medium for $\mathrm{Im}\,\epsilon \geq 0$.

The asymptotic expansion of Eq. (4-80) is different in the various physical regions of figure 19. If the observation point lies in the illuminated region, a direct ray from the source as well as a ray reflected from the obstacle according to the laws of geometrical optics contribute to the field. The direct ray is given by G_1 in Eq. (4-80). The reflected ray may be derived by applying the saddle point method of evaluation to the integral G_2 in Eq. (4-80). If the observation point lies in the shadow region, the first order asymptotic evaluation of G_2 yields an expression similar to the asymptotic expression of G_1, but with an opposite algebraic sign. This indicates the cancellation of the field to the first order. A more detailed calculation of G in terms of the residues in the complex μ (or λ) plane lends itself to an interpretation in terms of diffracted rays. If the observation point lies in the transition region near the boundary between the illuminated and the shadow zones, both methods fail. Actually, in this region, the field cannot be expressed in simple ray terms. A numerical evaluation of the integrals yields a smooth transition function which

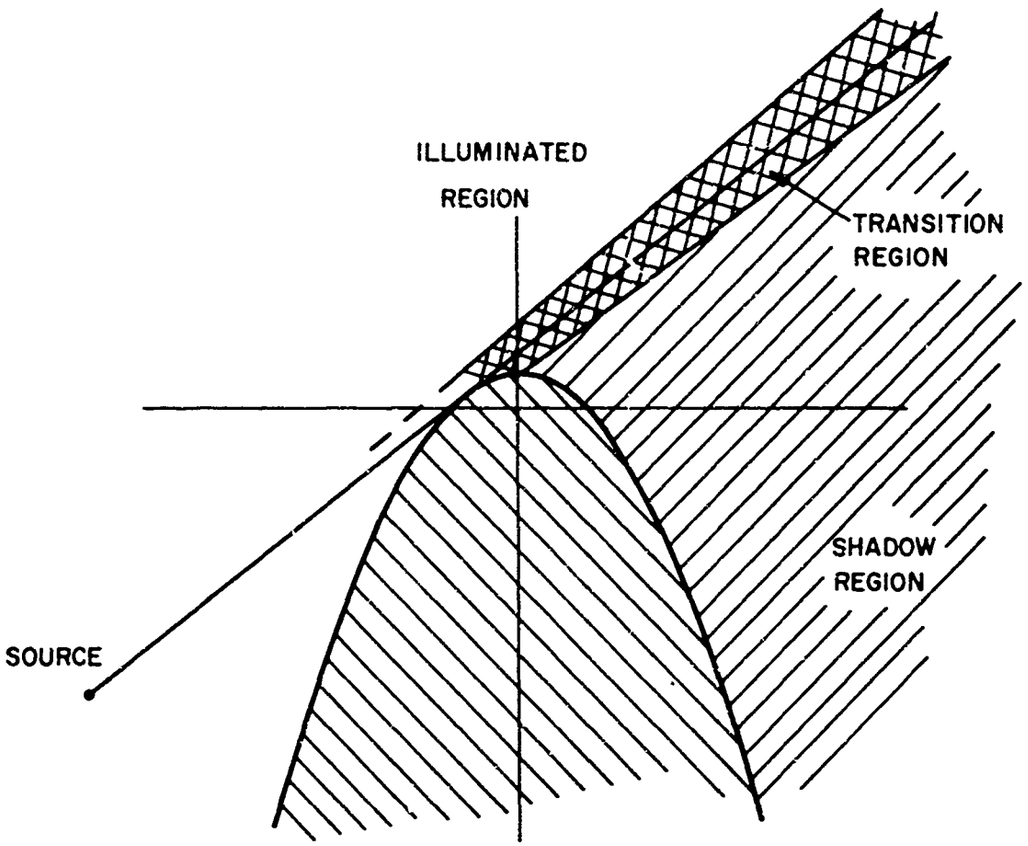

Fig. 19 Diffraction by a parabolic cylinder:
The illuminated, transition and shadow zones.

connects the different asymptotic forms on both sides of the transition zone because the shadow boundary does not introduce any physical discontinuity into the fields.

The asymptotic expression for the diffracted field in the shadow zone is calculated as follows:

The only poles of G to the left of the path of integration in the complex μ plane are given by Eq. (4-78). The path can be closed by an infinite semicircle enclosing the left half plane, and the integral is given exactly by the sum of residues:

$$G = i\pi \sum_{p=0}^{\infty} \frac{1}{\sin\mu_p \pi} D_{\mu_p}(h\xi_>) D_{\mu_p}(-h\xi_<) D_{-\mu_p-1}(h\eta_>) D_{-\mu_p-1}(h\eta_<) \frac{D'_{-\mu_p-1}(-h\eta_o)}{D'_{-\mu_p-1}(h\eta_o)} \qquad (4\text{-}83)$$

If the source point is removed to infinity and the result is normalized in such a way that $\frac{i}{4} H_o^{(1)}(k|\underline{R}-\underline{R}'|) \to \exp\left[-ik(u\sin\varphi' + v\cos\varphi')\right]$, then by using Eqs. (4-66) and (4-72) it can be shown that

$$D_\mu(-h\xi') D_{-\mu-1}(h\eta') \to \frac{(-1)^\mu (\tan\varphi'/2)^\mu}{i2\sqrt{2\pi}\cos\varphi'/2} \quad ; \tan\varphi' = \frac{u'}{v'}$$

The resulting Eq. (4-83) agrees with the expression derived by Rice[31] for the case of plane wave diffraction.

Keller[16] has shown that the exact expression given by Eq. (4-83) can be written asymptotically as

$$G \sim \sqrt{\frac{-2i}{\pi k \bar{d}'}} \sqrt{\frac{-2i}{\pi k \bar{d}}} \exp\left[ik\left(\bar{d}' + \bar{d} + \int_{\bar{Q}_1}^{\bar{P}_1} \bar{d}\ell\right)\right] \cdot$$

$$\cdot \sum_{p=0}^{\infty} \bar{D}_p(P) \bar{D}_p(Q) \exp\left[i\tau_p k^{1/3} \int_P^Q [\bar{b}(\ell)]^{-2/3} d\ell\right], \qquad (4\text{-}84)$$

with $\bar{b}$ denoting the radius of curvature along the diffracted ray path, and $\bar{D}_p$ the diffraction coefficient given by Eq. (4-56a) (see Eq. (4-56) and Fig. 16). It is noted that for complex values of ϵ, these quantities (as well as η, η', ξ and ξ' which are related to them) no longer remain real. Nevertheless, the calculation leading from Eq. (4-83) to Eq. (4-84) remains valid, because (as shown in the discussion following Eq. (4-81)) the same asymptotic forms of the parabolic cylinder functions may still be used when their arguments become complex as long as $\mathrm{Im}\,\epsilon \geq 0$. One may now write the asymptotic expression for G, Eq. (4-84), in terms of the original x-y coordinates by changing back

via Eqs. (4-81). The expression so obtained is exactly the one predicted in the preceding section (Eq. (4-53)), and therefore justifies use of the formula for complex ϵ. It is also shown in reference (16) that the series in Eq. (4-84) is equivalent to that in Eq. (4-83) only if the observation point lies in the shadow region. In the illuminated region, one performs a first order saddle point evaluation of the field using directly the integral representation of Eq. (4-80). For finding the saddle point locations, it is most convenient to substitute into Eq. (4-80) the asymptotic forms of the parabolic cylinder functions which are obtainable by applying the WKBJ method to Eqs. (4-70). The results are:

$$D_{-\frac{1}{2}-\frac{i\lambda}{2k}}(\eta\sqrt{-2ik}) \sim \frac{C_1}{\left[\eta^2-\lambda/k^2\right]^{1/4}} \exp\left[ik\int_{\sqrt{\lambda}/k}^{\eta}\sqrt{x^2-\lambda/k^2}\,dx\right] \qquad (4\text{-}85a)$$

$$D_{-\frac{1}{2}+\frac{i\lambda}{2k}}(\xi\sqrt{-2ik}) \sim \frac{C_2}{\left[\xi^2+\lambda/k^2\right]^{1/4}} \exp\left[ik\int_{0}^{\xi}\sqrt{x^2+\lambda/k^2}\,dx\right]. \qquad (4\text{-}85b)$$

These solutions reduce to Eq. (4-72) if $\eta^2 \gg \lambda/k^2$ and $\xi^2 \gg \lambda/k^2$, respectively, and must therefore have at least the same region of validity in the complex planes of $(\eta\sqrt{-2ik})$ and $(\xi\sqrt{-2ik})$. This assures us that the asymptotic evaluation of the field can be performed in the u-v space, and the result then expressed in terms of x; y. The calculation has been carried out by Jones[24] for the case of plane wave diffraction. Our case differs only in a few details, which are discussed in Appendix H.

F. RIGOROUS ANALYSIS FOR ANOTHER SPECIAL CASE: A CLOSED CYLINDER

Diffraction by a large elliptic cylinder is considered in this section, as a special case of a closed cylinder (Eq. (4-55)). In order to make use of the extensive literature on diffraction by a circular cylinder[22][24][33], an

elliptic cylinder has been chosen whose principal axes are parallel and perpendicular to the optic axis respectively, and related to each other as follows:

$$b = \sqrt{\epsilon}\, a \qquad \alpha = 1, \quad \epsilon > 0 \ , \tag{4-86}$$

where a and b are the half axes of the ellipse in the x and y directions, respectively. Such an elliptic cylinder transforms into a circular cylinder of radius a in the u-v space if we let $x=u$, $y=\sqrt{\epsilon}\, v$ (Fig. 20). While the configuration in Fig. 20 is convenient for the relatively simple confirmation of the assumptions and results of Section D leading to Eq. (4-55), it lacks in generality since the obstacle dimensions depend on the medium parameter ϵ. This model therefore does not permit the independent investigation of the solution as ϵ takes on complex values, as was possible in previous sections. However, this model is employed to test in detail another aspect of the procedure: the ability to apply the scale transformation to the asymptotic expressions in the isotropic region, and to recover therefrom the asymptotic result for the anisotropic case. The boundary value problem to be solved is the same as in Eqs. (4-61) with S given by the equation

$$\frac{x^2}{a^2} + \frac{y^2}{\epsilon\, a^2} = 1 \ . \tag{4-87}$$

Transformed into the u-v space, the boundary value problem to be solved is

$$\left(\frac{\partial^2}{\partial u^2} + \frac{\partial^2}{\partial v^2} + k^2\right) G(\underline{R}, \underline{R}') = -\delta(u-u')\, \delta(v-v') \ , \tag{4-88a}$$

$$\frac{\partial G}{\partial \hat{n}} = 0 \quad \text{on} \quad u^2 + v^2 = a^2 \ , \tag{4-88b}$$

$$\text{Radiation condition at } R = \sqrt{u^2+v^2} \to \infty \ . \tag{4-88c}$$

G is defined by Eq. (4-65d), and $k = k_o\sqrt{\epsilon}$. The rigorous solution to Eqs. (4-88) is well known, and various representations are available which have different convergence properties. The representation best suited to our purpose is given by[33]

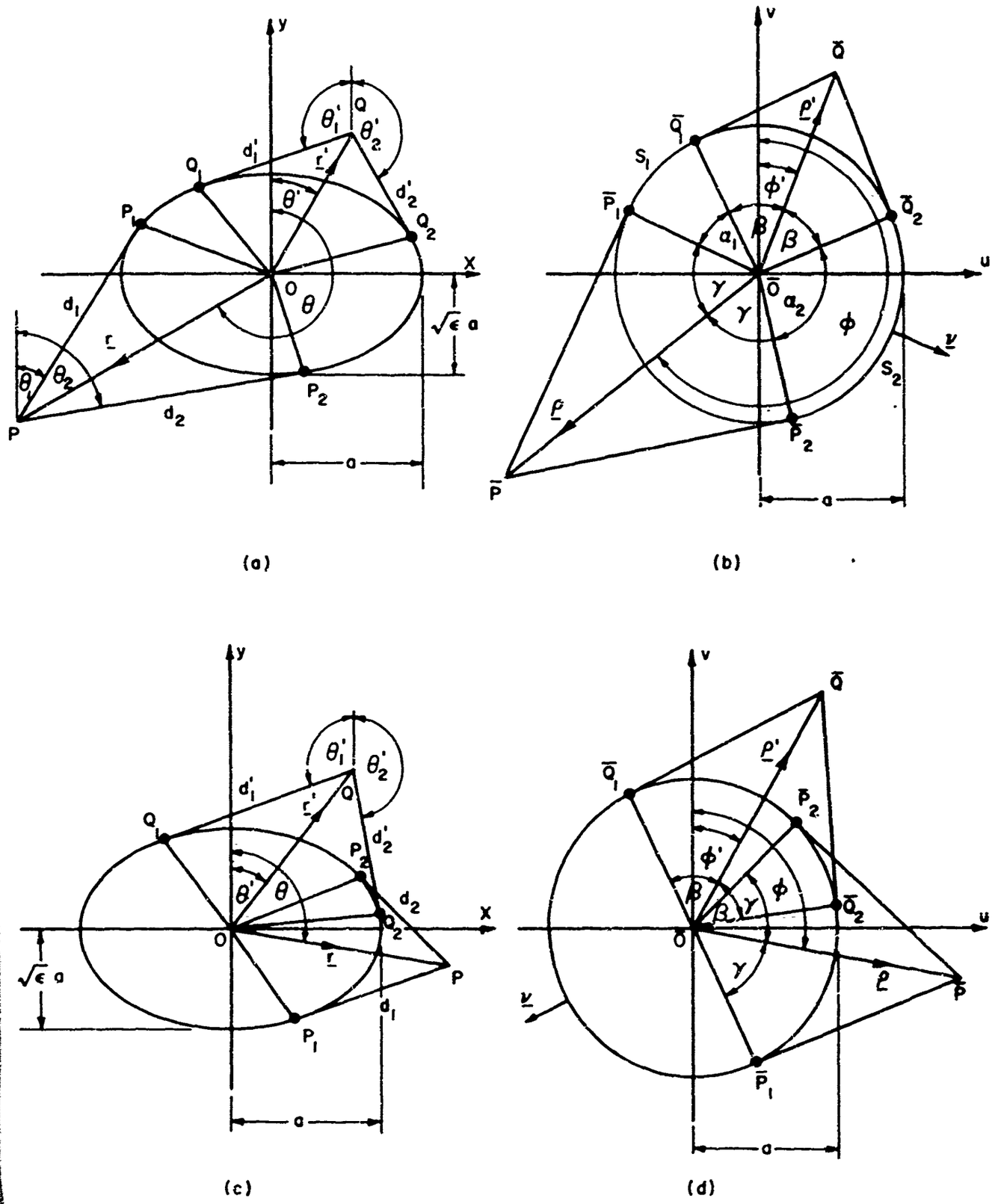

Fig. 20 Diffraction by an elliptic cylinder:
The xy and uv spaces for observation point in the shadow region (a, b) and in the illuminated region (c, d).

$$G(\underline{R},\underline{R}') = \frac{1}{i\pi}\int_C G_\rho(\rho,\rho';\mu)\,G_\varphi(\varphi,\varphi';\mu)\,\mu\,d\mu \tag{4-89}$$

$$\rho = \sqrt{u^2+v^2} \tag{4-89a}$$

$$\rho' = \sqrt{u'^2+v'^2} \tag{4-89b}$$

$$\varphi = \tan^{-1}\frac{u}{v} \tag{4-89c}$$

$$\varphi' = \tan^{-1}\frac{u'}{v'} \tag{4-89d}$$

$$G_\rho(\rho,\rho';\mu) = \frac{\pi i}{4}H_\mu^{(1)}(k\rho_>)\left[H_\mu^{(2)}(k\rho_<) - \frac{H_\mu'^{(2)}(ka)}{H_\mu'^{(1)}(ka)}H_\mu^{(1)}(k\rho_<)\right] \tag{4-89e}$$

$$G_\varphi(\varphi,\varphi';\mu) = \sum_{\ell=-\infty}^{\infty}(\mp 2i\mu)^{-1}\,e^{\pm i\mu|\varphi-(\varphi'+2\pi\ell)|};\quad \mathrm{Im}\,\mu \gtrless 0 \tag{4-89f}$$

$$H_\mu'^{(2)}(z) = \frac{\partial}{\partial z}H_\mu^{(2)}(z)\quad . \tag{4-89g}$$

Eq. (4-89) may alternatively be written in terms of a series of residues arising from the poles of the integrand, which are located at the points $\mu=\mu_p$, where

$$H_{\mu_p}'^{(1)}(ka) = 0\quad . \tag{4-90a}$$

These points have been calculated by several investigators[16][22] and for $ka \gg 1$, they are given asymptotically by

$$\mu_p \approx ka + \tau_p(ka)^{\frac{1}{3}}\quad , \tag{4-90b}$$

where τ_p are defined by Eq. (4-56c), and for the Neumann type boundary conditions

$$\tau_p \approx \frac{1}{2}\left[3\pi\left(p+\frac{1}{4}\right)\right]^{\frac{2}{3}} e^{i\frac{\pi}{3}} \quad , \quad p = 1, 2 \ldots \quad . \tag{4-90c}$$

In view of Eq. (4-89f), $G(\underline{\rho}, \underline{\rho}')$ can be interpreted as the field which results from an infinite number of line sources located in an angular space of infinite extent $(-\infty<\varphi<\infty)$ and separated from one another by a distance of 2π. Evidently, only one line source lies in the physical region $0\leq\varphi\leq 2\pi$, and this source alone accounts for the geometric optical parts of the total field. The sources outside the physical region of the angular space contribute only to the diffraction effects.

Eq. (4-89) may now be transformed back to the x-y space, (where it is a solution of Eqs. (4-61) and (4-87), and evaluated asymptotically. The details of this calculation are given in appendix I. It should be noted that the solution as given by Eq. (4-89) has different convergence properties, according to whether the observation point is located in a geometrically illuminated, or in a shadow region. Thus, the asymptotic evaluation and physical interpretation of the results are different from one another in those regions. If the observation point lies in the shadow region, then the total field is equal to the diffracted field. In that case it can be shown that Eq. (4-89) becomes[33]

$$G(\underline{R}, \underline{R}') = \frac{\pi}{2} \sum_p \frac{H'^{(2)}_{\mu_p}(ka)}{\frac{\partial}{\partial\mu} H'^{(1)}_{\mu}(ka)\Big|_{\mu_p}} H^{(1)}_{\mu_p}(k\rho) H^{(1)}_{\mu_p}(k\rho') \left[\sum_{\ell=-\infty}^{\infty} e^{i\mu_p|\varphi-(\varphi'+2\pi\ell)|}\right] , \tag{4-91}$$

whose asymptotic evaluation for $ka \gg 1$ (after transforming back to the x-y space) is carried out in appendix I and yields:

$$G = \sum_{p=1}^{\infty} \frac{-\frac{}{2\sqrt{2}} e^{i\frac{\pi}{3}} (ka)^{\frac{1}{3}}}{6^{\frac{1}{3}}\left[q_p A(q_p)\right]^2} \left[\frac{\exp\left\{ik_o\left[d_1 N(\theta_1)+d'_1 N(\theta'_1)+i\mu_p\frac{S_1}{a}\right]\right\}}{\sqrt{k_o d_1 N(\theta_1)}\sqrt{k_o d'_1 N(\theta'_1)}\left[1-e^{i2\pi\mu_p}\right]}\right. +$$

$$+ \frac{\exp\left\{ik_o\left[d_2 N(\theta) + d_2' N(\theta_2') + i\mu_p \frac{S_2}{a}\right]\right\}}{\sqrt{k_o d_2 N(\theta_2)}\sqrt{k_o d_2' N(\theta_2')}\left[1 - e^{i2\pi\mu_p}\right]}\Bigg] \tag{4-92}$$

where S_1 and S_2 are the arc lengths Q_1P_1 and Q_2P_2 (Fig. 20a), respectively, and $A(q_p)$ is the Airy function of argument q_p defined in Eq. (4-56d). Eq. (4-92) should be compared with Eq. (4-55).

To show that Eqs. (4-92) and (4-55) are identical, one notes first from Eq. (4-57a)

$$S_{1,2} = \int_{\overline{Q}_{1,2}}^{\overline{P}_{1,2}} \sqrt{du^2 + dv^2} = \frac{1}{\sqrt{\epsilon}} \int_{Q_{1,2}}^{P_{1,2}} N[\theta(\ell)]\, d\ell \tag{4-93}$$

Thus, from Eqs. (4-90), (4-92) and (4-93)

$$i\mu_p \frac{S_{1,2}}{a} = ik_o \int_{Q_{1,2}}^{P_{1,2}} N[\theta(\ell)]\, d\ell + ik_o^{\frac{1}{3}} \epsilon^{\frac{1}{3}} \tau_p \int_{Q_{1,2}}^{P_{1,2}} \frac{N[\theta(\ell)]}{\epsilon^{\frac{2}{3}} a^{\frac{2}{3}}}\, d\ell \tag{4-94}$$

From

$$\frac{\left[1 + \left(\frac{dy}{dx}\right)^2\right]^{\frac{3}{2}}}{\left|\frac{d^2y}{dx^2}\right|} = b(\ell) \quad , \tag{4-95}$$

(where $b(\ell)$ is the radius of curvature of the cylinder at ℓ), and the equation of the cylinder,

$$y = \pm\sqrt{\epsilon}\sqrt{a^2 - x^2} \tag{4-96}$$

it is not difficult to verify via Eq. (4-57a) that

$$\frac{N[\theta(\ell)]}{\epsilon^{\frac{2}{3}}\, a^{\frac{2}{3}}}\, d\ell = \frac{d\ell}{N[\theta(\ell)]\, b^{\frac{2}{3}}(\ell)} , \tag{4-97}$$

thereby confirming the structure of the exponent in Eq. (4-55) with Eq. (4-59). Moreover, from Eqs. (4-96) and (4-57a), it is noted that

$$N\, d\ell = \sqrt{\epsilon}\, a\, \frac{dx}{a^2 - x^2} \tag{4-98a}$$

so that

$$\oint N\, d\ell = 2\pi a \sqrt{\epsilon} \tag{4-98b}$$

where the $\oint$ is taken around the circumference of the cylinder. Thus, using Eqs. (4-59), (4-90b) and (4-98),

$$i 2\pi\mu_p = \oint \left\{ i k_o N[\theta(\ell)] - \alpha(\ell) \right\} d\ell \tag{4-99}$$

thereby making the denominators in Eqs. (4-55) and (4-92) equal. In a similar manner, the amplitude factor in Eq. (4-92) may be identified as the diffraction coefficient D_p. It has therefore been verified in this special case that the asymptotic evaluation of the scaled exact solution agrees with the result obtained when the scale transformation is applied directly to the asymptotic formula in the isotropic region.

If the observation point lies in the illuminated region, the field consists of a geometric optical part due to the $\ell = 0$ term in Eq. (4-89) and a diffracted part due to the $\ell \neq 0$ terms. Thus one may write in this region

$$G(\underline{R}, \underline{R}') = \frac{1}{\pi i} \int_{-\infty}^{\infty} G_\rho(\rho, \rho'; \mu)\, G_{\varphi_o}(\varphi, \varphi'; \mu)\, \mu\, d\mu \; +$$

$$+ \frac{\pi}{2} \sum_p \frac{H_{\mu_p}^{(2)}(ka)}{\frac{\partial}{\partial\mu} H_\mu^{(1)}(ka)\Big|_{\mu_p}} H_{\mu_p}^{(1)}(k\rho) H_{\mu_p}^{(1)}(k\rho') \left[\sum_{\ell=-\infty}^{\infty}{}' e^{i\mu_p |\varphi - (\varphi' + 2\pi\ell)|} \right] \tag{4-100}$$

where $\sum'$ stands for a summation over all integers ℓ excluding $\ell = 0$, and

$$G_{\varphi_o}(\varphi,\varphi';\mu) = \frac{e^{i\mu|\varphi-\varphi'|}}{-2i\mu} \tag{4-100a}$$

The series part of Eq. (4-100) is treated exactly as in Eq. (4-91) and leads to Eq. (4-92), except that the quantities d_1, d_1', d_2, S_1, S_2, etc. have to be taken now from Figs. (20c) and (20d). The integral in Eq. (4-100) furnishes the geometric-optical field.

It has therefore been verified that Eq. (4-92), which was obtained by performing the asymptotic evaluation in the anisotropic region, agrees with the previously derived Eq. (4-55) wherein the asymptotic result was obtained in the isotropic (scaled) system, with the scale transformation applied subsequently.

CHAPTER V

CONCLUDING REMARKS

The object of this study has been to gain an understanding of electromagnetic radiation and diffraction in anisotropic dielectric media. Emphasis has been placed not only on formal mathematical solutions but on approximate methods for the evaluation of explicit results as well as on a physical interpretation of relevant phenomena.

To achieve these aims, a special class of problems has been investigated in detail: two-dimensional problems of diffraction by variously shaped objects in a uniaxially anisotropic dielectric. By choosing the optic axis in the medium at right angles with respect to the axis of the cylindrical scatterers, one finds that the electromagnetic fields may be determined from a single scalar function, thereby reducing substantially the mathematical complexity and facilitating a thorough study of the resulting formal solutions. Two parameter ranges have received special consideration, corresponding, respectively, to "small" and "large" obstacle dimensions. In the first, the scattering properties are described essentially by multipoles of appropriate strength and orientation, while in the second, the radiation characteristics are specified conveniently in ray-optical terms. In each category, various representative problems, for which exact solutions may be constructed, have been analyzed in detail, and the results have been phrased in such a manner as to lend support to the above-mentioned physical mechanisms which are operative in establishing the radiation field.

A scaling method[2] may be employed to relate solutions for the present class of scattering problems in the anisotropic medium to equivalent, known solutions in an isotropic region when the dielectric tensor elements are positive real. Therefore, for this parameter range, the construction of solutions is elementary, and the remaining task has been an "invariant" phrasing of the results so as to include quantities which depend only and explicitly on the medium parameters, and on such structural features as the radius of curvature

of the obstacle surface and its orientation with respect to the optic axis. Further and non-trivial effort has been required to extend the range of validity of the results to complex values of the tensor elements, thereby providing solutions for a broad range of medium constants, including the "hyperbolic" range where one of the tensor elements is negative real and infinite values of refractive index may occur.

The results for various large obstacle problems have been compared with predictions made by generalizing Keller's geometrical theory of diffraction to anisotropic media. Since that theory proceeds on a ray-optical basis which retains its validity under quite general conditions, its confirmation for several special structures admitting of an exact analysis provides a basis of support similar to that achieved for the isotropic case. It may therefore be concluded that the present study has provided a general mechanism for the analysis of two-dimensional diffraction problems in uniaxially anisotropic media having the afore-mentioned orientation of the optic axis, and that the insight gained thereby may serve as a basis for the investigation of more complicated situations.

APPENDIX A

Derivation of the Green's function representation in elliptical coordinates (Eq. (3-11)).

The boundary value problem stated in Eqs. (3-8) is transformed via Eqs. (3-9a, b) into

$$\left[\frac{\partial^2}{\partial\xi^2}+\frac{\partial^2}{\partial\eta^2}+2h^2(\cosh 2\xi-\cos 2\eta)\right]G(\underline{R},\underline{R}') = -\delta(\xi-\xi')\,\delta(\eta-\eta') \,, \tag{A-1a}$$

$$\frac{\partial G}{\partial \xi} = 0 \quad \text{on} \quad \xi=\xi_o \,, \tag{A-1b}$$

$$\text{Radiation condition at} \quad 2h\cosh\xi \to \infty \,, \tag{A-1c}$$

where h is defined by Eq. (3-10a) and Fig. 4. The homogeneous equation (A-1a) can be separated, yielding

$$-\frac{d^2u_1}{d\xi^2}+(\lambda-2h^2\cosh 2\xi)\,u_1 = 0 \tag{A-2a}$$

$$\frac{d^2u_2}{d\eta^2}+(\lambda-2h^2\cos 2\eta)\,u_2 = 0 \tag{A-2b}$$

with λ denoting a separation constant. $U_2(\eta)$ has to be periodic in η with a period of 2π. This is one of the properties of the Mathieu functions of the first kind and integral order[9], $ce_m(\eta;h^2)$, $se_m(\eta;h^2)$, and $me_m(\eta;h^2)$ which is related to the former via Eqs. (3-18a, b). We note the completeness relation of these Mathieu functions,

$$\delta(\eta-\eta') = \frac{1}{2\pi}\sum_{m=-\infty}^{\infty} me_m(\eta')\,me_m(-\eta) \,. \tag{A-3}$$

We may assume an eigenfunction expansion

$$G(\underline{R};\underline{R}') = G(\xi,\eta;\xi',\eta') = \sum_{m=-\infty}^{\infty} g_m^o(\xi,\xi')\, me_m(-\eta) \quad . \tag{A-4}$$

Substituting Eq. (A-4) in Eq. (A-1a) and using Eqs. (A-2b) and (A-3) we get

$$\left(\frac{d^2}{d\xi^2} - \lambda + 2h^2\cosh 2\xi\right) g_m(\xi,\xi') = -\delta(\xi-\xi') \tag{A-5}$$

where

$$g_m(\xi,\xi') = -\frac{2\pi}{me_m(\eta')}\, g_m^o(\xi,\xi') \tag{A-5a}$$

The boundary conditions on $g_m(\xi,\xi')$ are

$$\frac{dg_m}{d\xi} = 0 \quad \text{at} \quad \xi=\xi_o \quad , \tag{A-5b}$$

$$\text{Radiation condition at} \quad \xi\to\infty \quad . \tag{A-5c}$$

Solutions of the homogeneous equation (A-5) are the "radial" Mathieu functions[10] $M_m^{(j)}(\xi;h)$. In particular, for our implied time dependence of $e^{-i\omega t}$, the pair of suitable functions is $M_m^{(1)}(\xi)$ and $M_m^{(3)}(\xi)$, which has the asymptotic behavior for $\xi\to\infty$,

$$M_m^{(1)}(\xi;h) \sim J_m(2h\cosh\xi) = J_m(kR) \quad , \tag{A-6a}$$

$$M_m^{(3)}(\xi;h) \sim H_o^{(1)}(2h\cosh\xi) = H_o^{(1)}(kR) \quad . \tag{A-6b}$$

Their Wronskian is given by

$$W\left[M_m^{(1)}(\xi;h),\ M_m^{(3)}(\xi;h)\right] = \frac{2i}{\pi} \quad . \tag{A-6c}$$

If we define

$$f_1(\xi) = M_m^{(3)}(\xi_>;h) \quad , \tag{A-7a}$$

$$f_2(\xi) = M_m^{(1)}(\xi_<;h) - \frac{M'^{(1)}_m(\xi_o;h)}{M'^{(3)}_m(\xi_o;h)}\, M_m^{(3)}(\xi_<;h) \quad , \tag{A-7b}$$

it is easy to show that

$$W\left[f_1, f_2\right] = W\left[M_m^{(1)}, M_m^{(3)}\right] = \frac{2i}{\pi} \quad , \tag{A-7c}$$

where $\xi_>$ and $\xi_<$ are defined by Eqs. (3-11a, b).

The solution of Eq. (A-5) subject to conditions (A-5b, c) is synthesized from f_1 and f_2 in the usual way[29]:

$$g_m(\xi, \xi') = \frac{f_1(\xi_>) f_2(\xi_<)}{W\left[f_1, f_2\right]} \; ; \tag{A-8}$$

thus, from Eqs. (A-4), (A-5a) and (A-8), we get Eq. (3-11).

APPENDIX B

The quadrupole radiation in the field scattered by a narrow strip.

From Eqs. (3-19), (3-20b) and (3-20d) we see that

$$g_2(\varphi,\varphi') = -\frac{\pi h^4}{4}\sin 2\varphi \sin 2\varphi' + O(h^6) \quad ; \tag{B-1}$$

also, using Eqs. (3-22), we have

$$\cos\varphi = \frac{U}{R} = \frac{u\cos\delta + v\sin\delta}{R} = \frac{\frac{x}{\sqrt{\alpha}}\sqrt{\epsilon}\sin\theta_o + \frac{y}{\sqrt{\epsilon}}\sqrt{\alpha}\cos\theta_o}{r\,N(\theta_o)N(\theta)}\sqrt{\alpha\epsilon} =$$

$$= \frac{\epsilon\sin\vartheta\sin\theta_o + \alpha\cos\vartheta\cos\theta_o}{N(\vartheta_o)N(\vartheta)} \tag{B-2}$$

$$\sin 2\varphi = 2\sin\varphi\cos\varphi = 2\sqrt{\alpha\epsilon}\,\frac{\sin(\theta_o-\theta)(\epsilon\sin\vartheta\sin\theta_o + \alpha\cos\vartheta\cos\theta_o)}{[N(\theta)\,N(\theta_o)]^2} \; . \tag{B-3}$$

An expression similar to (B-3), with ϑ' instead of ϑ, is obtained for $\sin 2\varphi'$. Using Eqs. (3-17a), (B-1) and (B-3) we get

$$g_2 \sim -\frac{\pi\alpha\epsilon}{64}(k_o a)^4\,\frac{\sin(\vartheta_o-\vartheta)\sin(\vartheta_o-\vartheta')}{[N(\vartheta)\,N(\vartheta')]^2}(\epsilon\sin\vartheta\sin\vartheta_o + \alpha\cos\vartheta\cos\theta_o)\cdot$$

$$\cdot\,(\epsilon\sin\vartheta'\sin\theta_o + \alpha\cos\vartheta'\cos\vartheta_o) + O(k_o a)^6 \tag{B-4}$$

To verify that Eq. (B-4) represents the radiation from an electric quadrupole line source, and to find the quadrupole radiation intensity in the scattered field (Eqs. (3-15)), consider Eqs. (3-24a, b) with the source term

$$\underline{J} = \underline{p}\,(\cos\vartheta_o\,\frac{\partial}{\partial y} + \sin\vartheta_o\,\frac{\partial}{\partial x})\,\delta(\underline{r}) \; . \tag{B-5}$$

Comparison of Eqs. (B-5) and (3-24c) shows that the source given by Eq. (B-5) corresponds to a linear quadrupole as shown in Fig. B-1.

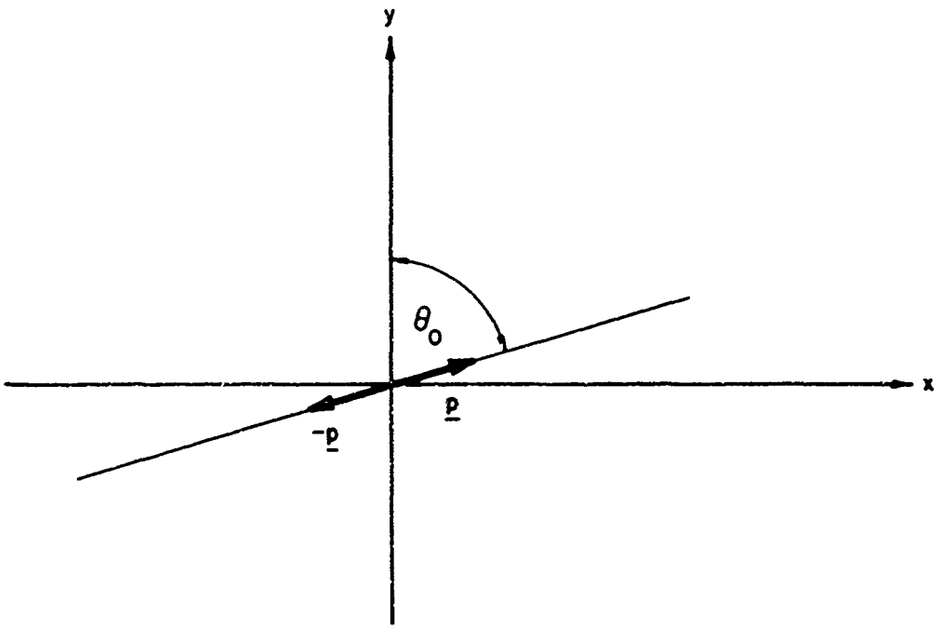

Fig. B-1 A linear quadrupole as a superposition of two dipoles.

Substituting Eq. (B-5) into Eqs. (3-24a, b) yields the following equation for H:

$$\left[\alpha \frac{\partial^2}{\partial x^2} + \epsilon \frac{\partial^2}{\partial y^2} + k^2\right] H = -B\,\delta(\underline{r}) \tag{B-6a}$$

where

$$B = p\left[\sin\vartheta_o \cos\vartheta_o \left(\alpha \frac{\partial^2}{\partial x^2} - \epsilon \frac{\partial^2}{\partial y^2}\right) + \left(\alpha \cos^2\theta_o - \epsilon \sin^2\theta_o\right) \frac{\partial^2}{\partial x\,\partial y}\right] \tag{B-6b}$$

If we consider H=BG, then the equation for G reduces to Eq. (3-8), whose solution, subject to a radiation condition at infinity, has already been given by $G_d(\underline{r}, o)$ in Eqs. (3-13). Thus, the solution of Eq. (B-6a) is

$$H(\underline{r}) = \frac{i}{4} B H_o^{(1)}\left[k_o \sqrt{\alpha y^2 + \epsilon x^2}\right] \tag{B-7a}$$

For $k_o r N(\vartheta) >> 1$ one may write

$$\frac{\partial^2}{\partial z^2} H_o^{(1)}(z) \sim H_2^{(1)}(z) \sim -H_o^{(1)}(z) \quad .$$

The derivation of Eq. (B-7b) from Eq. (B-7a) is analogous to the derivation of Eq. (3-29),

$$H(\underline{r}) \sim k_o^2 p \alpha \epsilon \frac{\sin(\hat{\theta}_o - \hat{\theta})}{N^2(\hat{\theta})} (\epsilon \sin\hat{\theta} \sin\theta_o + \alpha \cos\theta \cos\theta_o) \left\{ \frac{i}{4} H_o^{(1)}[k_o r N(\theta)] \right\} \tag{B-7b}$$

Comparison of Eqs. (B-7b) and (B-4) yields

$$p = -A_o \left[\frac{i\pi}{16} \frac{(k_o a)^4}{k_o^2} \frac{\sin(\hat{\theta}_o - \hat{\theta}')(\epsilon \sin\hat{\theta}' \sin\theta_o + \alpha \cos\theta' \cos\theta_o)}{N^2(\theta')} + O(k_o a)^6 \right] \tag{B-8}$$

where A_o is the intensity of the incident field at the location of the obstacle. Eq. (B-7b) shows that the leading term of g_2 in Eq. (B-4) is a linear quadrupole term, and Eq. (B-8) gives the intensity of the quadrupole induced in the strip by the incident field. It is easy to see from Eq. (B-7b) that the axes of zero radiation in the quadrupole radiation pattern are no longer perpendicular to each other. While one zero occurs at $\hat{\theta} = \hat{\theta}_o$, the other zero occurs at $\tan\hat{\theta} = -\frac{\alpha}{\epsilon} \cot\hat{\theta}_o$, which reduces to $\hat{\theta} = \hat{\theta}_o = \frac{\pi}{2}$ only when $\frac{\alpha}{\epsilon} = 1$ (isotropic case), or when $\hat{\theta}_o = 0, \frac{\pi}{2}$ (special orientation of the strip).

APPENDIX C

Reflection by a perfectly conducting plane in a homogeneous uniaxial medium.

To derive Eq. (4-10) from Eq. (4-1), consider Fig. 8. A ray passes through the point P(0, 0), is reflected at the point C(x, y) and then passes through the point Q(d, 0). Then,

$$\int_P^C N d\ell + \int_C^Q N d\ell = \int_P^C \sqrt{\cos^2\theta_1 + \epsilon \sin^2\theta_1}\ \frac{dy}{\cos\theta_1} + \int_C^Q \sqrt{\cos^2\theta_2 + \epsilon \sin^2\theta_2}\ \frac{dy}{\cos\theta_2}$$

$$= \sqrt{y^2 + \epsilon x^2} + \sqrt{y^2 + \epsilon (x-d)^2} = L(x, y) \qquad (C\text{-}1)$$

The variables x, y are subject to the constraint of lying on the conducting plane, i. e.,

$$f(x, y) = Bx + Ay - AB = 0 \qquad (C\text{-}2)$$

The equation which gives the extremum of (C-1) with the constraint (C-2) is

$$\begin{vmatrix} \frac{\partial L}{\partial x} & \frac{\partial L}{\partial y} \\ \frac{\partial f}{\partial x} & \frac{\partial f}{\partial y} \end{vmatrix} = A\left[\frac{\epsilon x}{\sqrt{y^2 + \epsilon x^2}} + \frac{\epsilon(x-d)}{\sqrt{y^2 + \epsilon(x-d)^2}}\right] -$$

$$- B\left[\frac{y}{\sqrt{y^2 + \epsilon x^2}} + \frac{y}{\sqrt{y^2 + \epsilon x^2}}\right] = 0 \qquad (C\text{-}3)$$

Substituting

$$\frac{x}{y} = \tan\theta_1\ ,\ \frac{x-d}{y} = \tan\theta_2,\ -\frac{A}{B} = \tan\theta_o \text{ and } \theta_i = \theta_1 + \pi;\ \theta_r = \theta_2$$

one gets from Eq. (C-3),

$$(\tan\theta_i - \tan\theta_r)\left[(\epsilon \tan^2\theta_o - 1)(\tan\theta_i + \tan\theta_r) + 2\tan\theta_o(\epsilon \tan\theta_i \tan\theta_r + 1)\right] = 0\ , \qquad (C\text{-}4)$$

which, upon exclusion of the case $\tan\vartheta_i = \tan\vartheta_r$, yields Eq. (4-10). In this derivation no restriction has been imposed on ϵ, so that the result is valid also for negative ϵ. While real rays propagate in this instance only when

$$|\tan\vartheta_1| \leq \tan\vartheta_c = \frac{1}{\sqrt{-\epsilon}} \tag{C-5}$$

Eq. (4-10) yields a real ϑ_r for <u>any</u> ϑ_i.

This is in accord with an image technique[2][15] by which the reflected field can be constructed as shown in Fig. C-1. A ray emanating from a source S gives rise to a reflected ray which appears to originate at an image source I. If $\epsilon < 0$, incident rays can propagate only within the wedge ASB.

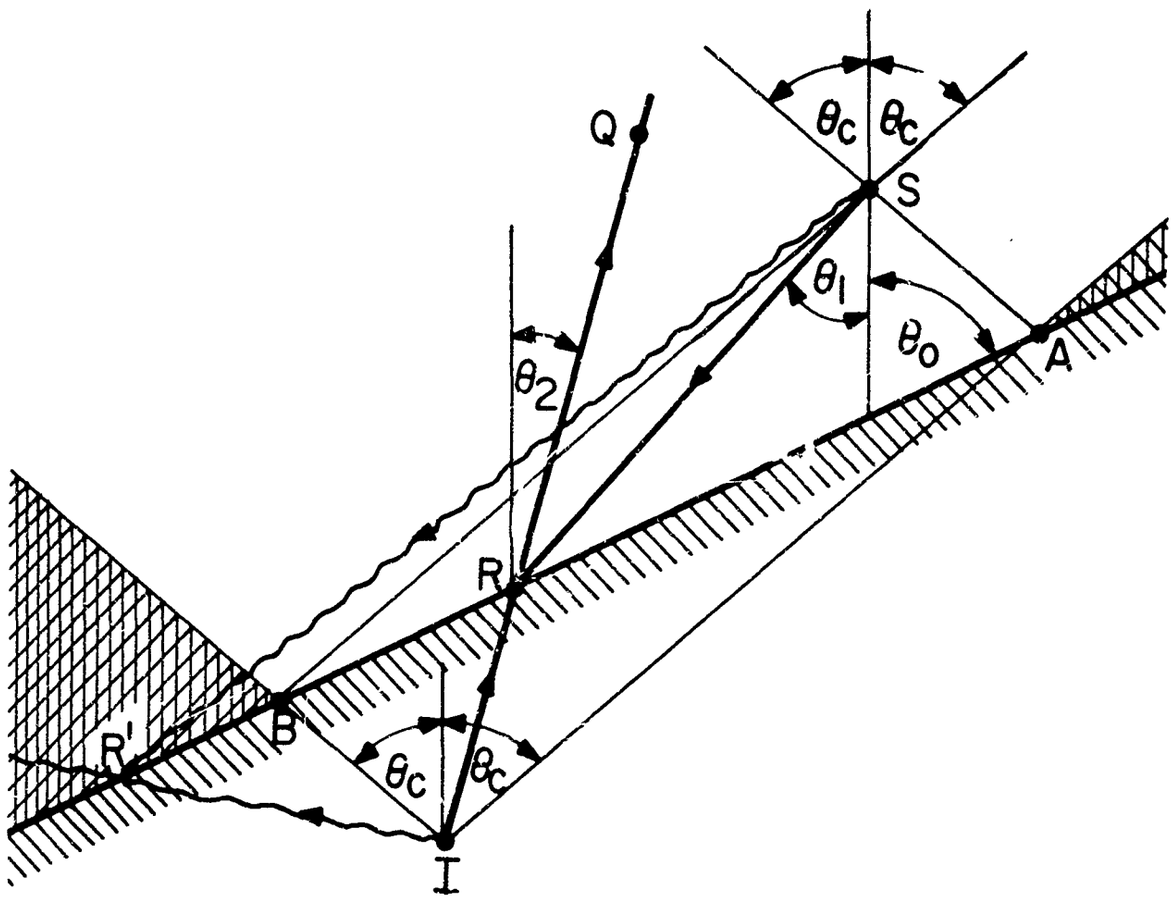

Fig. C-1 Reflection by a perfectly conducting plane.

The image source is then located at the head of the inverted wedge AIB, where the triangles ASB and AIB are congruent (or ASBI is a parallelogram, with the conducting plane as one of its diagonals). By using the sine law in triangle ASB, one gets

$$\frac{\overline{SB}}{\sin(\pi - \theta_c - \theta_o)} = \frac{\overline{SA}}{\sin(\theta_o - \theta_c)} , \qquad (C\text{-}6)$$

and since $\overline{AR}$ is common to triangles ASR and AIR,

$$\overline{AR} = \overline{AI}\,\frac{\sin(\theta_c - \theta_2)}{\sin(\pi - \theta_o + \theta_2)} = \overline{AS}\,\frac{\sin(\theta_c + \theta_1)}{\sin(\theta_o - \theta_1)} . \qquad (C\text{-}7)$$

Upon combining Eqs. (C-7) and (C-6), one may derive an expression connecting θ_1, θ_2, θ_o, and θ_c. If θ_c is eliminated by using Eq. (C-5), one gets precisely Eq. (4-10) relating θ_2 to θ_1, θ_o and ϵ. This confirms that the reflection law derived by Fermat's principle agrees with the one obtained from a solution of the boundary value problem.

The field above the conducting surface is given exactly by the sum of the contributions from the real and image sources, regardless of whether $\theta_1 > \theta_c$ or $\theta_1 < \theta_c$ [2]. If $\theta_1 > \theta_c$, Eq. (4-10) still yields a real θ_2, but then necessarily $|\theta_2| > |\theta_c|$, because an evanescent incident ray giving rise to a propagating reflected ray would violate the principle of conservation of energy. If the incident ray coincides with $\overline{SB}$, i.e. $\theta_i = \theta_c + \pi$, then the reflected ray coincides with IB, i.e. $\theta_r = -\theta_c$. All of this information can be deduced either from the analytic reflection formula in Eq. (4-10) or from the geometric image construction. In dealing with the conducting half-plane problem (sec. C) rather than with an infinite conducting plane, the geometric optical direct and reflected parts of the field can be constructed in the same way. If we assume in Fig. C-1 that the half-plane[2] coincides with that portion of the infinite plane which lies to the left of the point R (i.e., the edge of the half plane is at R), then the reflected ray $\overline{RQ}$ now constitutes the boundary between the region where both direct and reflected rays exist (to the left of $\overline{RQ}$) and the region where only the direct rays exist (to the right of $\overline{RQ}$). As has been shown in Eqs. (4-44), the location of this boundary may also be deduced from the rigorous solution of the problem. The solution for diffraction of a cylindrical wave by a half-plane shows

that the boundary between said regions has to be real even when the edge of the half plane is in the shadow of the source (point R′ in Fig. C-1, for example). Eq. (4-10) confirms that this is so, and that the pole contributions to the fields given by Eqs. (4-36) and (4-45) (see appendix E) yield exactly the geometric optical parts of the field.

δ

APPENDIX D

By solving the boundary value problem of reflection of a cylindrical wave from a perfectly conducting plane ($b \to \infty$) in a uniaxially anisotropic medium, Felsen[15] showed that the reflected field is given asymptotically by

$$|H_r(P)| = \left| \frac{H_o \sqrt{N(\theta_1)}}{\sqrt{N(\theta_1)}\, d' + N(\theta_2)\, d} \right| , \qquad \text{(D-1)}$$

with θ_1, θ_2, d and d′ defined in Fig. D-1, and H_o defined by Eq. (4-16).

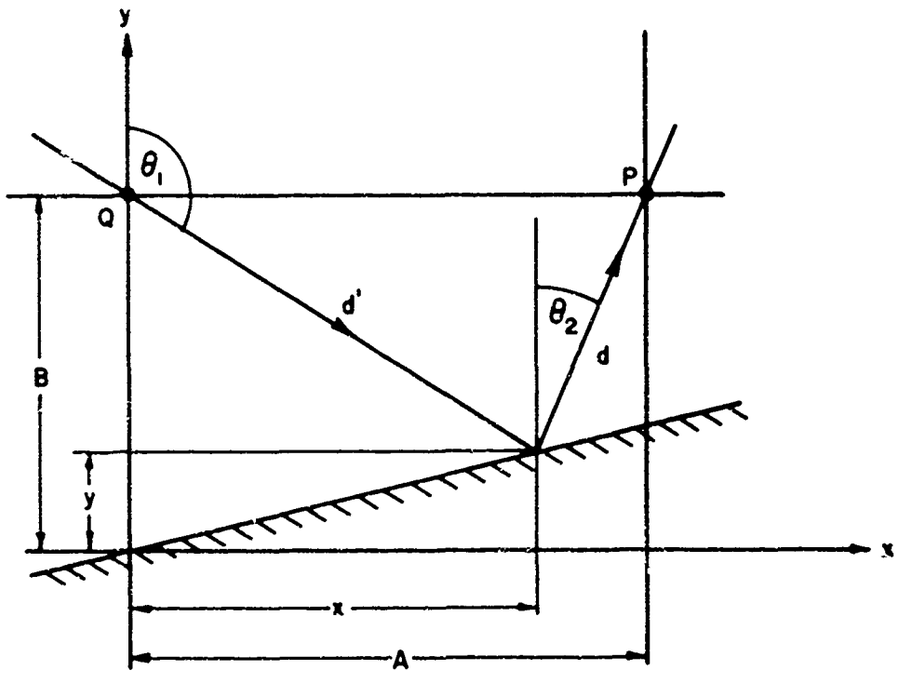

Fig. D-1 Reflection by a perfectly conducting plane.

(The choice of source Q and observation point P in Fig. (D-1) in a way such that $-d' \cos\theta_1 = d \cos\theta_2$, facilitates some of the following calculations without loss of generality).

We want to show that Eq. (4-17), which has been derived by employing geometric optical principles, reduces to Eq. (D-1), which has been derived from a rigorous solution. As in Appendix C, we write the equation of the plane

$$f(x, y) = x - y \tan \theta_o = 0 \qquad \text{(D-2a)}$$

and the optical path from Q to P

$$L(x, y) = \sqrt{(B-y)^2 + \epsilon x^2} + \sqrt{(B-y)^2 + \epsilon (A-x)^2} \quad . \qquad \text{(D-2b)}$$

It is also shown there that Fermat's principle implies

$$\frac{\partial f}{\partial x}\frac{\partial L}{\partial y} - \frac{\partial f}{\partial y}\frac{\partial L}{\partial x} = g(\theta_1, \theta_2) = 0 \quad . \qquad \text{(D-2c)}$$

Using the relations

$$\sin \theta_1 = \frac{x}{\sqrt{(B-y)^2 + x^2}} \quad , \qquad \text{(D-3a)}$$

$$\cos \theta_1 = \frac{-(B-y)}{\sqrt{(B-y)^2 + x^2}} \quad , \qquad \text{(D-3b)}$$

$$\sin \theta_2 = \frac{(A-x)}{\sqrt{(B-y)^2 + (A-x)^2}} \quad , \qquad \text{(D-3c)}$$

$$\cos \theta_2 = \frac{B-y}{\sqrt{(B-y)^2 + (A-x)^2}} \quad , \qquad \text{(D-3d)}$$

one can show from Eq. (D-2c) that

$$g(\theta_1, \theta_2) = \frac{N(\theta_2)}{\cos \theta_o \cos \theta_2 + \epsilon \sin \theta_o \sin \theta_2} + \frac{N(\theta_1)}{\cos \theta_o \cos \theta_1 + \epsilon \sin \theta_o \sin \theta_1} = 0 \qquad \text{(D-4)}$$

Also

$$\frac{\partial g}{\partial \theta_1} = -\frac{\epsilon \sin(\theta_o - \theta_1)}{N^3(\theta_1)} \quad , \qquad \text{(D-5a)}$$

$$\frac{\partial g}{\partial \theta_2} = \frac{\epsilon \sin(\theta_2 - \theta_o)}{N^3(\theta_2)} \quad . \tag{D-5b}$$

Thus, for the case $b \to \infty$ in Eq. (4-17)

$$\left.\frac{d\theta_2}{d\theta_1}\right|_{\theta_o = \text{const}} = \frac{\sin(\theta_o - \theta_1)\, N^3(\theta_2)}{\sin(\theta_2 - \theta_o)\, N^3(\theta_1)} \tag{D-5c}$$

From Eqs. (4-14) one finds (for general b)

$$\frac{d\theta_2}{d\theta_1} = \frac{d'}{a} \frac{\sin(\theta_o - \theta_2)}{\sin(\theta_1 - \theta_o)} \quad . \tag{D-6}$$

(see Fig. 9). But it is shown in Ref. (15) that for $b \to \infty$

$$d' N(\theta_1) = a\, N(\theta_2) \quad ; \tag{D-7}$$

thus, from Eqs. (D-5c), (D-6) and (D-7)

$$\frac{N(\theta_2)}{N(\theta_1)} = \frac{\sin(\theta_2 - \theta_o)}{\sin(\theta_o - \theta_1)} \tag{D-8}$$

and

$$\sqrt{\frac{N(\theta_2)\, d\theta_1}{N(\theta_1)\, d\theta_2}} = \sqrt{\frac{N(\theta_1)}{N(\theta_2)}} \tag{D-9}$$

for θ_o = constant or $b \to \infty$. From Eqs. (4-12), (4-13) and Fig. 9 one can deduce directly

$$|H_r(P)| = \left| \frac{H_o}{\sqrt{a+d}} \sqrt{\frac{N(\theta_2)\, d\theta_1}{N(\theta_1)\, d\theta_2}} \right| \tag{D-10}$$

which, upon using Eqs. (D-7) and (D-9), reduces to Eq. (D-1).

APPENDIX E

Rigorous solution of the half-plane diffraction problem.

The method by which $I(\alpha)$ in Eq. (4-35) is found, is described in detail in Ref. (4) chapters I, II for a half-plane in an isotropic medium. Though the following derivation is in principle identical with the one in the above mentioned reference, it differs in enough details to justify its presentation here.

Consider Eqs. (4-22) for the case of plane wave excitation,

$$L^{(2)}\varphi = 0 \qquad \text{(E-1a)}$$

$$L^{(1)}\varphi = 0 \quad \text{on} \quad Y=0;\ -\infty < X \leq 0 \qquad \text{(E-1b)}$$

with φ defined by Eq. (4-25b). Since φ_i in Eq. (4-25b) satisfies

$$L^{(2)}\varphi_i = 0 \ , \qquad \text{(E-2)}$$

the equation for φ_s become

$$L^{(2)}\varphi_s = 0 \qquad \text{(E-3a)}$$

$$L^{(1)}\varphi_s = -L^{(1)}\varphi_i = ik_o(A_3B_2 + A_2B_3)\exp[-ik_oB_2X] =$$

$$= \frac{ik_o\epsilon\,\sin(\theta_o-\theta')}{N(\theta')}\exp[-ik_oB_2X] \text{ on } \begin{cases} Y=0 \\ -\infty < X \leq 0 \end{cases} \qquad \text{(E-3b)}$$

Radiation condition at $r\to\infty$ (E-3c)

Edge condition at $r\to 0$ (E-3d)

$\Phi_+(\alpha)$ and $\Phi_-(\alpha)$ defined by Eqs. (4-28) are regular functions of α in the upper and lower halves of the complex α plane, respectively. (The analytic properties of functions defined by integrals are discussed in detail in detail in Ref. (4), Chap. I). In subsequent discussion, all functions with a subscript + (plus) or - (minus) will be regular in the upper or lower halves of the complex α plane. Also, we will denote by $\Psi(X,0+)$, $\Phi(\alpha,0+)$ the value of $\Psi(X,Y)$ or $\Phi(\alpha,Y)$ on the upper side of the half plane (and its extension at $X>0$), and by $\Psi(X,0-)$,

$\phi(\alpha, 0-)$ the same values on the lower side of the half-plane (and its extension). φ_s is continuous on the surface $Y=0$, $0 \leq X < \infty$; therefore

$$\phi_{s+}(\alpha, 0+) = \phi_{s+}(\alpha, 0-) = \phi_{s+}(0) \quad . \tag{E-4a}$$

The tangential component of $\underline{E}_s$ is continuous on the whole plane $Y=0$; therefore

$$L^{(1)}\hat{\varphi}_{s+}(\alpha, 0+) = L^{(1)}\hat{\varphi}_{s+}(\alpha, 0-) = L^{(1)}\hat{\phi}_{s+}(0) \tag{E-4b}$$

$$L^{(1)}\hat{\phi}_{s-}(\alpha, 0+) = L^{(1)}\hat{\phi}_{s-}(\alpha, 0-) = L^{(1)}\hat{\phi}_{s-}(0) \tag{E-4c}$$

Using Eqs. (E-4) and (4-30) one finds

$$\hat{\varphi}_s(\alpha, 0+) = \hat{\varphi}_{s+}(\alpha, 0) + \hat{\varphi}_{s-}(\alpha, 0+) = I(\alpha) \tag{E-5a}$$

$$\hat{\varphi}_s(\alpha, 0-) = \hat{\phi}_{s+}(\alpha, 0) + \hat{\varphi}_{s-}(\alpha, 0-) = -I(\alpha) \tag{E-5b}$$

$$L^{(1)}\hat{\phi}_{s+}(0) + L^{(1)}\hat{\varphi}_{s-}(0) = (i\alpha A_3 - i A_2 q_1) I(\alpha) = i\sqrt{\epsilon A_2}\sqrt{k_o^2 - \alpha^2/A_2}\, I(\alpha) \tag{E-5c}$$

$L^{(1)}\hat{\varphi}_{s-}(0)$ is a known function*: via Eq. (E-3b)

$$L^{(1)}\hat{\varphi}_{s-}(0) = \frac{1}{\sqrt{2\pi}} \int_{-\infty}^{0} dx\, e^{i\alpha x} L^{(1)}\varphi_s(x, 0) = \frac{k_o \epsilon \sin(\theta_o - \theta')}{N(\theta')\sqrt{2\pi}(\alpha - k_o B_2)} \tag{E-6}$$

Noting that

$$\sqrt{k_o^2 - \alpha^2/A_2} = \sqrt{k_o + \alpha/N(\theta_o)}\sqrt{k_o - \alpha/N(\theta_o)} \tag{E-7}$$

We get from Eqs. (E-5) and (E-6)

$$\frac{L^{(1)}\hat{\varphi}_{s+}(0)}{\sqrt{k_o + \alpha/N(\theta_o)}} + \frac{k_o \epsilon \sin(\theta_o - \theta')}{N(\theta')\sqrt{2\pi}\sqrt{k_o + \alpha/N(\theta_o)}(\alpha - k_o B_2)} =$$

$$= \frac{i\sqrt{\epsilon}}{2} N(\theta_o)\sqrt{k_o - \alpha/N(\theta_o)}\,[\hat{\varphi}_{s-}(0+) - \hat{\phi}_{s-}(0-)] = K_-(\alpha) \tag{E-8}$$

*It is assumed that for the class of functions under consideration here, the operators $L^{(1)}$ and $\int dx\, e^{i\alpha x}$ commute.

$$\frac{k_o \epsilon \sin(\theta_o-\theta')}{N(\theta')\sqrt{2\pi}\sqrt{k_o+\alpha/N(\theta_o)}(\alpha-k_oB_2)} = \frac{k_o \epsilon \sin(\theta_o-\theta')}{N(\theta')\sqrt{2\pi}\sqrt{k_o+k_oB_2/N(\theta_o)}(\alpha-k_oB_2)} +$$

$$+ \frac{k_o \epsilon \sin(\theta_o-\theta')}{N(\theta')\sqrt{2\pi}(\alpha-k_oB_2)}\left[\frac{1}{\sqrt{k_o+\alpha/N(\theta_o)}} - \frac{1}{\sqrt{k_o+k_oB_2/N(\theta_o)}}\right] = F_-(\alpha)+F_+(\alpha) \tag{E-9}$$

$K_-(\alpha)$ and $F_-(\alpha)$ are regular in the lower half, while $F_+(\alpha)$ is regular in the upper half, of the complex α plane. Using Eq. (E-9) in (E-8) we get

$$\frac{L^{(1)}\phi_{s+}(0)}{\sqrt{k_o+\alpha/N(\theta_o)}} + F_+(\alpha) = K_-(\alpha) - F_-(\alpha) \tag{E-10}$$

The position of the branch points is shown in Fig. 11. In Eq. (E-10) the left-side is regular in the upper half, and the right-hand side in the lower half, of the complex α plane, having as a common region of regularity the real axis. Thus each side can be equated to a polynomial $P(\alpha)$, the degree of which must be determined by the edge condition as follows:

We may assume that near the edge (i.e. for $r<<1$) φ_s can be represented by a series of the form

$$\varphi_s = r^{\mu}\sum_{n=o}^{\infty} a_n(\theta)\, r^n \; ; \tag{E-11}$$

the total energy $\hat{E}$ stored in the scattered electromagnetic field in a small cylindrical volume element surrounding the edge will be given by an expression of the form*

$$\hat{E} = \int_{\theta=o}^{2\pi}\int_{r=o}^{R}\left[a_{11}(\theta)\left(\frac{\partial\varphi_s}{\partial r}\right)^2 + a_{12}(\theta)\left(\frac{\partial\varphi_s}{\partial r}\right)\left(\frac{1}{r}\frac{\partial\varphi_s}{\partial\theta}\right) + a_{22}(\theta)\left(\frac{1}{r}\frac{\partial\varphi_s}{\partial\theta}\right)^2 + B(\theta)\varphi_s^2\right] r\,dr\,d\theta \tag{E-12}$$

In order for $\hat{E}$ to be finite for any finite R, it is seen that μ in Eq. (E-11) must be an arbitrary positive quantity. From this result, the asymptotic

*See footnote on p. 41 for elaboration.

behavior of Φ_{s+} and Φ_{s-} for $|\alpha| \to \infty$ may be derived, by using the identity

$$\int_0^{\pm\infty} x^{\mu} e^{i\alpha x} dx = \pm \Gamma(\mu+1)\, e^{i\frac{\pi}{2}(\mu+1)}\, \alpha^{-\mu-1} \qquad \text{(E-13)}$$

It follows from Eqs. (E-8), (E-9) and (E-10) that for $|\alpha| \to \infty$, $P(\alpha) = 0$, and thus

$$K_{-}(\alpha) - F_{-}(\alpha) = 0 \qquad \text{(E-14)}$$

One may find $I(\alpha)$ from Eqs. (E-5)(E-6) and (E-14), the result being Eq. (4-35).

APPENDIX F

Asymptotic evaluation of the integrals in Eqs. (4-36) and (4-45).

Equation (4-36) is the exact expression for the scattered part of the field due to a plane wave which falls upon a conducting half-plane in a uniaxially anisotropic medium. It is valid for all complex ϵ with $\mathrm{Im}\,\epsilon \geq 0$. If the incident wave is cylindrical (i.e. excited by a line source at finite distance from the edge), the appropriate expression for the scattered part of the field is given by Eq. (4-45). Both integrands have a pole, which for certain ranges of the observation point contributes a residue term to the solution. The other term of the solution arises from the integration over the given path. For $k_o r \gg 1$, i.e. for high frequencies and/or observation points far from the edge, this term can be calculated asymptotically by means of the saddle point method, and given in closed form. This conventional method fails and must be modified when the saddle point lies near the pole.

Via the transformation

$$\alpha = k_o N(\hat{\epsilon}_o) \sin\tau \tag{F-1}$$

the scattered part in Eq. (4-36) becomes

$$\Psi_s = \frac{\mp 1}{2\pi} \sqrt{1 - \frac{B_2}{N(\hat{\epsilon}_o)}} \int_p \frac{d\tau \cos\tau \exp\left[\mp i k_o r N(\hat{\epsilon}) \cos(\tau - \tau_s)\right]}{\sqrt{1 - \sin\tau}\left[\sin\tau - \frac{B_2}{N(\hat{\epsilon}_o)}\right]} \tag{F-2}$$

where the saddle point τ_s is defined by

$$\tan\tau_s = \mp \frac{A_3 Y - A_2 X}{\sqrt{F}\, Y} = \mp \frac{1 + \tan\theta_o \tan\tau}{\sqrt{F}\,(\tan\tau - \tan\tau_o)} , \tag{F-3}$$

with the $\mp$ sign applying for $Y \gtrless 0$ respectively. For $\hat{\epsilon} = 1$, Eq. (F-3) becomes

$$\tan\tau_s\big|_{\hat{\epsilon}=1} = \mp \tan\tau . \tag{F-3a}$$

where τ (Fig. 10) is the observation angle in the X-Y coordinate system. The pole of the integrand in Eq. (F-2) is located at

$$\sin w_p = \frac{B_2}{N(\theta_o)} \quad , \tag{F-4a}$$

which expression can be rearranged by using Eq. (4-25a) to read

$$\tan w_p = \frac{1 + \epsilon \tan\theta_o \tan\theta'}{\sqrt{\epsilon}\,(\tan\theta_o - \tan\theta')} \quad . \tag{F-4b}$$

By equating Eqs. (F-4b) and (F-3), one finds that when $w_p = w_s$,

$$\tan\theta = \frac{-(1 - \epsilon \tan^2\theta_o)\tan\theta' + 2\tan\theta_o}{(1 - \epsilon \tan^2\theta_o) + 2\epsilon \tan\theta_o \tan\theta'} \quad , \text{ for } Y > 0 \tag{F-5a}$$

$$\tan\theta = \tan\theta' \quad \text{for} \quad Y < 0 \tag{F-5b}$$

which limiting angles have already been noted in Eqs. (4-44). The path of integration and the locations of x_p and x_s in the complex w plane are shown in Fig. F-1(a), for ϵ real and positive. For other values of ϵ, the mapping from the α-plane to the x-plane will be different. For example, if $\epsilon < 0$ and

$$\tan\theta_o > \frac{1}{\sqrt{|\epsilon|}} \quad ,$$

the picture in the x-plane will be given by Fig. F-1(b). For $\epsilon < 0$ and

$$\tan\theta_o < \frac{1}{\sqrt{|\epsilon|}} \quad ,$$

the picture again looks different, but as the associated calculations are analogous to the former, this case will not be discussed separately.[15]

It is evident that if the original path p is deformed into the steepest descent path SDP through the saddle point x_s, the pole at x_p will be intercepted by the steepest descent path whenever $x_s > x_p$; this corresponds to observation points lying in region A of Fig. 12 if $Y > 0$, wherein a geometrically reflected part of the field exists. When $x_p = x_s$, then the observation point lies on the boundary between regions A and B. The angle of this boundary is given by Eq. (F-5a) and is recognized as the angle of the limiting ray which is

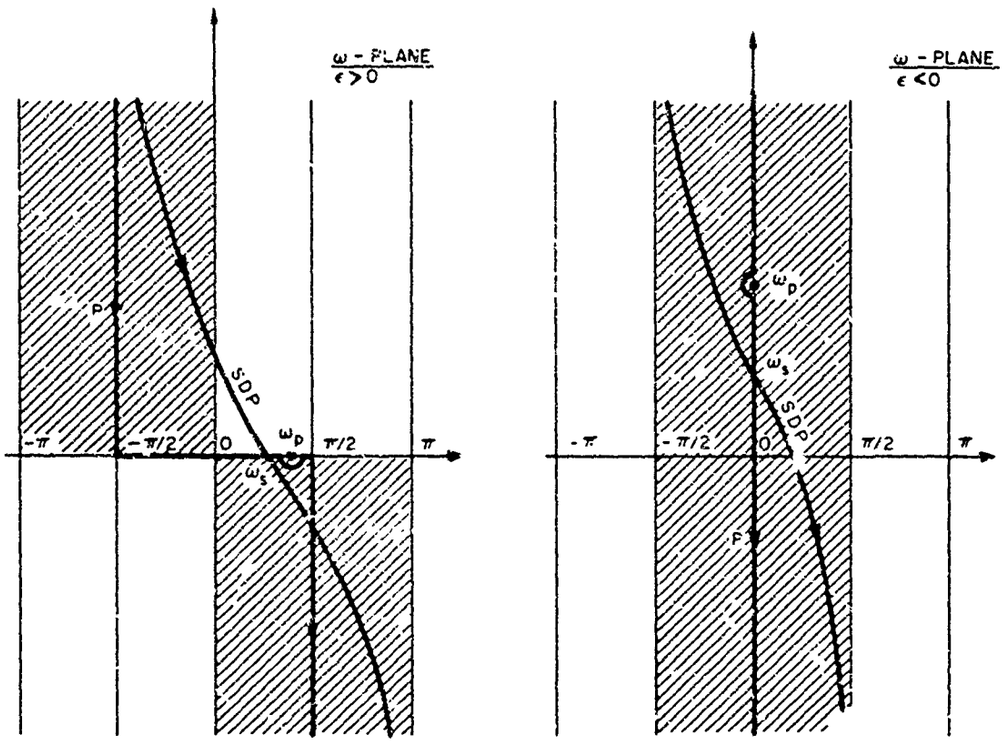

Fig. F-1
The original and the steepest descent paths of integration for $\epsilon > 0$ (a) and $\epsilon < 0$ (b)

reflected geometrically "at" the edge of the half-plane. The pole contribution to Φ_s is found by calculating the residue of Eq. (F-2) at $\omega = \omega_p$,

$$\Phi_g \simeq \pm \exp\left[\pm i k_o r N(-) \cos(\phi_p - \phi_s)\right] \text{ for } Y \gtrless 0 \quad . \tag{F-6}$$

Upon substitution of the correct ϕ_s for $Y \gtrless 0$, respectively, it can be shown that Eq. (F-6) gives exactly the geometrically reflected plane wave in region A and that it just cancels the incident wave in region C of Fig. 12. For calculating the saddle point contribution to the field, we use the formula

$$\int_P f(\omega)\, e^{\Omega g(\omega)} d\omega \simeq \sqrt{\frac{-2\pi}{\Omega g''(\omega_s)}}\; e^{\Omega g(\omega_s)}\, f(\omega_s) \tag{F-7a}$$

where in our case (Eq. F-2)

$$\zeta = k_o r N(\theta) \qquad \text{(F-7b)}$$

This yields the expressions given by Eqs. (4-43).

Eq. (4-45) can be derived from Eq. (4-36) as shown in Appendix G. The pole contribution to Eq. (4-45) in the region $Y<0$ will be calculated as an illustration. In that region, Φ_s in Eq. (4-45) is

$$\Phi_s = \frac{-i}{8\pi^2} \int_{-\infty}^{\infty} d\xi \, \frac{\exp\left[-i\xi X' + i q_1(\xi) Y'\right]}{\sqrt{k_o N(\theta_o) - \xi}} \int_{-\infty}^{\infty} d\alpha \, \frac{\exp\left[-i\alpha X + i q_2(\alpha) Y\right]}{\sqrt{k_o N(\theta_o) - \alpha}\,(\alpha + \xi)} \qquad \text{(F-8)}$$

The pole occurs at $\alpha = -\xi$, and by the residue method, the pole contribution to the second integral in Eq. (F-8) is found to be

$$2\pi i \, \frac{\exp\left[i\xi X + i q_2(-\xi) Y\right]}{\sqrt{k_o N(\theta_o) + \xi}} \qquad \text{(F-9a)}$$

Upon noting that $q_2(-\xi) = -q_1(\xi)$ (see Eq. (4-32), one obtains for the pole contribution to Φ_s,

$$\Phi_s\Big|_{\text{pole}} = \Phi_g = \frac{-i}{4\sqrt{\epsilon}} \int_{-\infty}^{\infty} d\xi \, \frac{\exp\left[i\xi(X-X') - i q_1(\xi)(Y-Y')\right]}{\sqrt{k_o^2 N^2(\theta_o) - \xi^2}}$$

$$= -\frac{i}{4} \int_{-\infty}^{\infty} d\xi \, \frac{\exp\left[i\xi(X-X') - i q_1(\xi)(Y-Y')\right]}{A_2(q_1 - q_2)}$$

$$= -\frac{i}{4} H_o^{(1)}\left[k_o N(-) \left| \underline{r} - \underline{r}' \right|\right] \quad , \qquad \text{(F-9)}$$

i.e., that part of Φ_s which cancels the incident cylindrical wave in the geometrical shadow zone (for verification of the last step in Eq. (F-9), see Eq. (16) in Ref. 15; attention should be called to the different definition of $q_{1,2}$ and A_1, A_2, A_3 in that reference).

The asymptotic evaluation of Eq. (4-45) by means of the saddle point technique is very similar to the evaluation of Eq. (4-36), because the equations

which define the saddle points in the complex α and ξ planes are independent of one another. Defining

$$\zeta = k_o N(\theta_o) \sin w \tag{F-10a}$$

$$\xi = k_o N(\theta_o) \sin z \tag{F-10b}$$

and substituting Eqs. (F-10) into Eq. (F-8),

$$\varphi_s = \frac{-1}{8\pi^2\sqrt{\varepsilon}} \int_{p(z)} \frac{dz \cos z \exp\left[ik_o r' N(\theta) \cos(z-z_s)\right]}{\sqrt{1-\sin z}} \times$$

$$\times \int_{p(x)} \frac{dw \cos w \exp\left[\pm ik_o r N(w) \cos(w-w_s)\right]}{\sqrt{1-\sin w}\,(\sin w + \sin z)} \,. \tag{F-11}$$

w_s is defined by Eq. (F-3), and z_s is given analogously by

$$\tan z_s = -\frac{A_3 Y' - A_2 X'}{\sqrt{\varepsilon}\, Y'} = -\frac{1+\varepsilon \tan\theta_o \tan\theta'}{\sqrt{\varepsilon}\,(\tan\theta' - \tan\theta_o)} \tag{F-12}$$

which is identical with Eq. (F-4b). The simple saddle point integration breaks down when

$$-w_s \sim z_s \,, \tag{F-13}$$

corresponding to observation points near the shadow boundary (see discussion of Eqs. (F-3), (F-4) and (F-5)). For all other observation points, Eq. (F-7a) can be used separately for the two integrals in Eq. (F-11), yielding the expression given in Eq. (4-46).

APPENDIX G

Derivation of Eq. (4-45) from Eq. (4-36).

The synthesis of the line source result (Eq. (4-45)) from the plane wave result (Eq. (4-36)) may be carried out as follows: If the source term in Eqs. (2-2) is of the form

$$\underline{M} = \underline{M}(\xi) = \underline{z}_o \, \delta(Y-Y') \frac{e^{i\xi X}}{\sqrt{2\pi}} \tag{G-1}$$

the differential equation for $\varphi(\xi)$ becomes

$$\left(A_1 \frac{\partial^2}{\partial X^2} + A_2 \frac{\partial^2}{\partial Y^2} + 2A_3 \frac{\partial^2}{\partial X \partial Y} + k^2\right) \varphi(\xi) = L^{(2)} \varphi(\xi) = -\delta(Y-Y') \frac{e^{i\xi X}}{\sqrt{2\pi}} \tag{G-2}$$

(A_1, A_2, A_3 are defined by Eqs. (4-24)). One assumes for $\varphi(\xi)$,

$$\varphi(X, Y; \xi) = h(Y) \, e^{i\xi X} \quad , \tag{G-3}$$

which implies that

$$\left(\frac{d^2}{dY^2} + 2i\xi \frac{A_3}{A_2} \frac{d}{dY} + \frac{k^2 - \xi^2 A_1}{A_2}\right) h(Y) = \frac{-\delta(Y-Y')}{A_2 \sqrt{2\pi}} \tag{G-4}$$

As $\varphi(\xi)$ is continuous across the plane $Y = Y'$, $h(Y)$ must also be, and from Eq. (G-4) we get by integration between the limits $Y'-\eta$ and $Y'+\eta$

$$\lim_{\eta \to 0} \left[\frac{dh}{dY} + 2i\xi \frac{A_3}{A_2} h\right]_{Y'-\eta}^{Y'+\eta} = \frac{-1}{A_2 2\pi} \quad . \tag{G-5}$$

The solution to Eq. (G-4) is constructed from the homogeneous solutions, which are given for $Y \lesseqgtr Y'$ by

$$h(Y) = C e^{iq_{1,2}(-\xi)(Y-Y')} = C e^{-iq_{2,1}(\xi)(Y-Y')} \tag{G-6}$$

with $q_{1,2}(\xi)$ defined by Eq. (4-32), and C being a constant. Imposition of con-

dition (G-5) on Eq. (G-6) leads to the solution of Eq. (G-2).

$$\varphi(\xi) = \frac{i}{2\pi} \frac{e^{-iq_{2,1}(Y-Y')+i\xi X}}{A_2(q_2-q_1)}$$

$$= \frac{ie^{iq_{2,1}Y'} e^{-iq_{2,1}Y+i\xi X}}{2\sqrt{2\pi\epsilon}\sqrt{k_o N(\theta_o)-\xi}\sqrt{k_o N(\theta_o)+\xi}} \qquad \text{(G-7)}$$

It can be shown that (see Eqs. (4-26))

$$\exp\left[i\xi X - iq_1 Y\right] = \exp\left[-ik_o B_2 X - ik_o B_3 Y\right] \qquad \text{(G-8)}$$

if we define

$$\xi = -k_o B_2 \quad . \qquad \text{(G-9)}$$

Then for $Y' > 0$, a plane wave falling onto the half plane at $Y = 0$ is given by Eq. (G-3), which is proportional to $\varphi(\xi)$ in this region. The scattered field $\varphi_{sp}(\xi)$ due to such a plane wave is given by Eq. (4-36), which, upon use of Eqs. (G-9), reads

$$\varphi_{sp}(\xi) = \pm \frac{\sqrt{k_o N(\theta_o)+\xi}}{2\pi} \int_{-\infty}^{\infty} \frac{d\alpha \exp\left[-i\alpha X + iq_{1,2}(\alpha) Y\right]}{\sqrt{\alpha - k_o N(\theta_o)}\,(\alpha+\xi)} \quad . \qquad \text{(G-10)}$$

This solution remains valid for $-\infty < \xi < \infty$ so that the scattered field due to the source in Eq. (G-1) is given for $Y' > 0$ by

$$\varphi_s(\xi) = \pm \frac{ie^{iq_1(\xi)Y'}}{4\pi\sqrt{2\pi\epsilon}\sqrt{k_o N(\theta_o)-\xi}} \int_{-\infty}^{\infty} \frac{d\alpha \exp\left[-i\alpha X + iq_{1,2}(\alpha) Y\right]}{\sqrt{\alpha - k_o N(\theta_o)}\,(\alpha+\xi)} \qquad \text{(G-11)}$$

By applying the inverse Fourier transform

$$f(X') = \frac{1}{\sqrt{2\pi}} \int_{-\infty}^{\infty} d\xi\, e^{-i\xi X'} F(\xi) \qquad \text{(G-12)}$$

to Eq. (G-2), we get

$$\left(A_1 \frac{\partial^2}{\partial X^2} + A_2 \frac{\partial^2}{\partial Y^2} + 2A_3 \frac{\partial^2}{\partial X \partial Y} + k^2\right)\varphi(X, Y; X', Y') = -\delta(X-X')\,\delta(Y-Y') \quad \text{(G-12)}$$

which is the desired form for line source excitation. The scattered part of φ will therefore be the inverse Fourier transform of $\varphi_s(\xi)$ (Eq. (G-11)), which is given by Eq. (4-45).

APPENDIX H

Asymptotic evaluation of Eq. (4-80) in the illuminated region.

The Weber functions $D_{-\frac{1}{2}+\frac{i\lambda}{2k}}(\pm\xi\sqrt{-2ik})$ and $D_{-\frac{1}{2}+\frac{i\lambda}{2k}}(\pm\eta\sqrt{-2ik})$ which appear in the integral representation of the field (Eq. (4-80)), satisfy the equations

$$\left[\frac{d^2}{d\xi^2}+k^2(\xi^2+\lambda/k^2)\right] D_{-\frac{1}{2}+\frac{i\lambda}{2k}}(\pm\xi\sqrt{-2ik}) = 0 \qquad \text{(H-1a)}$$

$$\left[\frac{d^2}{d\eta^2}+k^2(\eta^2-\lambda/k^2)\right] D_{-\frac{1}{2}-\frac{i\lambda}{2k}}(\pm\eta\sqrt{-2ik}) = 0 \qquad \text{(H-1b)}$$

For high frequencies (large k) one may construct asymptotic forms of these functions by the WKBJ method as follows

$$D_{-\frac{1}{2}+\frac{i\lambda}{2k}}(\xi\sqrt{-2ik}) \sim \frac{A}{\left[\xi^2+\lambda/k^2\right]^{1/4}} \exp\left\{ik\int_0^{\xi}\sqrt{x^2+\lambda/k^2}\,dx\right\} \qquad \text{(H-2a)}$$

$$D_{-\frac{1}{2}-\frac{i\lambda}{2k}}(\eta\sqrt{-2ik}) \sim \frac{B}{\left[\eta^2-\lambda/k^2\right]^{1/4}} \exp\left\{ik\int_{\sqrt{\lambda}/k}^{\eta}\sqrt{x^2-\lambda/k^2}\,dx\right\} \qquad \text{(H-2b)}$$

$$D_{-\frac{1}{2}-\frac{i\lambda}{2k}}(-\eta\sqrt{-2ik}) \sim \frac{C}{\left[\eta^2-\lambda/k^2\right]^{1/4}} \exp\left\{ik\int_{\sqrt{\lambda}/k}^{\eta}\sqrt{x^2-\lambda/k^2}\,dx\right\} +$$

$$+ \frac{D}{\left[\eta^2-\lambda/k^2\right]^{1/4}} \exp\left\{-ik\int_{\sqrt{\lambda}/k}^{\eta}\sqrt{x^2-\lambda/k^2}\,dx\right\} \qquad \text{(H-2c)}$$

Assuming that ξ, η are real, Eq. (H-2a) is valid for $\lambda/k^2 > -\xi^2$, while Eqs. (H-2b, c) are valid for $\lambda/k^2 < \eta^2$. Outside these regions the exponentials become real. For $|\lambda/k^2| >> \eta^2, \xi^2$ Eqs. (H-2) reduce to Eq. (4-75a), and the exponents

become proportional to $\sqrt{\lambda}\,\xi$ and $\sqrt{\lambda}\,\eta$, respectively.

The coefficients A, B, C and D in Eqs. (H-2) may be evaluated by comparing Eqs. (H-2) in the region where $\eta^2, \xi^2 \gg |\lambda/k^2|$ with the asymptotic forms given by Eqs. (4-72).

It is useful to note that

$$ik\int_{c}^{\xi}\sqrt{x^2+\lambda/k^2}\,dx = \frac{ik}{2}\left[\xi\sqrt{\xi^2+\lambda/k^2} + \frac{\lambda}{k^2}\ln\frac{\xi+\sqrt{\xi^2+\lambda/k^2}}{\sqrt{\lambda}/k}\right] \qquad \text{(H-3a)}$$

$$ik\int_{\lambda/k}^{r}\sqrt{x^2-\lambda/k^2}\,dx = \frac{ik}{2}\left[r\sqrt{\eta^2-\eta/k^2} - \frac{\lambda}{k^2}\ln\frac{\eta+\sqrt{\eta^2-\eta/k^2}}{\sqrt{\lambda}/k}\right] \qquad \text{(H-3b)}$$

If we substitute the asymptotic forms (H-2a-c) into Eq. (4-80) we get

$$G_1 = \frac{i}{4k}\int_{-\infty}^{\infty}\frac{d\lambda}{\sin\left(\frac{i\lambda}{2k}-\frac{1}{2}\right)\pi} D_{-\frac{1}{2}+\frac{i\lambda}{2k}}(\xi\sqrt{-2ik})\,D_{-\frac{1}{2}+\frac{i\lambda}{2k}}(-\xi'\sqrt{-2ik}) \quad x$$

$$x \quad D_{-\frac{1}{2}-\frac{i\lambda}{2k}}(r\sqrt{-2ik})\,D_{-\frac{1}{2}-\frac{i\lambda}{2k}}(-r'\sqrt{-2ik}) \sim$$

$$\sim -\frac{i}{4k}\left\{A^2BC\int_{-\infty}^{\infty}\frac{d\lambda}{\sin\left(\frac{i\lambda}{2k}-\frac{1}{2}\right)\pi}\left[\left(\xi^2+\frac{\lambda}{k^2}\right)\left(\xi'^2+\frac{\lambda}{k^2}\right)\left(\eta^2-\frac{\lambda}{k^2}\right)\left(\eta'^2-\frac{\lambda}{k^2}\right)\right]^{-\frac{1}{4}}\exp\left[\frac{ik}{2}\,q_1(\lambda)\right] + \right.$$

$$\left. + A^2BD\int_{-\infty}^{\infty}\frac{d\lambda}{\sin\left(\frac{i\lambda}{2k}-\frac{1}{2}\right)\pi}\left[\left(\xi^2+\frac{\lambda}{k^2}\right)\left(\xi'^2+\frac{\lambda}{k^2}\right)\left(\eta^2-\frac{\lambda}{k^2}\right)\left(\eta'^2-\frac{\lambda}{k^2}\right)\right]^{-\frac{1}{4}}\exp\left[\frac{ik}{2}\,q_2(\lambda)\right]\right\} \qquad \text{(H-4a)}$$

where

$$q_{1,2}(\lambda) = \left[\xi\sqrt{\xi^2+\frac{\lambda}{k^2}} + \eta\sqrt{\eta^2+\frac{\lambda}{k^2}} + |\xi'|\sqrt{\xi'^2+\frac{\lambda}{k^2}} \pm \eta'\sqrt{\eta'^2-\frac{\lambda}{k^2}}\right] +$$

$$+ \frac{\lambda}{k^2}\left[\ln\frac{\xi+\sqrt{\xi^2+\frac{\lambda}{k^2}}}{\sqrt{\lambda}/k} + \ln\frac{|\xi'|+\sqrt{\xi'^2+\frac{\lambda}{k^2}}}{\sqrt{\lambda}/k} - \ln\frac{\eta+\sqrt{\eta^2-\frac{\lambda}{k^2}}}{\sqrt{\lambda}/k^2} \mp \ln\frac{\eta'+\sqrt{\eta'^2-\frac{\lambda}{k^2}}}{\sqrt{\lambda}/k}\right] \qquad \text{(H-4b)}$$

Eqs. (H-4) are really valid only in the region

$$-\min\left\{\xi^2, \xi'^2\right\} < \frac{\lambda}{k^2} < \min\left\{\eta^2, \eta'^2\right\} \tag{H-5}$$

where $\min\{a, b\}$ stands for "the smaller of a and b". Thus, if there is a real saddle point in that interval one may obtain a closed asymptotic form for G_1 from Eq. (H-4a), which will represent a propagating wave. If no saddle point is found in the interval (H-5), the asymptotic form in Eq. (H-4a) becomes useless. Eq. (4-75a) indicates that in this case the integral has no real saddle points at all, and does not represent a propagating wave. Next it will be shown that the first part of Eq. (h-4a) has one real saddle point in the region (H-5), whereas the second part has none. Thus G_1 is given asymptotically by the first integral alone.

One may easily verify that

$$\frac{d}{d\lambda}\left[x\sqrt{x^2 \pm \frac{\lambda}{k^2}} \pm \frac{\lambda}{k^2} \ln\frac{x+\sqrt{x^2 \pm \frac{\lambda}{k^2}}}{\sqrt{\lambda}/k}\right] = \pm \ln \frac{x+\sqrt{x^2 \pm \frac{\lambda}{k^2}}}{\sqrt{\lambda}/k} . \tag{H-6}$$

Thus

$$\frac{dq_1(\lambda)}{d\lambda} = \ln\left\{\frac{\xi+\sqrt{\xi^2+\frac{\lambda}{k^2}}}{\eta+\sqrt{\eta^2-\frac{\lambda}{k^2}}} \quad \frac{|\xi'|+\sqrt{\xi'^2+\frac{\lambda}{k^2}}}{\eta'+\sqrt{\eta'^2-\frac{\lambda}{k^2}}}\right\}, \tag{H-7a}$$

and the saddle point condition for the first part of G_1 becomes

$$\frac{\xi+\sqrt{\xi^2+\frac{\lambda_s}{k^2}}}{\eta+\sqrt{\eta^2-\frac{\lambda_s}{k^2}}} \quad \frac{|\xi'|+\sqrt{\xi'^2+\frac{\lambda_s}{k^2}}}{\eta'+\sqrt{\xi'^2-\frac{\lambda_s}{k^2}}} = 1 \tag{H-7b}$$

This condition has a simple geometrical interpretation as shown in Fig. H-1. From Eqs. (4-66), it follows that

$$\eta = \sqrt{R+v} = \sqrt{R(1+\cos\varphi)} = \sqrt{2R}\cos\frac{\varphi}{2} \tag{H-8a}$$

$$\eta' = \sqrt{R'+v'} = \sqrt{R'(1+\cos\varphi')} = \sqrt{2R'}\cos\frac{\varphi'}{2} \tag{H-8b}$$

$$\xi = \sqrt{R - v} = \sqrt{R(1 - \cos\varphi)} = \sqrt{2R}\,\sin\frac{\varphi}{2} \qquad \text{(H-8c)}$$

$$\xi' = \sqrt{R' - v'} = \sqrt{R'(1 - \cos\varphi')} = \sqrt{2R'}\,\sin\frac{\varphi'}{2} \qquad \text{(H-8d)}$$

Also

$$\varphi = \gamma - \alpha$$

$$\varphi' = \gamma + \alpha' + \pi \qquad \text{(H-8f)}$$

$$t = R \sin\alpha \sin\gamma = R' \sin\alpha' \sin\gamma \quad . \qquad \text{(H-8g)}$$

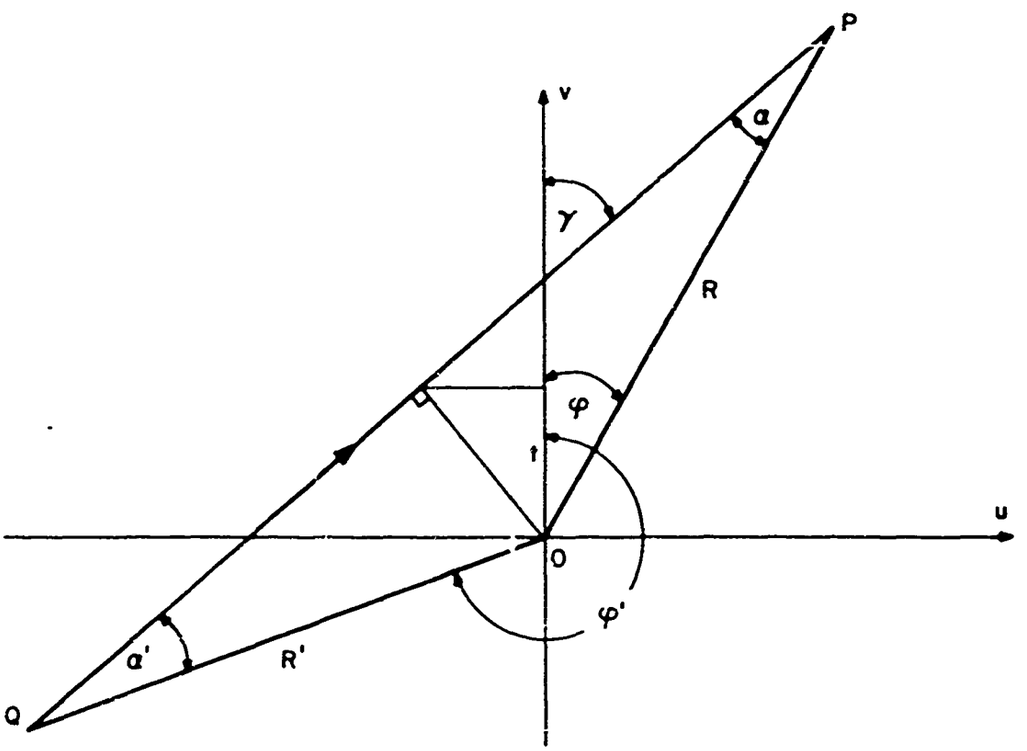

It is seen that if we identify

$$\lambda_s = 2k^2 t \quad . \qquad \text{(H-9)}$$

then by using Eqs. (H-8), we can show that

$$\frac{\xi+\sqrt{\xi^2+\frac{\lambda_s}{k^2}}}{\xi+\sqrt{\xi^2-\frac{\lambda_s}{k^2}}} = \frac{\sqrt{1-\cos\varphi}+\sqrt{1-\cos\varphi+2\sin\gamma\sin\alpha}}{\sqrt{1+\cos\varphi}+\sqrt{1+\cos\varphi-2\sin\gamma\sin\alpha}} = \frac{\sin\frac{\gamma-\alpha}{2}+\sin\frac{\gamma+\alpha}{2}}{\cos\frac{\gamma-\alpha}{2}+\cos\frac{\gamma+\alpha}{2}} = \tan\frac{\gamma}{2}, \tag{H-10a}$$

and similarly,

$$\frac{|\xi|'+\sqrt{\xi'^2+\frac{\lambda_s}{k^2}}}{\eta'+\sqrt{\eta'^2-\frac{\lambda_s}{k^2}}} = \cot\frac{\gamma}{2}, \tag{H-10b}$$

which satisfies the saddle point condition Eq.(H-7b). Now it is seen from Eq. (H-4b) that

$$q_1(\lambda_s) = \left[\xi\sqrt{\xi^2+\frac{\lambda_s}{k^2}}+|\xi'|\sqrt{\xi'^2+\frac{\lambda_s}{k^2}}+\eta\sqrt{\eta^2-\frac{\lambda_s}{k^2}}+\eta'\sqrt{\eta'^2-\frac{\lambda_s}{k^2}}\right] \tag{H-11a}$$

But

$$\xi\sqrt{\xi^2+\frac{\lambda_s}{k^2}}+\eta\sqrt{\eta^2-\frac{\lambda_s}{k^2}} =$$

$$= \sqrt{R(1-\cos\varphi)}\sqrt{R(1-\cos\varphi)+2t}+\sqrt{R(1+\cos\varphi)}\sqrt{R(1+\cos\varphi)-2t} =$$

$$= R\left[\sqrt{1-\cos(\gamma-\alpha)}\sqrt{1-\cos(\gamma+\alpha)}+\sqrt{1+\cos(\gamma-\alpha)}\sqrt{1+\cos(\gamma+\alpha)}\right] = 2R\cos\alpha \tag{H-11b}$$

and similarly

$$|\xi|'\sqrt{\xi'^2+\frac{\lambda_s}{k^2}}+\eta'\sqrt{\eta'^2-\frac{\lambda_s}{k^2}} = 2R'\cos\alpha' . \tag{H-11c}$$

Thus,

$$\exp\left[\frac{ik}{2}q_1(\lambda_s)\right] = \exp\left[ik(R\cos\alpha+R'\cos\alpha')\right] = \exp\left[ik|\underline{R}-\underline{R}'|\right] \tag{H-12}$$

which is exactly the phase term at the point P of a wave emanating at Q (Fig. H-1). The saddle point condition for $q_2(\lambda)$ in Eq. (H-4b) would be

$$\frac{\xi+\sqrt{\xi^2+\frac{\lambda_s}{k^2}}}{\eta+\sqrt{\eta^2-\frac{\lambda_s}{k^2}}}\;\frac{|\xi|'+\sqrt{\xi'^2+\frac{\lambda_s}{k^2}}}{\sqrt{\frac{\lambda_s}{k}}}\;\frac{\eta'+\sqrt{\eta'^2-\frac{\lambda_s}{k^2}}}{\sqrt{\frac{\lambda_s}{k}}} = 1 \tag{H-13}$$

Eqs. (H-8a-d) show that a condition like Eq. (H-9), i.e.; a λ_s which is independent of φ and φ', cannot be found here.

The second part of Eq. (4-80) yields

$$G_2 = \frac{i}{4k}\int_{-\infty}^{\infty} \frac{d\lambda}{\sin(\frac{i\lambda}{2k}-\frac{1}{2})\pi} \frac{D'_{-\frac{1}{2}-\frac{i\lambda}{2k}}(-\eta_o\sqrt{-2ik})}{D'_{-\frac{1}{2}-\frac{i\lambda}{2k}}(\eta_o\sqrt{-2ik})} D_{-\frac{1}{2}+\frac{i\lambda}{2k}}(\xi\sqrt{-2ik}) \times$$

$$\times D_{-\frac{1}{2}+\frac{i\lambda}{2k}}(-\xi'\sqrt{-2ik})\, D_{-\frac{1}{2}-\frac{i\lambda}{2k}}(\eta'\sqrt{-2ik}) \sim$$

$$\sim -\frac{i}{4k}\left\{A^2BC\int_{-\infty}^{\infty} \frac{d\lambda}{\sin(\frac{i\lambda}{2k}-\frac{1}{2})\pi}\left[(\xi^2+\frac{\lambda}{k^2})(\xi'^2+\frac{\lambda}{k^2})(\eta^2-\frac{\lambda}{k^2})(\eta'^2-\frac{\lambda}{k^2})\right]^{-\frac{1}{4}} \exp\left[\frac{ik}{2}q_1(\lambda)\right] + \right.$$

$$\left. + A^2BD\int_{-\infty}^{\infty} \frac{d\lambda}{\sin(\frac{i\lambda}{2k}-\frac{1}{2})\pi}\left[(\xi^2+\frac{\lambda}{k^2})(\xi'^2+\frac{\lambda}{k^2})(\eta^2-\frac{\lambda}{k^2})(\eta'^2-\frac{\lambda}{k^2})\right]^{\frac{1}{4}} \exp\left[\frac{ik}{2}\, q_3(\lambda)\right]\right\} \tag{H-14a}$$

where

$$q_3(\lambda) = q_1(\lambda) - 2\int_{\sqrt{\lambda}/k}^{\eta_o}\sqrt{x^2-\frac{\lambda}{k^2}}\,dx =$$

$$= q_1(\lambda) - 2\eta_o\sqrt{\eta_o^2-\frac{\lambda}{k^2}} + 2\frac{\lambda}{k^2}\ln\frac{\eta_o+\sqrt{\eta_o^2-\frac{\lambda}{k^2}}}{\sqrt{\lambda}/k} \tag{H-14b}$$

$q_1(\lambda)$ is given by Eq. (H-4b).

It is seen that the first part of G_2 cancels (asymptotically) the first part of G_1. It must be noted, though, that Eq. (H-14a) is valid only in the region

$$-\min(\xi^2, \xi'^2) < \frac{\lambda}{k^2} < \eta_o^2 \tag{H-15}$$

This implies that the geometrical interpretation of Fig. H-1 and Eq. (H-9) for the first part of G_2 is valid only when the observation point lies in the shadow region, where $t < \eta_o/2$. In the illuminated region ($t > \eta_o/2$), the interpretation still holds for G_1, but the first part of G_2 has no saddle point when $\lambda/k^2 > \eta_o^2$

and is therefore of a smaller order of magnitude than G_1 .

The asymptotic evaluation of the second part of G_2 is done as follows:

From Eqs. (H-14) and (H-6) it is seen that the saddle point condition is given by

$$\frac{\xi + \sqrt{\xi^2 + \frac{\lambda_2}{k^2}}}{\eta + \sqrt{\eta^2 - \frac{\lambda_s}{k^2}}} \; \frac{|\xi'| + \sqrt{\xi'^2 + \frac{\lambda_s}{k^2}}}{\eta' + \sqrt{\eta'^2 - \frac{\lambda_s}{k^2}}} \; \frac{\left(\eta_o + \sqrt{\eta_o^2 - \frac{\lambda_s}{k^2}}\right)^2}{\frac{\lambda_s}{k^2}} = 1 \qquad \text{(H-16)}$$

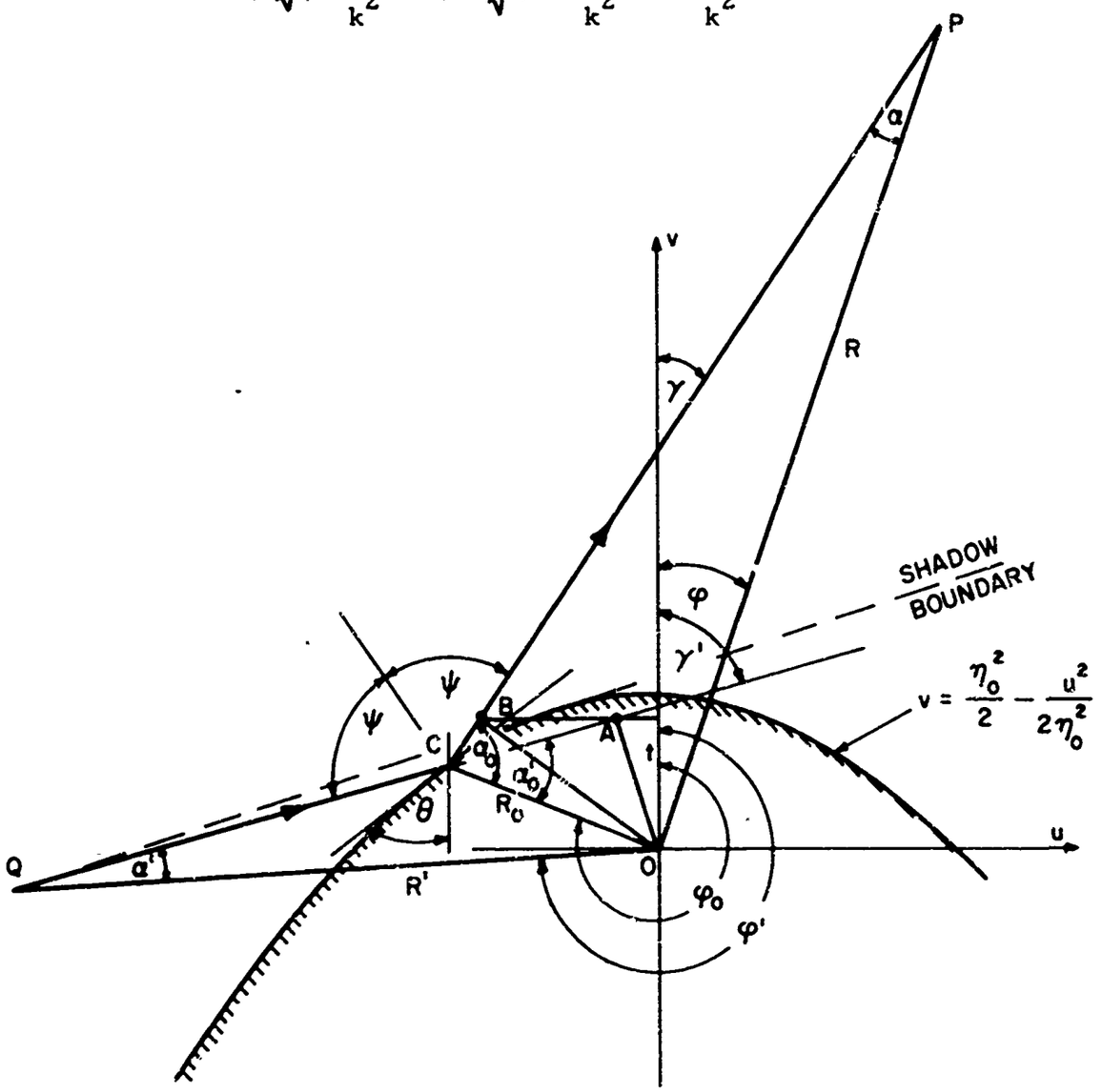

It can be shown that Eq. (H-16) is satisfied if λ_s is given by Eq. (H-9). QCP is the path of a ray which emanates at Q and reaches P after being reflected at the surface according to the laws of geometrical optics. $\overline{OA}$ and $\overline{OB}$ are perpendicular lines to $\overline{QC}$ and $\overline{CP}$ respectively whose projections on the v axis are equal and denoted by t in Eq. (H-9) and Fig. H-2. To show that these projections are equal, one has to utilize the fact that the reflecting surface is a parabolic cylinder which implies that

$$\theta = \frac{1}{2}(\varphi_o - \pi) \tag{H-17a}$$

and

$$\alpha_o = \gamma'; \quad \alpha_o' = \gamma \tag{H-17b}$$

(θ is the angle between the tangent to the parabola at C and the v axis). Using Eqs. (H-8a-d), (H-17) and the additional relations

$$\eta_o = \sqrt{R_o - v_o} = \sqrt{R_o(1-\cos\varphi_o)} = \sqrt{2R_o}\,\sin\frac{\varphi_o}{2} \tag{H-18a}$$

$$\varphi' = \alpha' + \gamma' + \pi \tag{H-18b}$$

$$\varphi = \gamma - \alpha \tag{H-18c}$$

$$\varphi_o = \alpha_o + \gamma + \pi = \alpha_o' + \gamma' + \pi \tag{H-18d}$$

$$t = \begin{cases} R\sin\alpha\sin\gamma & \text{(H-18e)} \\ R'\sin\alpha'\sin\gamma' & \text{(H-18f)} \\ R_o\sin\alpha_o\sin\gamma = R_o\sin\alpha_o'\sin\gamma' & \text{(H-18g)} \end{cases}$$

Eqs. (H-16) and (H-9) can be shown to be compatible by a calculation similar to that in Eqs. (H-10). A calculation similar to that is in Eqs. (H-11) shows also that

$$\exp\left[\frac{ik}{2}q_3(\lambda_s)\right] = \exp\left[ik(R\cos\alpha + R'\cos\alpha' + R_o\cos\alpha_o - R_o\cos\alpha_o')\right] = \exp\left[ik(\overline{QC}+\overline{CP})\right] \tag{H-19}$$

which is the phase of a wave emanating from Q and reaching P by being

reflected from the parabolic cylinder.

From Fig. H-2 it can be seen that $t \to \frac{\eta_o^2}{2}$ or $\frac{\lambda_s}{k^2} \to \eta_o^2$ when the observation point P nears the shadow boundary. The geometrical interpretation of the second part of G_2 is valid only in the illuminated region. Thus it is seen that the exact solution, Eq. (4-80), yields correctly the terms expected from geometrical optics as a first order asymptotic result at high frequencies. It would be satisfying if we could show that the asymptotic evaluation of the exact solution in the illuminated region yields also the amplitude factor which has been predicted by geometrical optics (Eq. (4-17). Jones[24] claims that it can indeed be shown for the case of a plane wave diffracted by a conducting parabolic cylinder in an isotropic region, but no detailed calculation is given in this reference. At the time of writing, this correspondence has not been obtained in the present study although there is reason to believe that the calculation can be performed.

When ϵ is complex or negative real, the parameters ξ, ξ', η, η' and η_o become complex according to Eqs. (4-81). If these expressions are substituted into Eqs. (H-7b) and (H-16), one obtains complex expressions of λ_s as functions of the complex parameter ϵ. The resulting equations for the loci of λ_s in the complex λ-plane, as functions of ϵ, are extremely complicated, and their detailed study (for some fixed $\underline{r}$ and $\underline{r}'$) is probably done best by computing machine.

APPENDIX I

Asymptotic evaluation of Equation (4-89).

According to whether the observation point lies in the illuminated or the shadow region, there will be two slightly different treatments of Eq. (4-89). In the shadow region, we follow Figs. 20(a) and 20 (b), assigning coordinates to the following points:

$$Q \equiv (x', y'),\ Q_1 \equiv (x_1', y_1'),\ P \equiv (x, y),\ P_1 \equiv (x_1, y_1),\quad O \equiv (0,0)\ ,$$
$$\overline{Q} \equiv (u', v'),\ \overline{Q}_1 \equiv (u_1', v_1'),\ \overline{P} \equiv (u, v),\ \overline{P}_1 \equiv (u_1, v_1),\quad \overline{O} \equiv (0,0)\ ,$$

The distance between two points A and B will be denoted by (AB); thus

$$\rho = (\overline{P}\,\overline{O}) = \begin{cases} \sqrt{(\overline{P}\,\overline{P}_1)^2 + (\overline{P}_1\,\overline{O})^2} = \sqrt{(u-u_1)^2 + (v-v_1)^2 + u_1^2 + v_1^2} \\ \sqrt{(\overline{P}\,\overline{P}_2)^2 + (\overline{P}_2\,\overline{O})^2} = \sqrt{(u-u_2)^2 + (v-v_2)^2 + u_2^2 + v_2^2} \end{cases} \tag{I-1}$$

$$\rho' = (\overline{Q}\,\overline{O}) = \begin{cases} \sqrt{(\overline{Q}\,\overline{Q}_1)^2 + (\overline{Q}_1\,\overline{O})^2} = \sqrt{(u'-u'_1)^2 + (v'-v_1') + u_1'^2 + v_1'^2} \\ \sqrt{(\overline{Q}\,\overline{Q}_2)^2 + (\overline{Q}_2\,\overline{Q})^2} = \sqrt{(u'-u'_2)^2 + (v'-v_2')^2 + u_2'^2 + v_2'^2} \end{cases} \tag{I-2}$$

$$a = (\overline{O}\,\overline{Q}_1) = (\overline{O}\,\overline{Q}_2) = (\overline{O}\,\overline{P}_1) = (\overline{O}\,\overline{P}_2) =$$
$$= \sqrt{u_1^2 + v_1^2} = \sqrt{u_2^2 + v_2^2} = \sqrt{u_1'^2 + v_1'^2} = \sqrt{u_2'^2 + v_2'^2} \tag{I-3}$$

$$\alpha_1 = 2\pi - |\varphi - \varphi'| - \beta - \gamma = 2\pi - |\varphi - \varphi'| - \cos^{-1}\frac{a}{\rho} - \cos^{-1}\frac{a}{\rho'} = \frac{S_1}{a} \tag{I-4}$$

$$\alpha_2 = |\varphi - \varphi'| - \beta - \gamma = |\varphi - \varphi'| - \cos^{-1}\frac{a}{\rho} - \cos^{-1}\frac{a}{\rho} = \frac{S_2}{a} \tag{I-5}$$

By using the relations

$$x = u \quad , \quad y = \frac{v}{\sqrt{\epsilon}} \quad , \tag{I-6}$$

one finds from Eqs. (I-1), (I-2), and (I-3),

$$k\rho = k_o\sqrt{(y-y_{1,2})^2+\epsilon\,(x-x_{1,2})^2+y_{1,2}^2+\epsilon\,x_{1,2}^2} \tag{I-7a}$$

$$k\rho' = k_o\sqrt{(y'-y'_{1,2})^2+\epsilon(x'-x'_{1,2})^2+y_{1,2}'^2+\epsilon\,x_{1,2}'^2} \tag{I-7b}$$

$$ka = k_o\sqrt{y_1^2+\epsilon\,x_1^2} = k_o\sqrt{y_1'^2+\epsilon\,x_1'^2} = k_o\sqrt{y_2^2+\epsilon\,x_2^2}$$

$$= k_o\sqrt{y_2'^2+\epsilon\,x_2'^2} \tag{I-7c}$$

In the shadow region, from Eq. (4-91)

$$\sum_{\ell=-\infty}^{\infty} e^{i\mu_p|\varphi-(\varphi'+2\pi\ell)|} = \left(\sum_{\ell=-1}^{-\infty} + \sum_{\ell=0}^{\infty}\right) e^{i\mu_p|\varphi-(\varphi'+2\pi\ell)|} =$$

$$= \left(1-e^{i2\pi\mu_p}\right)^{-1}\left\{e^{i\mu_p[2\pi-|\varphi-\varphi'|]} + e^{i\mu_p|\varphi-\varphi'|}\right\} =$$

$$= \left(1-e^{i2\pi\mu_p}\right)^{-1}\left\{e^{i\mu_p\left(\pi-\frac{S_2-S_1}{2a}\right)} + e^{i\mu_p\left(\pi+\frac{S_2-S_1}{2a}\right)}\right\} \tag{I-9}$$

with the last step obtained by subtracting Eq. (I-4) from Eq. (I-5), and substituting for $|\varphi-\varphi'|$. S_1 and S_2 are the arcs connecting $\overline{Q}_1$ to $\overline{P}_1$ and $\overline{Q}_2$ to $\overline{P}_2$ in Fig. (20b) respectively, and may be expressed in terms of $X_{1,2}$ and $X'_{1,2}$ (see Eq. (4-94)).

The asymptotic form of the Hankel function,

$$H^{(1)}_{\mu_p}(z) \sim \sqrt{\frac{2}{i\pi\sqrt{z^2-\mu_p^2}}}\exp\left[i\sqrt{z^2-\mu_p^2} - i\mu_p^2\cos^{-1}\frac{\mu_p}{z}\right] , \tag{I-10}$$

is valid for source and observation points which do not lie on or very near the

cylinder surface. Eq. (4-90b) is used for μ_p in Eq. (I-10)

$$\frac{\mu_p}{k\rho} \sim \frac{a}{\rho} + O(ka)^{-\frac{2}{3}} \approx \cos\gamma, \text{as } ka \gg 1 \tag{I-11}$$

$$\frac{\mu_p}{k\rho'} \sim \frac{a}{\rho'} + O(ka)^{-\frac{2}{3}} \approx \cos\theta, \text{as } ka \gg 1 \tag{I-12}$$

By adding Eqs. (I-4) and (I-5) we get

$$\cos^{-1}\frac{\mu_p}{k\rho} + \cos^{-1}\frac{\mu_p}{k\rho'} \sim \beta + \gamma = \pi - \frac{S_1+S_2}{2a} \tag{I-13}$$

and with the relations derived above (Eqs. (I-7), (I-9), (I-10), and (I-13)),

$$\frac{\pi}{2}H^{(1)}_{\mu_p}(k\rho)\,H^{(1)}_{\mu_p}(k\rho')\sum_{\ell=-\infty}^{\infty} e^{i\mu_p|\varphi-(\varphi'+2\pi\ell)|} \sim$$

$$\sim \frac{\exp\left[ik_o\sqrt{(y-y_1)^2+\epsilon(x-x_1)^2}+ik_o\sqrt{(y'-y_1')^2+\epsilon(x_1'-x_1')^2}+i\mu_p\frac{S_1}{a}\right]}{k_o\left[(y-y_1)^2+\epsilon(x-x_1)^2\right]^{\frac{1}{4}}\left[(y'-y_1')^2+\epsilon(x'-x_1')^2\right]^{\frac{1}{4}}\left[1-e^{i2\pi\mu_p}\right]} +$$

$$+ \frac{\exp\left[ik_o\sqrt{(y-y_2)^2+\epsilon(x-x_2)^2}+ik_o\sqrt{(y'-y_2')^2+\epsilon(x'-x_2')^2}+\mu_p\frac{S_2}{a}\right]}{k_o\left[(y-y_2)^2+\epsilon(x-x_2)^2\right]^{\frac{1}{4}}\left[(y'-y_2')^2+\epsilon(x'-x_2')^2\right]^{\frac{1}{4}}\left[1-e^{i2\pi\mu_p}\right]} =$$

$$= \frac{\exp\left[ik_o d_1 N(\theta_1)+ik_o d_1' N(\theta_1')+i\mu_p\frac{S_1}{a}\right]}{\sqrt{k_o d_1 N(\theta_1)}\sqrt{k_o d_1' N(\theta_1')}\left[1-e^{i2\pi\mu_p}\right]} +$$

$$+ \frac{\exp\left[ik_o d_2 N(\theta_2)+ik_o d_2' N(\theta_2')+i\mu_p\frac{S_2}{a}\right]}{\sqrt{k_o d_2 N(\theta_2)}\sqrt{k_o d_2' N(\theta_2')}\left[1-e^{i2\pi\mu_p}\right]} \tag{I-14}$$

The coefficient which appears in Eq. (4-91)

$$\frac{H_{\mu_p}'^{(2)}(k a)}{\frac{\partial}{\partial \mu} H_{\mu}'^{(1)}(k a)\Big|_{\mu_p}}$$

is identical with the one appearing in the corresponding isotropic problem (diffraction by a circular cylinder in an isotropic medium), and has been evaluated asymptotically for large $k a$ by various authors[16][17].

For the illuminated region, we follow Figs. (20c) and (20d) for various definitions and note that S_1 and S_2 are now the arcs connecting $\overline{Q}_1$ to $\overline{P}_1$ and $\overline{Q}_2$ to $\overline{P}_2$, respectively (Fig. (20d)). They are interpretable as paths of creeping rays which shed from the surface toward the observation point P located in the illuminated region. Thus the arc S_2 is now the long arc connecting the points $\overline{Q}_2$ and $\overline{P}_2$ in Fig. (20d). From the same figure one notes that Eqs. (I-4) and (I-5) have to be replaced by:

$$2\pi - |\varphi - \varphi'| - \beta - \gamma = 2\pi - |\varphi - \varphi'| - \cos^{-1}\frac{a}{\rho} - \cos^{-1}\frac{a}{\rho} = \frac{S_1}{a} \tag{I-15}$$

$$2\pi + |\varphi - \varphi'| - \beta - \nu = 2\pi + |\varphi - \varphi'| - \cos^{-1}\frac{a}{\rho} - \cos^{-1}\frac{a}{\rho'} = \frac{S_2}{a} \tag{I-16}$$

Proceeding as above, one may then derive a result like Eq. (I-14), except that the $\ell = 0$ term is not included in the summation. Thus the expression given by Eq. (4-92) (or equivalently Eq. 4-55) is valid both in the shadow and the illuminated regions, but in the illuminated region one has as well the integral in Eq. (4-100).

BIBLIOGRAPHY

1. Budden, K. G.: "Radio Waves in the Ionosphere", Cambridge University Press, chap. 3, (1961).

2. Felsen, L. B.: "Propagation and Diffraction in Uniaxially Anisotropic Regions", Proc. IEE (London) 111, pp. 445-464, (1963).

3. Keller, J. B.: "The Geometrical Theory of Diffraction ", J. Opt. Soc. Amer. 52, pp. 116-130, (1962). This paper contains additional pertinent references.

4. Noble, B.: "Methods Based on the Wiener-Hopf Technique", Pergamon Press, London, chap. II, (1958).

5. Arbel, E. and Felsen, L. B.: "Theory of Radiation from Sources in Anisotropic Media" in "Electromagnetic Theory and Antennas", pp. 391-459. (Proceedings of Symposium in Copenhagen, June 1962) Pergamon Press, New York, (1963).

6. Ref. 1, sec. 13.19.

7. Arbel, E. and Felsen, L. B.: "Radiation from a Dipole in an Infinite, Homogeneous Anisotropic Plasma", Research Report No. PIBMRI-1070-62, (Sept. 1962).

8. Meixner, J. and Schäfke, F. W.: "Mathieusche Funktionen und Sphäroidfunktionen" Springer Verlag, Berlin, (1954).

9. Ref. 8: Sections 2.2. and 2.7.

10. Ref. 8: Sections 2.4. and 2.7.

11. Morse, P. M. and Feshbach, H.: "Methods of Theoretical Physics", McGraw-Hill, New York, (1953), sec. 11.2.

12. Burke, J. E. and Twersky, V.: "On Scattering of Waves by an Elliptical Cylinder", Jour. Opt. Soc. Amer. 54, pp. 732-744, (June 1964) and Report EDL-M266, Sylvania Electronic Defense Labs, (1960).

13. Brandstatter, J. J.: "An Introduction to Waves, Rays and Radiation in Plasma Media", chap. VII, New York, McGraw-Hill, (1963).

14. Wait, J. R.: "Electromagnetic Waves in Stratified Media", Oxford, New York, Pergamon Press, (1962).

15. Felsen, L. B.: "Radiation from a Uniaxially Anisotropic Plasma Half Space", IEEE Trans. AP-11, pp. 469-484, (1963).

16. Keller, J. B.: "Diffraction by a Convex Cylinder", IRE Trans., AP-4, pp. 312-321, (1956).

17. Franz, W.: "Theorie der Beugung Electromagnetischer Wellen", p. 49, Springer Verlag, Berlin, (1957).

18. MacDonald, H. M.: "A Class of Diffraction Problems", Proc. Lond. Math. Soc. 14, p. 410, (1915).

19. Rulf, B. and Felsen, L. B.: "Diffraction by Objects in Anisotropic Media", Proc. Symp. on Quasi Optics, pp. 107-148. Polytechnic Press, New York, (1964).

20. Ref. 4, pp. 31-36.

21. Fock, V. A.: "Fresnel Diffraction from Convex Bodies", UFN (Russian) 36, pp. 308-319, (1948).

22. Ref. 17, the whole chapter on diffraction by a circular cylinder, in particular p. 42.

23. King, R. W. P. and Wu, T. T.: "The Scattering and Diffraction of Waves", Harvard University Press, (1959).

24. Jones, D. S.: "The Theory of Electromagnetism", chap. 8, Pergamon Press, (1964).

25. Levy, B. R.: "Diffraction by an Elliptic Cylinder", Jour. Math. and Mech. 9, pp. 147-165, (1960).

26. Marcuvitz, N.: "Field Representations in Spherically Stratified Regions", Comm. Pure and Appl. Math. 4, p. 263, (1951).

27. Magnus, W. and Oberhettinger, F.: "Formulas and Theorems for the Functions of Mathematical Physics", Chelsea Publishing Co., New York, (1954).

28. Erdelyi, A., Director, Bateman Manuscript Project Staff: "Higher Transcendental Functions", vol. II, chap. VIII, New York, McGraw-Hill, (1953).

29. Felsen, L. B. and Marcuvitz, N.: "Modal Analysis and Synthesis of Electromagnetic Fields", Chap. III, Report R-726-59, PIB-654 Polytechnic Institute of Brooklyn, (June 1959).

30. Ref. 11, Sec. 4.5.

31. Rice, S. O.: "Diffraction of a Plane Radio Wave by a Parabolic Cylinder", Bell Sys. Tech. Jour. 33, pp. 4-17-504, (March 1959).

32. Keller, J. B. and Levy, B. R.: "Decay Exponents and Diffraction Coefficients for Surface Waves on Surfaces of Nonconstant Curvature", Trans. IRE, AP-7 p. 352 (Dec. 1959).

33. Felsen, L. B. and Marcinkowski, C. J. · "Diffraction by a Cylinder with Variable Surface Impedance", Proc. Roy. Soc., A, 267, pp. 329-350, (1962).

AD 618 689

AFCRL-65-429 26 April 1965
Contract No. AF 19(628)-2357

ERRATA - 20 September 1965

The following corrections are applicable to AFCRL-65-429 entitled "Diffraction and Scattering of Electromagnetic Waves in Anisotropic Media" UNCLASSIFIED Report, dated 26 April 1965:

Front Cover

Title Page

Project Number and Task Number were reversed. Should read

Project No. 5635
Task No. 563501

The above report was issued by the Polytechnic Institute of Brooklyn, Department of Electrophysics, Report No. PIBMRI-1262-65.

X